# Part IV

# SAMPLED DATA MULTI-INPUT MULTI-OUTPUT SYSTEMS

# Chapter 15

# MIMO Sampled-Data Systems

We assume that the reader has mastered the chapters on SISO sampled-data systems as well the chapters on MIMO continuous systems. When the extension of results to MIMO sampled-data systems is straightforward the discussion will be brief and sometimes limited to simply defining the appropriate notation.

## 15.1 Fundamentals of MIMO Sampled-Data Systems

### 15.1.1 Sampled-Data Feedback

The block diagram of a typical sampled-data feedback loop is shown in Fig. 15.1-1A. Thick lines are used to represent the paths along which the signals are continuous. Equations (7.1–1) to (7.10–11) carry through to the MIMO case, with vectors instead of scalars. $C(z)$ denotes the discrete controller implemented through a digital computer. $H_0(s)$ models the D/A converter. We have

$$H_0(s) = h_0(s)I \qquad (15.1-1)$$

where $h_0(s)$ is the zero-order hold given by (7.1–12) and $I$ is the identity matrix with dimension equal to the number of controller outputs. The block $\Gamma(s)$ represents an anti-aliasing prefilter. The problem of aliasing was discussed in Sec. 7.1. Assuming that the the same sampling time is used for all the process outputs, it is reasonable to choose

$$\Gamma(s) = \gamma(s)I \qquad (15.1-2)$$

where $I$ has dimension equal to the number of the process outputs. $P(s)$ is the continuous system transfer matrix described in Sec. 10.1.1.

When the continuous output $y$ is not observed directly but after the prefilter and only at the sampling points, then Fig. 15.1-1A can be simplified to Fig. 15.1-1B, where

$$d^*_\gamma(z) = \mathcal{Z}\mathcal{L}^{-1}\{\Gamma(s)d(s)\} = \mathcal{Z}\mathcal{L}^{-1}\{\gamma(s)d(s)\} \qquad (15.1-3)$$

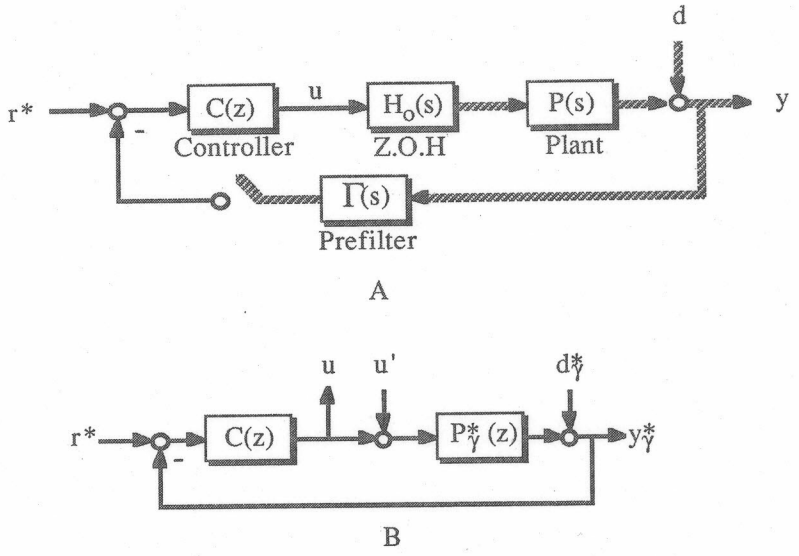


*Figure 15.1-1.* Block diagram of computer controlled system A: Sampled-data structure with thick lines indicating analog signals. B: Discrete structure with all signals discrete.

$$y_\gamma^*(z) = \mathcal{ZL}^{-1}\{\Gamma(s)y(s)\} = \mathcal{ZL}^{-1}\{\gamma(s)y(s)\} \qquad (15.1-4)$$

and all signals are discrete. Note that when the operator $\mathcal{ZL}^{-1}$ is applied to a vector or matrix, it is simply applied to each element separately. We define

$$P_\gamma^*(z) = \mathcal{ZL}^{-1}\{\Gamma(s)P(s)H_0(s)\} = \mathcal{ZL}^{-1}\{h_0(s)P(s)\gamma(s)\} \qquad (15.1-5)$$

$$P^*(z) = \mathcal{ZL}^{-1}\{P(s)H_0(s)\} = \mathcal{ZL}^{-1}\{h_0(s)P(s)\} \qquad (15.1-6)$$

All the elements of a vector or matrix pulse transfer function are always rational in $z$, although the continuous transfer functions may include time delays. In order to be physically realizable the transfer matrices (or vectors) have to be proper or causal.

**Definition 15.1-1.** *A vector or matrix $G^*(z)$ is proper or causal if all its elements are proper and strictly proper if all its elements are strictly proper. All systems $G^*(z)$ which are not proper are called improper or noncausal .*

### 15.1.2 Poles and Zeros

Let

$$G^*(z) = \mathcal{ZL}^{-1}\{h_0(s)G(s)\} \qquad (15.1-7)$$

where $G(s)$ is the transfer matrix representation of the system of differential and algebraic equations of Sec. 10.1.1. Then $G^*(z)$ is the z-transfer matrix that describes the system of difference equations

$$x(kT+T) = \Phi x(kT) + \Gamma u(kT) \qquad (15.1-8)$$

$$y(kT) = Cx(kT) + Du(kT) \qquad (15.1-9)$$

where $T$ is the sampling time and

$$\Phi = e^{AT} \qquad (15.1-10)$$

$$\Gamma = \int_0^T e^{At}\,dt\;B \qquad (15.1-11)$$

Taking the $z$-transform of (15.1–8), (15.1–9) we get

$$x(z) = (zI - \Phi)^{-1}\Gamma u(z) \qquad (15.1-12)$$

$$y(z) = Cx(z) + Du(z) \qquad (15.1-13)$$

and substituting (15.1–12) into (15.1–13) yields

$$y(z) = G^*(z)u(z) \qquad (15.1-14)$$

where

$$G^*(z) \triangleq C(zI - \Phi)^{-1}\Gamma + D \qquad (15.1-15)$$

The matrix $G^*(z)$ will be assumed to be of full normal rank. The poles and zeros of $G^*(z)$ are defined in exactly the same way as those of $G(s)$.

**Definition 15.1-2.** *The eigenvalues $\pi_i, i = 1, \ldots, n_p$, of the matrix $\Phi$ are called the poles of the system (15.1–8), (15.1–9). The pole polynomial $\pi(z)$ is defined as*

$$\pi(z) = \prod_{i=1}^{n_p}(z - \pi_i) \qquad (15.1-16)$$

**Definition 15.1-3.** *$\zeta$ is a zero of $G^*(z)$ if the rank of $G^*(\zeta)$ is less than the normal rank of $G^*(z)$.*

The zero polynomial is defined as

$$\zeta(z) = \prod_{i=1}^{n_z}(z - \zeta_i) \qquad (15.1-17)$$

where $n_z$ is the number of finite zeros of $G^*(z)$.

### 15.1.3 Internal Stability

Assuming that no unstable poles of the continuous process have become unobservable after sampling, the internal stability of the system in Fig. 15.1-1A can be assessed from the internal stability of the system in Fig. 15.1-1B.

**Theorem 15.1-1.** *The sampled-data system in Fig. 15.1-1A is internally stable if and only if the transfer matrix in (15.1-18)*

$$\begin{pmatrix} y_\gamma^* \\ u \end{pmatrix} = \begin{pmatrix} P_\gamma^* C(I + P_\gamma^* C)^{-1} & (I + P_\gamma^* C)^{-1} P_\gamma^* \\ C(I + P_\gamma^* C)^{-1} & -C(I + P_\gamma^* C)^{-1} P_\gamma^* \end{pmatrix} \begin{pmatrix} r^* \\ u' \end{pmatrix} \qquad (15.1-18)$$

*is stable — i.e. if and only if all its poles are strictly inside the unit circle.*

Another test for internal stability is the Nyquist criterion, which was discussed for continuous systems in Sec. 10.2.2. The derivation follows exactly the same steps. The difference is that when we are dealing with z-transfer functions instead

of Laplace transfer functions, the Nyquist D-contour encircles the area outside the UC instead of the RHP.

**Theorem 15.1-2 (Nyquist Stability Criterion).** *Let the map of the Nyquist D-contour under* $\det(I + P_\gamma^*(z)C(z))$ *encircle the origin* $n_F$ *times in the clockwise direction. Let the number of open-loop unstable poles of* $P_\gamma^* C$ *be* $n_{PC}$*. Then the closed-loop system is stable if and only if*

$$n_F = -n_{PC} \tag{15.1-19}$$

### 15.1.4 IMC Structure

The block diagram of the sampled-data MIMO IMC structure is shown in Fig. 15.1-2A, where

$$\tilde{P}_\gamma^*(z) = \mathcal{Z}\mathcal{L}^{-1}\{\Gamma(s)\tilde{P}(s)H_0(s)\} = \mathcal{Z}\mathcal{L}^{-1}\{\gamma(s)\tilde{P}(s)h_0(s)\} \tag{15.1-20}$$

$$\tilde{P}^*(z) = \mathcal{Z}\mathcal{L}^{-1}\{\tilde{P}(s)H_0(s)\} = \mathcal{Z}\mathcal{L}^{-1}\{\tilde{P}(s)h_0(s)\} \tag{15.1-21}$$

When the IMC controller $Q$ and the feedback controller $C$ are related through

$$C = Q(I - \tilde{P}_\gamma^* Q)^{-1} \tag{15.1-22}$$

$$Q = C(I + \tilde{P}_\gamma^* C)^{-1} \tag{15.1-23}$$

then $u(z)$ and $y(s)$ react to inputs $r^*(z)$ and $d(s)$ in exactly the same way for both the classic feedback and the IMC structure.

Figure 15.1-2B is a different representation of the sampled-data IMC structure, which is equivalent to that in Fig. 15.1-2A, but not suitable for computer implementation because of the presence of the continuous model $\tilde{P}(s)$. If only the sampled signals are of interest, then Fig. 15.1-2A is equivalent to Fig. 15.1-2C, where all signals are digital.

### 15.1.5 Model Uncertainty Description

In Sec. 7.3.2, we demonstrated how the modeling error in the description of the discretized plant is related to that in the continuous plant description. We pointed out that some conservativeness is introduced when the uncertainty bounds for the discrete plant are derived from those for the continuous plant. However, the conservativeness is quite small for the type of unstructured SISO system

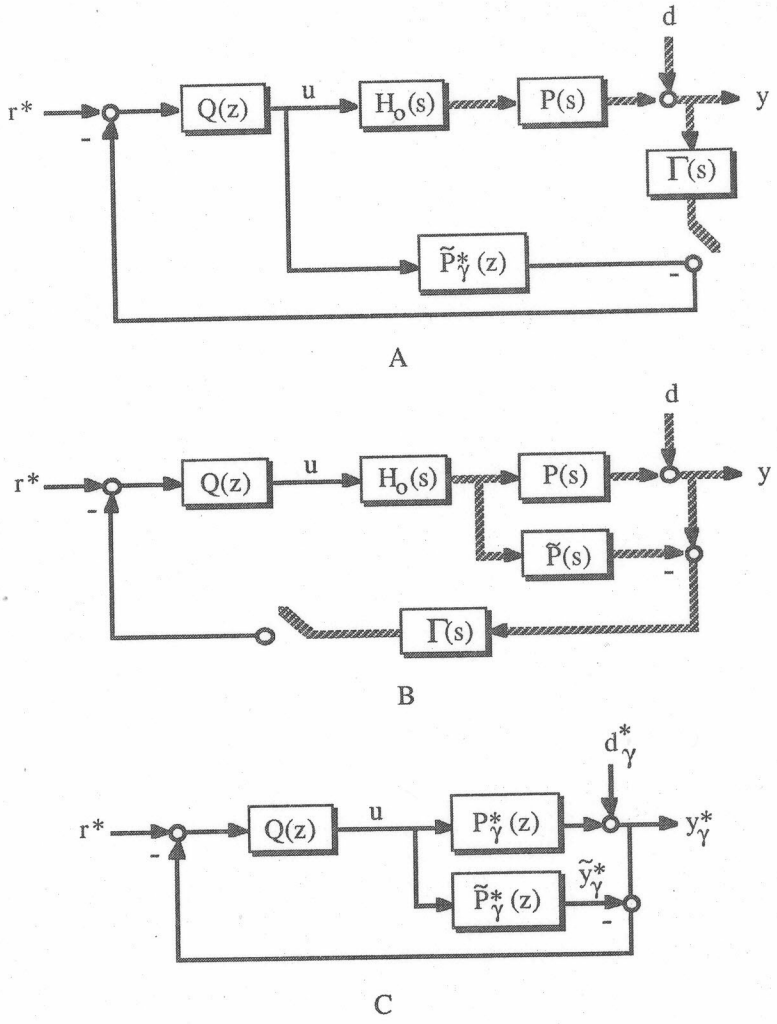


*Figure 15.1-2.* IMC structure: A: Sampled-data structure; B: Structure equivalent to (A) but not implementable; C: Discrete structure (all signals discrete).

uncertainty that was used in Chaps. 7 through 9. The same is true for a few types of MIMO-system uncertainty. For example, let us assume that the additive uncertainty for the continuous plant is bounded by $\bar{\ell}_A$:

$$\bar{\sigma}(P(i\omega) - \tilde{P}(i\omega)) \leq \bar{\ell}_A(\omega) \qquad (15.1-24)$$

For the discretized plant we have from (15.1–6), (15.1–21)

$$P^*(z) - \tilde{P}^*(z) = \mathcal{Z}\mathcal{L}^{-1}\{h_0(s)(P(s) - \tilde{P}(s))\} \qquad (15.1-25)$$

Then from the z-transform property (7.1–5), the singular value property $\bar{\sigma}(A+B) \leq \bar{\sigma}(A) + \bar{\sigma}(B)$, and (15.1–24), (15.1–25), it follows that

$$\bar{\sigma}(P^*(e^{i\omega T}) - \tilde{P}^*(e^{i\omega T})) \leq \frac{1}{T}\sum_{k=-\infty}^{\infty} |h_0(i\omega + ik2\pi/T)|\bar{\ell}_A(i\omega + ik2\pi/T) \triangleq \bar{\ell}_a^*(\omega) \qquad (15.1-26)$$

The ZOH $h_0(s)$ is small at frequencies higher than $\pi/T$ and goes to 0 as fast as $1/\omega$ as $\omega \to \infty$. Therefore only a few terms around $k = 0$ are important in the infinite sum. Also note that for a physical system, $\bar{\ell}_A(\omega) \to 0$ at least as fast as $1/\omega$ as $\omega \to \infty$, and hence the sum converges.

However, it is not always possible to obtain a mathematical description for the uncertainty in the $z$-domain in a non-conservative way, starting from the uncertainty in the $s$-domain. In the absence of first-principles models, these descriptions may be the result of experiments conducted with different sampling rates, one of which may be small enough to approximate the continuous system. A discussion of identification techniques is beyond the scope of this book. We will assume in this chapter that non-conservative uncertainty descriptions for the discrete and the continuous plant are available.

## 15.2 Nominal Internal Stability

### 15.2.1 IMC Structure

The same arguments as in Sec. 12.2 imply that the following matrix must be stable for internal stability of the IMC structure in Fig. 15.1-2C.

$$S_1 = \begin{pmatrix} P_\gamma^* Q & (I - P_\gamma^* Q)P_\gamma^* & P_\gamma^* \\ Q & -QP_\gamma^* & 0 \\ P_\gamma^* Q & -P_\gamma^* Q P_\gamma^* & P_\gamma^* \end{pmatrix} \qquad (15.2-1)$$

Note that stability of the structure in Fig. 15.1-2C implies stability of that in Fig. 15.1-2A, provided that no open-loop unstable poles of the plant become unobservable after sampling.

**Theorem 15.2-1.** *For $P = \tilde{P}$, the IMC system in Fig. 15.1-2A is internally stable if and only if both the plant $P$ and the controller $Q$ are stable.*

Hence for open-loop unstable plants, the IMC structure cannot be implemented. In such cases, the IMC design procedure is used to design the controller, which is then implemented through the classic feedback structure.

### 15.2.2 Feedback Structure

When there is no modeling error, substitution of (15.1–22) into (15.1–18) yields for the internal stability matrix

$$S_2 = \begin{pmatrix} P_\gamma^* Q & (I - P_\gamma^* Q) P_\gamma^* \\ Q & -Q P_\gamma^* \end{pmatrix} \qquad (15.2-2)$$

All four transfer matrices in (15.2–2) have to be stable for nominal stability of the classic feedback structure in Fig. 15.1-1A.

Theorem 15.2-2 provides a parametrization of all proper stabilizing controllers in terms of a stable transfer matrix $Q_1$. The following assumptions are analogous to those made in Sec. 12.3.

**Assumption A1.** *If $\pi$ is a pole of $\tilde{P}^*$ outside the UC, then (a) The order of $\pi$ is equal to 1 and (b) $\tilde{P}$ has no zeros at $z = \pi$.*

**Assumption A2.** *Any poles of $\tilde{P}^*$ or $P^*$ on the UC are at $z = 1$. Also $\tilde{P}^*$ has no zeros on the UC.*

**Theorem 15.2-2.** *Assume that Assns. A1 and A2 hold and that $Q_0(z)$ is a proper transfer matrix that stabilizes $\tilde{P}^*$ — i.e., it yields a stable $S_2$. Then all proper $Q$'s that make $S_2$ stable are given by*

$$Q(z) = Q_0(z) + Q_1(z) \qquad (15.2-3)$$

*where $Q_1(z)$ is any proper and stable transfer matrix such that $P^*(z)Q_1(z)P^*(z)$ is stable.*

*Proof.* The fact that $Q_1$ has to be proper in order for $Q$ to be proper and vice versa, follows from the properness of $Q_0$. For the following part of the proof we will use the fact that $P^*$ and $P_\gamma^*$ have the same unstable poles.

$\Rightarrow$ We shall show that any $Q$ given by (15.2–3) makes $S_2$ stable. From substitution of (15.2–3) into (15.2–2) it follows that all that is required is that $(P^*Q_1 \quad Q_1P^* \quad P^*Q_1P^*)$ be stable. From the properties of $Q_1$, it follows that the third element in the above matrix is stable. Stability of the other

two elements follows by pre- and post-multiplication of $P^*Q_1P^*$ by $(P^*)^{-1}$, since according to assumptions A1 and A2, $P^*$ has no zeros at the location of its unstable poles and these are the only possible unstable poles of $S_2$.

$\Leftarrow$ Assume that $Q$ makes $S_2$ stable. Then the difference matrix

$$\Delta S_2 = S_2(Q) - S_2(Q_0) = \begin{pmatrix} P^*(Q-Q_0) & P^*(Q-Q_0)P^* \\ (Q-Q_0) & (Q-Q_0)P^* \end{pmatrix} \qquad (15.2-4)$$

is stable. This implies that $(Q - Q_0) = Q_1$ and $P^*Q_1P^*$ are stable. □

## 15.3 Nominal Performance

### 15.3.1 Sensitivity and Complementary Sensitivity Function

The development in this section follows that in Sec. 7.5.1. Therefore we shall limit ourselves to simply setting the appropriate notation for the MIMO systems.

From Fig. 15.1-2A we get for $P = \tilde{P}$

$$y(s) = h_0(s)P(s)Q(e^{sT})(r^*(e^{sT}) - d_\gamma^*(e^{sT})) + d(s) \qquad (15.3-1)$$

Define

$$e(s) = y(s) - r(s) \qquad (15.3-2)$$

Then for an $r(s)$ that remains constant between sampling points, we have $r(s) = h_0(s)r^*(e^{sT})$ and we can define the sensitivity and complementary sensitivity operators that relate $r(s)$ to $-e(s)$ and $y(s)$, correspondingly as

$$\tilde{E}_r(s) \triangleq I - P(s)Q(e^{sT}) \qquad (15.3-3)$$

$$\tilde{H}_r(s) \triangleq P(s)Q(e^{sT}) \qquad (15.3-4)$$

An approximate sensitivity function for the relation between $y(s)$ and $d(s)$ can only be obtained when the assumption is made that the disturbance is limited to the frequency band up to $\pi/T$.

$$y(i\omega) \cong \tilde{E}_d(i\omega)d(i\omega) \qquad (15.3-5)$$

where

$$\tilde{E}_d(s) = I - P(s)\hat{Q}(s) \qquad (15.3-6)$$

$$\hat{Q}(s) = \frac{1}{T} h_0(s) Q(e^{sT}) \gamma(s) \qquad (15.3-7)$$

Sampling of (15.3–1) yields

$$y^*(z) = P^*(z)Q(z)(r^*(z) - d^*_\gamma(z)) + d^*(z) \qquad (15.3-8)$$

from which we can obtain the *pulse* sensitivity and complementary sensitivity functions, relating $e^*(z)$ to $r^*(z)$ and $d^*(z)$ (for $\gamma(s) = 1$) or $d^*_\gamma(z)$ (when $d^*_\gamma$ is substituted for $d^*$ in (15.3–8)):

$$\tilde{E}^*(z) \triangleq I - P^*(z)Q(z) \qquad (15.3-9)$$

$$\tilde{H}^*(z) \triangleq P^*(z)Q(z) \qquad (15.3-10)$$

### 15.3.2 $H_2^*$ Performance Objectives

We define as $L_2^{*,n}$ the Hilbert space of complex valued vector functions $y(z)$ with $n$ elements, defined on the unit circle and square integrable with respect to $\theta$ — i.e., for which the following quantity is finite:

$$\|y\|_2 = \left( \frac{1}{2\pi} \int_{-\pi}^{\pi} y(e^{i\theta})^H y(e^{i\theta}) \quad d\theta \right)^{1/2} \qquad (15.3-11)$$

Note that (15.3–11) defines a norm on $L_2^{*,n}$. In the case where $y(z)$ has no poles outside the UC, Parseval's theorem yields a time domain expression for $\|y\|_2$:

$$\|y\|_2 = \left( \sum_{k=0}^{\infty} y_k^T y_k \right)^{1/2} \qquad (15.3-12)$$

For matrix valued functions $G(z)$ of dimensions $n \times m$, the space $L_2^{*,n\times m}$ is defined similarly with norm

$$\|G\|_2 = \left( \frac{1}{2\pi} \int_{-\pi}^{\pi} \text{trace}[G(e^{i\theta})^H G(e^{i\theta})] \quad d\theta \right)^{1/2} \qquad (15.3-13)$$

The spaces $H_2^{*,n}$ and $H_2^{*,n\times m}$ are defined as subspaces of the corresponding $L_2$ spaces as in the scalar case.

The $H_2^*$ performance objective is to minimize over all stabilizing $\tilde{Q}$ the weighted sum of squared errors for the response to an input or a set of inputs of interest. Several $H_2^*$–type objective functions will be considered. For a specific external input $v^*$ ($r^*$ or $d^*$ or $d^*_\gamma$) define by using (15.3-9)

$$\Phi(v^*) \triangleq \|We^*\|_2^2 = \|W\tilde{E}^*v^*\|_2^2 = \|W(I - P^*\tilde{Q})v^*\|_2^2 \qquad (15.3-14)$$

where $W$ is a frequency dependent matrix or scalar weight. One objective could be

*Objective O1:*

$$\min_{\tilde{Q}} \Phi(v^*)$$

for a particular input $v^* = (\, v_1 \quad v_2 \quad \ldots \quad v_n \,)^T$.

A more meaningful objective would be to minimize $\Phi(v)$ not just for one input vector $v^*$, but for every input in a set $\mathcal{V}$:

$$\mathcal{V} = \{v^i(z) | i = 1, \ldots n\} \qquad (15.3-15)$$

where $v^1(z)$,...,$v^n(z)$ are vectors that describe the directions and the frequency content of the expected external system inputs and $n$ is the dimension of $P$. Thus, the objective is

*Objective O2:*

$$\min_{\tilde{Q}} \Phi(v^*) \qquad \forall v^* \in \mathcal{V}$$

However a linear time invariant $\tilde{Q}(z)$ that solves *O2* does not always exist. The conditions necessary for its existence are expressed in Thm. 15.6-3. An alternative is

*Objective O3:*

$$\min_{\tilde{Q}} [\Phi(v^1) + \ldots + \Phi(v^n)]$$

In this case the objective is the sum of the squared errors caused by each of the $v^i$'s, when applied separately.

For every external input $v^*$ that will be considered in this chapter the following assumptions will be made. They are analogous to those discussed in Sec. 12.6.1 and their physical meaning is identical.

**Assumption A3.** *Every nonzero element of $v^*$ includes all the poles of $\tilde{P}$ outside the UC, each with degree 1, and those are the only poles of $v^*$ outside the UC.*

**Assumption A4.** *Let $\ell_i$ be the maximum number of poles at $z = 1$ of any element in the $i^{th}$ row of $P$. Then the $i^{th}$ element of $v^*$, $v_i$, has at least $\ell_i$ poles at $z = 1$. Also $v^*$ has no other poles on the UC and its elements have no zeros on the UC.*

For the case, where a set $\mathcal{V}$ of inputs is considered, define

$$V \triangleq (v^1 \quad v^2 \quad \dots \quad v^n) \qquad (15.3-16)$$

where $v^1, \dots, v^n$ satisfy Assn. A3. An additional assumption on $V$ is needed:

**Assumption A5.** *$V$ has no zeros at the location of its unstable poles or on the UC and $V^{-1}$ cancels the unstable poles of $\tilde{P}$ in $V^{-1}\tilde{P}$.*

### 15.3.3 $H_\infty$ Performance Objective

The $H_\infty$ objective discussed in Sec. 10.4.4 can now be extended to discrete systems with band-limited disturbances. The development is similar to that for the SISO case (Sec. 7.5.5). The objective can be written as

$$\|W\tilde{E}_v\|_\infty < 1 \qquad (15.3-17)$$

where $W$ is the frequency weight and $\tilde{E}_v(s)$ is either the approximate disturbance sensitivity function $\tilde{E}_d$ given by (15.3–6) or the setpoint sensitivity function $\tilde{E}_r$ given by (15.3–3). Since the disturbance is assumed to be limited to the frequency band up to $\pi/T$ and $h_0(s)r^*(e^{sT})$ is also limited because of $h_0$, the weight should satisfy

$$\bar{\sigma}(W(\omega)) << 1, \qquad \omega > \pi/T \qquad (15.3-18)$$

Hence (15.3–17) can be written as

$$\bar{\sigma}(W(\omega)\tilde{E}_v(i\omega)) < 1, \qquad 0 \le \omega \le \pi/T \qquad (15.3-19)$$

If $W$ is a scalar, (15.3–19) becomes

$$\bar{\sigma}(\tilde{E}_v(i\omega)) < |w(\omega)|^{-1}, \qquad 0 \le \omega \le \pi/T \qquad (15.3-20)$$

## 15.4 Robust Stability

In Sec. 15.1 we explained that if no open-loop unstable poles of the plant or the model become unobservable after sampling, then stability of the structures in Figs. 15.1-1A and 15.1-2A is equivalent to stability of those in Figs. 15.1-1B and 15.1-2C correspondingly. In Sec. 15.2 we developed the nominal internal stability conditions. We shall now concentrate on the robust stability of completely discrete structures like the ones in Figs. 15.1-1B and 15.1-2C. The development of robustness conditions follows exactly the same steps as those in Chap. 11.

First the $M - \Delta$ structure (Fig. 11.1-2) which is needed in the structured singular value theory, has to be generated from the given discrete control structure. For this purpose the same type of block manipulations have to be carried

out as were demonstrated in Chap. 11. Then, if $M$ and $\Delta$ are stable, the condition for robust stability is that the map of the discrete Nyquist D-contour under $\det(I - M\Delta)$ does not encircle the origin. Recall that for discrete systems the D-contour encircles the area outside the UC. We can now use the SSV to obtain the following theorem.

**Theorem 15.4-1.** *Assume that the nominal systems $M$ is stable and that the perturbation $\Delta$ is such that the perturbed closed-loop system is stable if and only if the map of the Nyquist contour under* $\det(I - M\Delta)$ *does not encircle the origin. Then the system in Fig. 11.1-2 is stable for all $\Delta \in X_1$ if and only if*

$$\mu(M(e^{i\omega T})) < 1 \qquad 0 \leq \omega \leq \pi/T \tag{15.4-1}$$

Note that because of the periodicity of the $z$-transforms and the property described by (7.1-8), only the frequencies up to $\pi/T$ need to be considered.

## 15.5 Robust Performance

### 15.5.1 Sensitivity Function Approximation

First, we shall obtain an approximate sensitivity function in a similar way as in Sec. 15.3.1. Then we shall use this function to assess robust performance. From Fig. 15.1-2A it follows that

$$e(s) \triangleq y(s) - r(s)$$

$$= (d(s) - r(s)) - P(s)H_0(s)Q(e^{sT})$$

$$(I + (P^*_\gamma(e^{sT}) - \tilde{P}^*_\gamma(e^{sT}))Q(e^{sT}))^{-1}(d^*_\gamma(z) - r^*(z)) \tag{15.5-1}$$

We shall now obtain an approximation to (15.5–1) by considering the frequencies $0 \leq \omega \leq \pi/T$. Note that because of the periodicity of $Q(z)$, these are the only frequencies which one can influence independently by using a digital controller. It follows from (7.1–5) that if $a(s)$ is small for $\omega > \pi/T$, then

$$a^*(e^{i\omega T}) \cong \frac{1}{T}a(i\omega), \qquad 0 \leq \omega \leq \pi/T \tag{15.5-2}$$

Use of (15.5–2) for all the $z$-transforms in (15.5–1) except for $r^*$ for which we assume $r(s) = h_0(s)r^*(e^{sT})$, yields the approximation

$$e(i\omega) \cong E_d(i\omega)d(i\omega) - E_r(i\omega)r(i\omega), \qquad 0 \leq \omega \leq \pi/T \tag{15.5-3}$$

where

$$E_r(i\omega) \triangleq I - P(i\omega)Q(e^{i\omega T})\cdot$$
$$\left[I + (P(i\omega) - \tilde{P}(i\omega))Q(e^{i\omega T})\gamma(i\omega)h_0(i\omega)/T\right]^{-1} \qquad (15.5-4)$$

$$E_d(i\omega) \triangleq I - P(i\omega)Q(e^{i\omega T})\gamma(i\omega)h_0(i\omega)/T\cdot$$
$$\left[I + (P(i\omega) - \tilde{P}(i\omega))Q(e^{i\omega T})\gamma(i\omega)h_0(i\omega)/T\right]^{-1} \qquad (15.5-5)$$

Note that the above approximation is valid when the input signals $r$ and $d$ are small for $\omega > \pi/T$. If we assume that $r(t)$ is a staircase function then it has the desired property. If one expects disturbances with high frequency content at $\omega > \pi/T$ then one should reduce $T$ or use the anti-aliasing prefilter whose function is to cut off signals with frequencies higher than $\pi/T$.

### 15.5.2 $H_\infty$ Performance Objective

We require that the objective defined in Sec. 15.3.3 be satisfied for all plants $P(s)$ in the uncertainty set $\Pi$ (note that $E_v(\tilde{P}) = \tilde{E}_v$).

$$\max_{0\le\omega\le\pi/T} \bar{\sigma}(W(\omega)E_v(i\omega)) < 1 \qquad \forall P \in \Pi \qquad (15.5-6)$$

From this point on the treatment of the problem is identical to that presented in Sec. 11.3.1. Note that only the continuous plant $P(s)$ appears in $E_v(s)$ and therefore all the uncertain $\Delta$'s are continuous transfer functions. Hence the need mentioned in Sec. 15.1.4 for continuous as well as discrete (used for test of robust stability) uncertainty bounds.

## 15.6 IMC Design: Step 1 ($\tilde{Q}$)

### 15.6.1 $H_2^*$-Optimal Control

The plant $P^*$ can be factored into an allpass portion $P_A^*$ and a minimum phase portion $P_M^*$:

$$P^* = P_A^* P_M^* \qquad (15.6-1)$$

Here $P_A^*$ is stable and such that $P_A^*(e^{i\theta})^H P_A^*(e^{i\theta}) = I$. Also $(P_M^*)^{-1}$ is stable. $P_M^*$ has the additional property that both $P_M^*$ and $(P_M^*)^{-1}$ are proper. In the case where $P^*$ is scalar, this factorization can be easily accomplished as described by (8.1–2). In the general multivariable case, this "inner-outer factorization" can be accomplished by using the bilinear transformation $z = (1+s)/(1-s)$, to reduce

the problem to the one for the $s$-domain, which was discussed in Sec. 12.6.4. The steps involved in this procedure are explained in Sec. 15.6.4.

*Objective O1: Specific Input*

Let $v_0(z)$ be the scalar allpass with the property $v_0(1) = 1$, which includes the *common* zeros outside the UC and the *common* delays of the elements of $v^*(z)$. Write

$$v^*(z) = v_0(z)\hat{v}(z) \qquad (15.6-2)$$

where $\hat{v}(z)$ is a vector. Hence $\hat{v}$ is proper with at least one element semi-proper and there is no point $z$ outside the UC where $\hat{v}$ becomes identically zero.

**Theorem 15.6-1.** *Assume that Assns. A1-A4 hold. Any stabilizing $\tilde{Q}$ that solves Obj. O1 satisfies*

$$\tilde{Q}\hat{v} = z(WP_M^*)^{-1}\{z^{-1}W(P_A^*)^{-1}\hat{v}\}_* \qquad (15.6-3)$$

*where the operator $\{\cdot\}_*$ denotes that after a partial fraction expansion of the operand, only the strictly proper terms are retained except those corresponding to poles of $(P_A^*)^{-1}$. Furthermore, for $n \geq 2$ the number of stabilizing controllers that satisfy (15.6–3) is infinite. Guidelines for the construction of such a controller are given in the proof.*

Note that not every $\tilde{Q}$ satisfying (15.6–3) is necessarily a stabilizing controller. Equation (15.6–3) should be compared to (9.2–4) for SISO systems. If we assume that the disturbance and the plant have the same open-loop poles outside the UC, then the two equations are identical.

*Proof of Theorem 15.6-1.* We shall assume $W = I$. The proof of the weighted case is left as an exercise. Let $V_0$ be a diagonal matrix where each column satisfies Assn. A3 and every element has $\ell_v$ poles at $z = 1$, where $\ell_v$ is the maximum number of such poles in any element of $v$. Assume that there exists $Q_0$, which stabilizes $P^*$ in the sense of Thm. 15.2-2 and also makes $(I - P^*Q_0)V_0$ stable. Its existence will be proven by construction. Substitution of (15.2–3) into (15.3–14) and use of the fact that pre- or post-multiplication of a function with an allpass does not change its $L_2$-norm, yields:

$$\Phi(v^*) = \|z^{-1}(P_A^*)^{-1}(I - P^*Q_0)\hat{v} - z^{-1}P_M^*Q_1\hat{v}\|_2^2$$

$$\triangleq \|f_1 - f_2Q_1\hat{v}\|_2^2 \qquad (15.6-4)$$

The term $f_1$ has no poles at $z = 1$ because $(I - P^*Q_0)V_0$ has no such poles. Any rational function $f_1(z)$ with no poles on the UC, can be uniquely decomposed

into a strictly proper, stable part $\{f_1\}_+$ in $H_2^*$ and a strictly unstable part $\{f_1\}_-$ in $(H_2^*)^\perp$:

$$f_1 = \{f_1\}_+ + \{f_1\}_- \qquad (15.6-5)$$

Note that according to the definition of $H_2^*, (H_2^*)^\perp$, any improper terms as well as the constant term in a partial fraction expansion of $f_1$, belong in $\{f_1\}_-$. Next we want to show that $f_2Q_1\hat{v}$ has to be stable. The fact that $(I - P^*Q_0)V_0$ is stable implies that $(I - P^*Q_0)\hat{v}$ is stable. We require that $(I - P^*Q)v$ has no poles outside the UC and therefore that $(I - P^*Q)\hat{v} = (I - P^*Q_0)\hat{v} - P^*Q_1\hat{v}$ have no poles outside the UC. But since $(I - P^*Q_0)\hat{v}$ is stable, this requirement reduces to $P^*Q_1\hat{v}$ having no poles outside the UC. Also in order for $\Phi(v^*)$ to be finite, $Q_1$ must be such that $(I - P^*Q)\hat{v}$ has no poles on the UC. But since $(I - P^*Q_0)\hat{v}$ is stable, this is equivalent to $P^*Q_1\hat{v}$ having no poles on the UC. Hence the optimal $Q_1$ must be such that $P^*Q_1\hat{v}$ is stable. Then the only possible unstable poles of $f_2Q_1\hat{v} = z^{-1}(P_A^*)^{-1}P^*Q_1\hat{v}$ are the poles of $(P_A^*)^{-1}$. But Assns. A1, A2 imply that the poles of $(P_A^*)^{-1}$ are not among those of $f_2Q_1\hat{v}$ and therefore $f_2Q_1\hat{v}$ has to be stable. To proceed we will assume that $Q_1$ has this property. We will verify later that the solution indeed has this property.

Hence we can write

$$\Phi(v^*) = \|\{f_1\}_-\|_2^2 + \|\{f_1\}_+ - f_2Q_1\hat{v}\|_2^2 \qquad (15.6-6)$$

The first term on the RHS of (15.6–6) does not depend on $Q_1$. Hence for solving O1 we only have to look at the second term. The obvious solution is

$$Q_1\hat{v} = f_2^{-1}\{f_1\}_+ \qquad (15.6-7)$$

Clearly such a $Q_1$ produces a stable $f_2Q_1\hat{v}$ as was assumed. It should now be proved that $Q_1$'s that satisfy the internal stability requirements exist among those described by (15.6–7), so that the obvious solution is a true solution. For $n = 1$, (15.6–7) yields a unique $Q_1$, which can be shown to satisfy the requirements by following the arguments in the proof of Thm. 15.6-2. For $n \geq 2$ write

$$\hat{v} \triangleq (\,\hat{v}_1 \quad \hat{v}_2 \quad \ldots \quad \hat{v}_n\,)^T \qquad (15.6-8)$$

$$\hat{V}_2 \triangleq (\,\hat{v}_2 \quad \ldots \quad \hat{v}_n\,)^T \qquad (15.6-9)$$

$$Q_1 \triangleq (\,q_1 \quad q_2\,) \qquad (15.6-10)$$

where without loss of generality the first element of $v^*$, and thus $\hat{v}_1$, is assumed to be nonzero. Also $q_1$ is $n \times 1$ and $q_2$ is $n \times (n-1)$. Then from (15.6–7) it follows that

$$Q_1 = ( \hat{v}_1^{-1}(f_2^{-1}\{f_1\}_+ - q_2\hat{V}_2) \quad q_2 ) \qquad (15.6-11)$$

We now need to show that a proper, stable $q_2$ exists such that $Q_1$ is proper, stable and produces a stable $P^*Q_1P^*$. Select a $q_2$ of the form:

$$q_2(z) = \hat{q}_2(z)(1-z^{-1})^{3l_v}\prod_{i=1}^{k}(1-\pi_i z^{-1})^3 \qquad (15.6-12)$$

where $\hat{q}_2$ is proper and stable and $\{\pi_1, \ldots, \pi_k\}$ are the poles of $P^*$ outside the UC. Then from (15.6–11) it follows that in order for $P^*Q_1P^*$ to be stable it is sufficient that $P^*\hat{v}_1^{-1}f_2^{-1}\{f_1\}_+\{P^*\}_{1^{st}row}$ has no poles on or outside the UC. But $P^*f_2^{-1} = zP_A^*$ is stable and the only possible poles of $\hat{v}_1^{-1}\{P^*\}_{1^{st}row}$ on or outside the UC are poles of $\hat{v}_1^{-1}$ outside the UC, because of Assns. A3 and A4. These are also the only possible unstable poles of $Q_1$. Let $\alpha$ be such a pole (zero of $\hat{v}_1$). Then for stability we need to find $\hat{q}_2$ such that

$$\hat{q}_2(\alpha)\hat{V}_2(\alpha) = (1-\alpha^{-1})^{-3l_v}\prod_{i=1}^{k}(1-\pi_i\alpha^{-1})^{-3}f_2^{-1}(\alpha)\{f_1\}_+\Big|_{z=\alpha} \qquad (15.6-13)$$

The above equation always has a solution because the vector $\hat{V}_2(\alpha)$ is not identically zero since any common zeros in $v^*$ outside the UC were factored out in $v_0$.

We now need to examine the properness of $Q_1$. Since $(P_M^*)^{-1}$ is proper and $\{f_1\}_+$ is strictly proper, $f_2^{-1}\{f_1\}_+$ is proper. Then if $\hat{v}_1^{-1}$ is improper ($\hat{v}_1$ strictly proper) there exists at least one element in $\hat{V}_2$ that is semi-proper. Hence by solving a system of linear equations we can always select a $\hat{q}_2(z)$ such that of the first impulse response coefficients of $f_2^{-1}\{f_1\}_+ - q_2\hat{V}_2$, as many are zero as needed to make the first element of the matrix in (15.6–11) proper.

We shall now proceed to obtain an expression for $Q\hat{v}$. (15.2–3) and (15.6–11) yield

$$Q\hat{v} = z(P_M^*)^{-1}\left[z^{-1}(P_A^*)^{-1}P^*Q_0\hat{v} - \{z^{-1}(P_A^*)^{-1}P^*Q_0\hat{v}\}_+ + \{z^{-1}(P_A^*)^{-1}\hat{v}\}_+\right]$$

$$= z(P_M^*)^{-1}\left[\{z^{-1}(P_A^*)^{-1}P^*Q_0\hat{v}\}_{0-} + \{z^{-1}(P_A^*)^{-1}\hat{v}\}_+\right] \qquad (15.6-14)$$

where $\{\cdot\}_{0-}$ indicates that in the partial fraction expansion all poles on or outside the UC are retained. For (15.6–14), these poles are the poles of $\hat{v}$ on or outside

the UC; $(P_A^*)^{-1}P^*Q_0 = P_M^*Q_0$ is strictly stable and proper because of Assn. A1 and the fact that $Q_0$ is a stabilizing controller. The fact that $(I - P^*Q_0)V_0$ has no poles at $z = 1$ imply that $(I - P^*Q_0)$ and its derivatives up to and including the $(\ell_v - 1)^{th}$ are equal to zero at $z = 1$. Also, the fact that $(I - P^*Q_0)V_0$ is stable and that the columns of this diagonal $V_0$ satisfy Assn. A3, imply that $(I - P^*Q_0) = 0$ at $1, \pi_1, \ldots, \pi_k$. Thus (15.6-14) simplifies to (15.6–3).

We now need to establish that a stabilizing controller $Q_0$ exists with the property that $(I - P^*Q_0)V_0$ is stable. The selection of a $V_0$ with the properties mentioned at the beginning of this section and its use instead of $V$ in (15.6–16) yields such a controller. □

*Objectives O2 and O3: Set of $v^*$'s.*

Factor $V$ similarly to $P^*$ (see Sec. 15.6.4):

$$V = V_M V_A \qquad (15.6-15)$$

**Theorem 15.6-2.** *Assume that Assns. A1-A5 hold. The controller*

$$\tilde{Q} = z(WP_M^*)^{-1}\{z^{-1}W(P_A^*)^{-1}V_M\}_*V_M^{-1} \qquad (15.6-16)$$

*is the unique solution to O3. Here the operator $\{\cdot\}_*$ denotes that after a partial fraction expansion of the operand, only the strictly proper terms are retained except those corresponding to poles of $(P_A^*)^{-1}$.*

*Proof.* Again we assume $W = I$ and leave the weighted case as an exercise. From (15.3–13), (15.3–14), and (15.3–16) it follows that

$$\Phi(v^1) + \Phi(v^2) + \ldots + \Phi(v^n) = \|(I - P\tilde{Q})V\|_2^2 \triangleq \Phi(V) \qquad (15.6-17)$$

The minimization of $\Phi(V)$ follows the steps in the proof of Thm. 15.6-1 up to (15.6–7), with $V_M$ used instead of $\hat{v}$. In this case $\ell_v$ is the maximum number of poles at $z = 1$ in any element of $V$. From the equivalent to (15.6–7) we obtain

$$Q_1 = f_2^{-1}\{f_1\}_+V_M^{-1} \qquad (15.6-18)$$

We now have to establish that $Q_1$ is stable, proper and produces a stable $P^*Q_1P^*$. In $P^*Q_1P^*$ the unstable poles of the $P^*$ on the left cancel with those of $(P_M^*)^{-1}$ in $f_2^{-1}$. As for the $P^*$ on the right, cancellation follows from Assn. A5. Then in the same way that (15.6–3) follows from (15.6–14), (15.6–16) follows from (15.6–18). □

A more meaningful objective would be to solve Obj. O2. However a $\tilde{Q}$ that solves Obj. O2 will also solve Obj. O3. Then from Thm. 15.6-2 it follows that

if a solution to O2 exists, it is given by (15.6–16). Factor each of the $v^i$ in the same way as in (15.6–2):

$$v^i(z) = v_0^i(z)\hat{v}^i(z) \qquad (15.6-19)$$

Define

$$\hat{V} \triangleq (\hat{v}^1 \quad \hat{v}^2 \quad \dots \quad \hat{v}^n) \qquad (15.6-20)$$

**Theorem 15.6-3.** *Assume that Assns. A1-A5 hold.*

*(i) If $\hat{V}(z)$ is non-minimum phase (i.e., $\hat{V}^{-1}$ is unstable or improper), then there exists no solution to Obj. O2.*

*(ii) If $\hat{V}(z)$ is minimum phase, then use of $\hat{V}$ instead of $V_M$ in (15.6–16) yields exactly the same $\tilde{Q}$, which also solves Obj. O2. In addition $\tilde{Q}$ minimizes $\Phi(v^*)$ for any $v^*(z)$ that is a linear combination of $v^i$'s that have the same $v_0^i$'s.*

*Proof.* ($W = I$). A stabilizing controller that solves Obj. O2 has to solve Obj. O1 for all $v^i$, $i = 1, \dots, n$. Satisfying (15.6–3) for every $v^i$ is equivalent to

$$\tilde{Q} = z(P_M^*)^{-1}\{z^{-1}(P_A^*)^{-1}\hat{V}\}_*\hat{V}^{-1} \qquad (15.6-21)$$

Hence the above $\tilde{Q}$ is the only potential solution for Obj. O2. However, it is not necessarily a stabilizing controller since not only stabilizing $\tilde{Q}$'s satisfy (15.6–3) for some $v^*$. Indeed, if $\hat{V}$ is non-minimum phase, $\hat{V}^{-1}$ is unstable and/or improper and this results in an unstable and/or improper $\tilde{Q}$, which is therefore unacceptable. Hence in such a case, there exists no solution for Obj. O2, which completes the proof of part (i) of the theorem.

In the case where $\hat{V}^{-1}$ is stable and proper ($\hat{V}$ minimum phase), the controller given by (15.6–21) is stable and proper and therefore it is the same as the one given by (15.6–16). This fact can be explained as follows. We have

$$V = \hat{V}V_0 \qquad (15.6-22)$$

where

$$V_0 = \text{diag}\{v_0^1, v_0^2, \dots, v_0^n\} \qquad (15.6-23)$$

Since $\hat{V}^{-1}$ is stable and proper, (15.6–22) represents a factorization of V similar to that in (15.6–15). From spectral factorization theory it follows that

$$\hat{V}(z) = V_M(z)A \qquad (15.6-24)$$

where $A$ is a constant matrix such that $AA^H = I$. Then (15.6–16) is not altered when $\hat{V}$ is used instead of $V_M$ because $A$ cancels.

Let us now assume without loss of generality that the first $j$ $v^i$'s have the same $v_0^i$'s. Consider a $v^*$ that is a linear combination of $v^1, \ldots, v^j$:

$$v^*(z) = \alpha_1 v^1(z) + \ldots + \alpha_j v^j(z) \qquad (15.6-25)$$

Then it follows that

$$v_0(z) = v_0^1(z) = \ldots = v_0^j(z) \qquad (15.6-26)$$

$$\hat{v}(z) = \alpha_1 \hat{v}^1(z) + \ldots + \alpha_j \hat{v}^j(z) \qquad (15.6-27)$$

One can easily check that a $\tilde{Q}$ that satisfies (15.6–3) for $\hat{v}^1, \ldots, \hat{v}^j$, will also satisfy (15.6–3) for the $\hat{v}$ given by (15.6–27) because of the property

$$\{\alpha_1 f_1(z) + \ldots + \alpha_j f_j(z)\}_* = \alpha_1\{f_1(z)\}_* + \ldots + \alpha_j\{f_j(z)\}_* \qquad (15.6-28)$$

But then from Thm. 15.6-1 it follows that if a stabilizing controller $\tilde{Q}$ satisfies (15.6–3) for $\hat{v}$, then it minimizes the $L_2$ error $\Phi(v^*)$. □

The following corollary to Thm. 15.6-3 holds for a specific choice of $V$.

**Corollary 15.6-1.** *Let*

$$V = \mathrm{diag}\{v_1, v_2, \ldots, v_n\} \qquad (15.6-29)$$

*where $v_1(z), \ldots, v_n(z)$ are scalars. Then use of $\hat{V}$ instead of $V_M$ in (15.6–16) yields exactly the same $\tilde{Q}$, which minimizes $\Phi(v^*)$ for the following n vectors:*

$$v^* = \begin{pmatrix} v_1 \\ 0 \\ \vdots \\ 0 \end{pmatrix}, \begin{pmatrix} 0 \\ v_2 \\ \vdots \\ 0 \end{pmatrix}, \ldots, \begin{pmatrix} 0 \\ 0 \\ \vdots \\ v_n \end{pmatrix} \qquad (15.6-30)$$

*and their multiples, as well as for the linear combinations of those directions that correspond to $v_i$'s with the same zeros outside the UC with the same degree and the same time delays.*

**Example 15.6-1 (Minimum phase $P$).** $P^*(z)$ cannot be truly MP for a physical system. Even if the Laplace transfer matrix representing the continuous

plant is MP but strictly proper, the discretized plant $P^*(z)$ will still have a delay of one unit because of sampling. Hence $P_A^* = z^{-1}I$, $P_M^* = zP^*$ and (15.6-16) yields for $W$ = constant

$$\tilde{Q} = (P^*)^{-1}(I - KV_M^{-1}) \qquad (15.6-31)$$

where $K$ is the constant term in a partial fraction expansion of $V_M$. This is equal to the first non-zero matrix in the impulse response description of $V(z)$, which can be obtained by long division. □

### 15.6.2 Setpoint Prediction

In the case of setpoint tracking, future values of $r^*$ are often known and supplied to the computer ahead of time. If at time $t$ the setpoint value that is provided to the control algorithm as $\mathcal{Z}^{-1}\{r^*(z)\}$ is the one we wish the plant output to reach at time $t + NT$, then the objective function has to be modified to:

$$\Phi_N(r^*) = \|W(z^{-N}I - P^*\tilde{Q})r^*\|_2^2 \qquad (15.6-32)$$

If the above objective function is used for Objs. O1, O2, O3, then the resulting expressions for the $H_2^*$-optimal controller are the same as in Thms. 15.6-1, 15.6-2, and 15.6-3, but with the term $z^{-N-1}$ instead of $z^{-1}$ inside $\{\cdot\}_*$. All the steps in the proofs remain the same when (15.6–32) is used rather than (15.3–14).

### 15.6.3 Intersample Rippling

The $H_2^*$-optimal controller minimizes the sum of squared errors and completely disregards the plant's output behavior between the sample points. Therefore the performance of the $H_2^*$-optimal controller may be excellent at the sample points but may suffer from severe intersample rippling. This problem was demonstrated in Sec. 7.5.3. A modification was introduced in Secs. 8.1.2 and 9.2.2 to substitute poles in $\tilde{q}$ close to (-1,0) with poles at $z = 0$. The new $\tilde{q}$ was shown to be free of the problem of intersample rippling and to combine desirable deadbeat type characteristics with those of the $H_2^*$-optimal controller. This section extends the modification to MIMO systems and general open-loop stable and unstable plants. It should be pointed out that this modification is sufficient only if there are no open-loop oscillatory poles in the continuous plant transfer function, which have become unobservable after sampling.

Let $\tilde{Q}_H(z)$ be the $H_2^*$-optimal $\tilde{Q}$ obtained according to the previous sections. Also let $\delta(z)$ be the least common denominator of the elements of $P^*(z)$, and $\kappa_i$, $i = 1, \ldots, \rho$ be the roots of $\delta(z)$ close to (-1,0) (or in general with negative real

part). Define

$$\tilde{q}_-(z) = z^{-\rho} \prod_{j=1}^{\rho} \frac{z - \kappa_j}{1 - \kappa_j} \qquad (15.6-33)$$

Then $\tilde{Q}_H$ is modified as follows:

$$\tilde{Q}(z) = \tilde{Q}_H(z)\tilde{q}_-(z)B(z) \qquad (15.6-34)$$

where the scalar $B(z)$ is selected so that the matrix $S_2$ (15.2–2) and $(I - P^*\tilde{Q})V$ remain stable. Let $\pi_i, i = 1, \ldots, \xi$ be the unstable roots (including $\pi_1 = 1$) of the least common denominator of $P^*(z), V(z)$. Let the multiplicity of each of them be $m_i$. Note that the poles outside the UC have multiplicity one, according to Assns. A1 and A3. Remember also that according to Assns. A3 and A4, $V$ has at least as many poles at $z = 1$ as $P^*$ and that each pole of $V$ outside the UC is also a pole of $P^*$. Then, since $\tilde{Q}_H$ makes $S_2$ and $(I - P^*\tilde{Q}_H)V$ stable, it follows that the requirements on $B(z)$ are:

$$\frac{d^k}{dz^k}(1 - \tilde{q}_-(z)B(z))\Big|_{z=\pi_i} = 0, \qquad k = 0, \ldots, m_i - 1; \quad i = 1, \ldots, \xi \qquad (15.6-35)$$

We can write

$$B(z) = \sum_{j=0}^{M-1} b_j z^{-j} \qquad (15.6-36)$$

where

$$M = \sum_{i=0}^{\xi} m_i \qquad (15.6-37)$$

and then compute the coefficients $b_j, j = 0, \ldots, M-1$ from (15.6–35). Note that since none of the $\pi_i$'s is 0 or $\infty$, (15.6–35) is equivalent to

$$\frac{d^k}{d\lambda^k}(1 - \tilde{q}_-(\lambda^{-1})B(\lambda^{-1}))\Big|_{\lambda=\pi_i^{-1}} = 0, \qquad k = 0, \ldots, m_i - 1; \quad i = 1, \ldots, \xi \qquad (15.6-38)$$

Both $\tilde{q}_-(\lambda^{-1})$ and $B(\lambda^{-1})$ are polynomials in $\lambda$ and therefore their derivatives with respect to $\lambda$ can be computed easily. Then (15.6–38) yields a system of $M$ linear equations with $M$ unknowns $(b_0, b_1, \ldots, b_{M-1})$. The resulting controller $\tilde{Q}$ combines the desirable properties of the $H_2^*$-optimal controller and deadbeat type controllers.

**Example 15.6-2.** This example is presented to demonstrate the problem of intersample rippling in the $H_2^*$-optimal controller and the modification discussed above. Consider the continuous system

$$P(s) = \begin{pmatrix} \frac{0.50}{s+1} & \frac{1.42}{6s+1} \\ \frac{1.00}{2s+1} & \frac{1.00}{4s+1} \end{pmatrix} \qquad (15.6-39)$$

The discretized system (zero order hold included) for a sampling time of $T = 1$, is

$$P^*(z) = \begin{pmatrix} \frac{0.316}{z-0.368} & \frac{0.218}{z-0.846} \\ \frac{0.393}{z-0.607} & \frac{0.221}{z-0.779} \end{pmatrix} \qquad (15.6-40)$$

Computation of the roots of $\det P(z) = 0$ shows that the system in (15.6–40) has two finite zeros, at $a_1 = -0.95$ and $a_2 = 0.75$. The first zero is close to (-1,0) and is expected to cause intersample rippling when the $H_2$-optimal controller is used.

We find from (15.6-40) that $P_A^* = z^{-1}I$, $P_M^* = zP$. We shall consider step setpoint changes as external inputs – i.e.,

$$V(z) = \frac{z}{z-1}I \qquad (15.6-41)$$

Then (15.6-16) yields

$$\tilde{Q}_H(z) = z^{-1}P^{-1} \qquad (15.6-42)$$

Figure 15.6-1A shows the time response of this control system for a unit step change in the setpoint of output 1:

$$v^*(z) = r^*(z) = \begin{pmatrix} z/(z-1) \\ 0 \end{pmatrix} \qquad (15.6-43)$$

The prediction of intersample rippling is verified. Note that at the sample points the outputs are indeed exactly at the setpoints yielding the minimum sum of squared errors.

The IMC controller is now obtained from (15.6–34) with $B(z) = 1$ and

$$\tilde{q}_-(z) = \frac{z+0.95}{1.95z} \qquad (15.6-44)$$

The response for this control system is shown in Fig. 15.6-1B. Clearly the rippling problem has disappeared. Note the inverse responses caused by the RHP zero of the continuous system $P(s)$. □

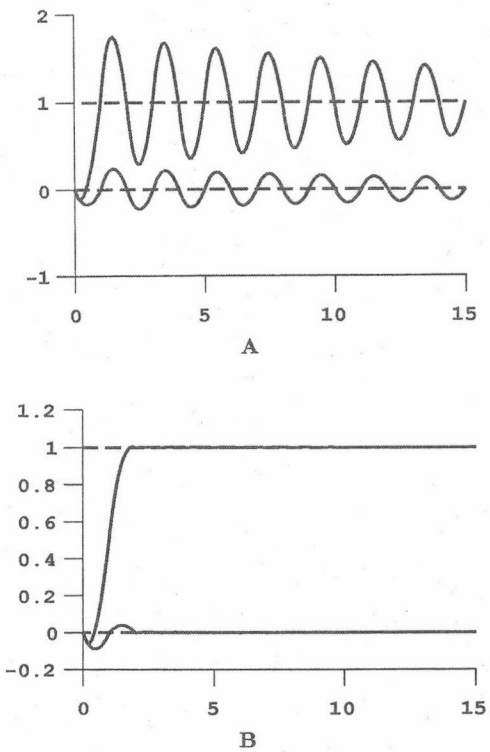


*Figure 15.6-1.* Response to unit setpoint change $r = (1,0)^T$. A: $H_2^*$-optimal controller, B: IMC.

### 15.6.4 Inner-Outer Factorization

As mentioned in Sec. 15.6.1, the factorization (15.6–1) is accomplished by employing the bilinear transformation

$$z = \frac{1+s}{1-s} \qquad (15.6-45)$$

to reduce the problem into the one discussed in detail in Sec. 12.6.4. The theorems below provide the formulas for the transformation of state space descriptions implied by (15.6–45) or its inverse

$$s = \frac{-1+z}{1+z} \qquad (15.6-46)$$

The following lemma is used in the proofs of the theorems.

**Lemma 15.6-1.** *Let* $G(x) = C(xI - A)^{-1}B + xD$. *Then*

$$xG(x) = C(xI - A)^{-1}AB + CB + xD \qquad (15.6-47)$$

*Proof.* We have

$$\begin{aligned} xG(x) &= C(xI - A)^{-1}(A + xI - A)B + xD \\ &= C(xI - A)^{-1}AB + CB + xD \end{aligned}$$

□

**Theorem 15.6-4.** *Let $G^*(z) = C(zI - \Phi)^{-1}\Gamma + D$ have no poles at $z = -1$. Then*

$$\hat{G}(s) \triangleq G^*\left(\frac{1+s}{1-s}\right) = \hat{C}(sI - \hat{A})^{-1}\hat{B} + \hat{D} \qquad (15.6-48)$$

*where*

$$\hat{A} = (\Phi + I)^{-1}(\Phi - I) \qquad (15.6-49)$$

$$\hat{B} = 2(\Phi + I)^{-2}\Gamma \qquad (15.6-50)$$

$$\hat{C} = C \qquad (15.6-51)$$

$$\hat{D} = D - C(\Phi + I)^{-1}\Gamma \qquad (15.6-52)$$

*Proof.* Since $P^*(z)$ is assumed to have no poles at $z = -1$, $\Phi + I$ is nonsingular. We can then write

$$\hat{G}(s) = C\Big(\frac{1+s}{1-s}I - \Phi\Big)^{-1}\Gamma + D$$

$$= (1-s)C(s(\Phi + I) + I - \Phi)^{-1}\Gamma + D$$

$$= (1-s)C(sI - (\Phi + I)^{-1}(\Phi - I))^{-1}(\Phi + I)^{-1}\Gamma + D \qquad (15.6-53)$$

Use of Lem. 15.6-1 in (15.6-53) yields

$$\hat{G}(s) = C(sI - (\Phi + I)^{-1}(\Phi - I))^{-1}(\Phi + I)^{-1}\Gamma$$

$$- \left[C(sI - (\Phi + I)^{-1}(\Phi - I))^{-1}(\Phi + I)^{-1}(\Phi - I)(\Phi + I)^{-1}\Gamma + C(\Phi + I)^{-1}\Gamma\right] + D$$

$$= C(sI-(\Phi+I)^{-1}(\Phi-I))^{-1}(I-(\Phi+I)^{-1}(\Phi-I))(\Phi+I)^{-1}\Gamma+D-C(\Phi+I)^{-1}\Gamma$$

$$= C(sI-(\Phi+I)^{-1}(\Phi-I))^{-1}2(\Phi+I)^{-2}\Gamma+D-C(\Phi+I)^{-1}\Gamma$$

□

**Theorem 15.6-5.** *Let $\hat{G}(s)=\hat{C}(sI-\hat{A})^{-1}\hat{B}+\hat{D}$ have no poles at $s=1$. Then*

$$G^*(z) \triangleq \hat{G}\Big(\frac{-1+z}{1+z}\Big) = C(zI-\Phi)^{-1}\Gamma+D \qquad (15.6-54)$$

*where*

$$\Phi = (I-\hat{A})^{-1}(I+\hat{A}) \qquad (15.6-55)$$

$$\Gamma = 2(I-\hat{A})^{-2}\hat{B} \qquad (15.6-56)$$

$$C = \hat{C} \qquad (15.6-57)$$

$$D = \hat{D}+\hat{C}(I-\hat{A})^{-1}\hat{B} \qquad (15.6-58)$$

*Proof.* $I-\hat{A}$ is nonsingular because $\hat{G}(s)$ is assumed to have no poles at $s=1$. We have

$$G^*(z) = \hat{C}(\frac{-1+z}{1+z}I-\hat{A})^{-1}\hat{B}+\hat{D}$$
$$= (1+z)\hat{C}(z(I-\hat{A})-(I+\hat{A}))^{-1}\hat{B}+\hat{D}$$

$$= (1+z)\hat{C}(zI-(I-\hat{A})^{-1}(I+\hat{A}))^{-1}(I-\hat{A})^{-1}\hat{B}+\hat{D} \qquad (15.6-59)$$

Application of Lem. 15.6-1 to (15.6–59) yields

$$G^*(z) = \hat{C}(zI-(I-\hat{A})^{-1}(I+\hat{A}))^{-1}(I-\hat{A})^{-1}\hat{B}$$

$$+\Big[\hat{C}(zI-(I-\hat{A})^{-1}(I+\hat{A}))^{-1}(I-\hat{A})^{-1}(I+\hat{A})(I-\hat{A})^{-1}\hat{B}+\hat{C}(I-\hat{A})^{-1}\hat{B}\Big]+\hat{D}$$

$$= \hat{C}(zI-(I-\hat{A})^{-1}(I+\hat{A}))^{-1}(I+(I-\hat{A})^{-1}(I+\hat{A}))\hat{B}+\hat{D}+\hat{C}(I-\hat{A})^{-1}\hat{B}$$

$$= \hat{C}(zI - (I - \hat{A})^{-1}(I + \hat{A}))^{-1}2(I - \hat{A})^{-2}\hat{B} + \hat{D} + \hat{C}(I - \hat{A})^{-1}\hat{B}$$

□

The factorization

$$P^*(z) = P_A^*(z)P_M^*(z) \qquad (15.6-1)$$

involves the following steps:

*Step 1:* Use the variable transformation (15.6–45) on $P^*(z)$ to obtain $\hat{P}(s)$. Note that the assumption of Thm. 15.6-4 that $P^*(z)$ has no poles at $z = -1$ holds for the $P^*$'s under consideration in this chapter because of Assn. A2.

*Step 2:* Apply Thm. 12.6-4 on $\hat{P}(s)$ to obtain the factorization

$$\hat{P}(s) = \hat{P}_A(s)\hat{P}_M(s) \qquad (15.6-60)$$

Note that for a strictly proper system $D = 0$ and therefore from (15.6–52) we have $\hat{D} = -C(\Phi + I)^{-1}\Gamma = P^*(-1)$. According to Assn. A2, $P^*(z)$ has no zeros on the UC and therefore $P^*(-1)$ has full rank. Hence, the assumption of no zeros on the imaginary axis including infinity in Thm. 12.6-4, holds for $\hat{P}(s)$.

*Step 3:* Use the variable transformation (15.6–46) on $\hat{P}_A(s)$ and $\hat{P}_M(s)$ to obtain $P_A^*(z)$ and $P_M^*(z)$ correspondingly. Note that $\hat{P}_A(s)$ satisfies the assumption of no poles at $s = 1$, since by construction all its poles are in the LHP. Also, $\hat{P}_M(s)$ has the poles of $\hat{P}(s)$, which do not include a pole at $s = 1$, since $P^*(z)$ has no poles at $z = \infty$.

The result of the above steps is a stable, all-pass $P_A^*$ and a minimum phase $P_M^*$. Both $P_A^*$ and $P_M^*$ are proper because $\hat{P}_A$ and $\hat{P}_M$ have no poles at $s = 1$. Also note that since $\hat{P}_M(s)$ is minimum phase, it does not have a zero at $s = 1$ and therefore $P_M^*(z)$ has no zero at $z = \infty$, which means that $(P_M^*(z))^{-1}$ is proper.

To obtain the factorization

$$V = V_M V_A \qquad (15.6-15)$$

one should follow the same steps as above with the difference that in Step 2, Thm. 12.6-4 is applied on $\hat{V}(s)^T$ as described in Sec. 12.6-4.

## 15.7 IMC Design: Step 2 ($F$)

The controller $\tilde{Q}$ obtained in Step 1 of the IMC design procedure is detuned in Step 2 to satisfy the robustness conditions by augmenting it with the IMC filter $F(z)$:

$$Q = Q(\tilde{Q}, F) \qquad (15.7-1)$$

First we will postulate reasonable filter structures. Then we will define appropriate minimization problems to be solved over the filter parameters and discuss the computational issues involved.

### 15.7.1 Filter Structure

Some structure has to be assumed for $F$, which can be as general as the designer wishes. However, in order to keep the number of variables in the optimization problems small, a rather simple structure like a diagonal $F$ with first- or second-order terms would be recommended. In most cases this is not restrictive because the controller $\tilde{Q}$ that was designed in the first step of the IMC procedure is in general a full high-order transfer matrix. More complex filter structures may be necessary in cases of ill-conditioned systems ($\bar{\sigma}(\tilde{P}^*)/\underline{\sigma}(\tilde{P}^*)$ very large). For such systems a two-filter structure was discussed in detail in Sec. 12.7.1. The elements of each of the two filters in that structure can be designed as described below.

The filter $F(z)$ is chosen to be a diagonal rational function that satisfies the following requirements.

a. Internal Stability. $S_1$ in (15.2–1) must be stable.

b. Asymptotic setpoint tracking and/or disturbance rejection. $(I - \tilde{P}^*\tilde{Q}F)v^*$ must be stable.

Write

$$F(z) = \text{diag}\{f_1(z), \ldots, f_n(z)\} \qquad (15.7-2)$$

Then, Assns. A1-A5 and the fact that by construction $\tilde{Q}(z)$ makes $S_1$ and $(I - \tilde{P}^*\tilde{Q})V$ stable, imply that the requirements on an element $f_\ell$ of $F$ are:

$$\frac{d^j}{dz^j}(1 - f_\ell(z))\Big|_{z=\pi_1} = 1, \qquad j = 0, \ldots, m_{1\ell} - 1 \qquad (15.7-3)$$

$$f_\ell(\pi_i) = 1, \qquad i = 2, \ldots, \xi \qquad (15.7-4)$$

where $\pi_1 = 1$ and $m_{1\ell}$ is the highest multiplicity of such a pole in any element of the $\ell^{th}$ row of $V$ and $\pi_i$, $i = 2, \ldots, \xi$ are the poles of $P^*$ outside the UC, each with multiplicity 1, according to Assn. A1.

One can now select the filter elements to be of the form discussed in Sec. 9.3

$$f(z) = \phi(z) f_1(z) \qquad (9.3-3)$$

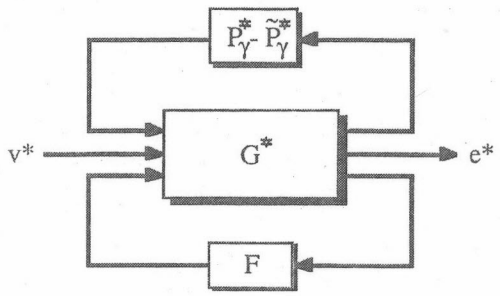


*Figure 15.7-1.* Discrete interconnection structure.

where

$$f_1(z) = \frac{(1-\alpha)z}{z-\alpha} \qquad (8.2-1)$$

$$\phi(z) = \sum_{j=0}^{w} \beta_j z^{-j} \qquad (9.3-4)$$

and the coefficients $\beta_0, \ldots, \beta_w$ are computed so that (15.7–3), (15.7–4) are satisfied for some specified $\alpha$. The parameter $\alpha$ can be used as a tuning parameter.

Note that for $\xi = 1, \pi_1 = 1, m_{1\ell} = 1$, we only need $\phi(z) = 1$. For the general case, (15.7–3) and (15.7–4) a system of $M_\ell$ linear equations with $\beta_0, \ldots \beta_w$ as unknowns where $M_\ell$ is given by

$$M_\ell = m_{1\ell} + \xi \qquad (15.7-5)$$

The procedure for solving these equations is identical to the one described in Sec. 9.3, with $m_{1\ell}$ and $M_\ell$ replacing $m_1$ and $M$. Also, when the two-filter structure of Sec. 12.7.1 is used in the case of ill-conditioned plants, $\hat{m}_1 = \max_\ell m_{1\ell}$ should be used for all $\ell$ in the place of $m_{1\ell}$ in $F_1(z)$. This is required for internal stability and no steady-state offset.

### 15.7.2 Robust Stability Interconnection Structure

Consider the block diagram in Fig. 15.1-2C. The same block manipulations that were used to obtain Fig. 12.7-1A from Fig. 12.1-1B, can be used on Fig. 15.1-2C to obtain Fig. 15.7-1. The only difference is that $P_\gamma^*$ and $\tilde{P}_\gamma^*$ take the place of $P$ and $\tilde{P}$. All the transfer matrices in Fig. 15.7-1 are discrete.

The development described in Sec. 12.7.2 can now be applied to the block structure of Fig. 15.7-1 to put it in the form shown in Figs. 12.7-1B, C. The difference is that the uncertainty block $\Delta$ represents a discrete transfer function. If simple uncertainty descriptions of the form discussed in Sec. 12.7.2 are available for the discrete plant $P_\gamma^*$, then the corresponding formulas carry over to the discrete case, where $\bar{\ell}_A$, $\bar{\ell}_O$, $\bar{\ell}_I$, $W_{e1}$, $W_{e2}$ are now discrete. Therefore only their values up to $\pi/T$ need be considered.

Theorem 15.4-1 provides the robust stability condition. The matrix $M$ in (15.4–1) is $G_{11}^{*F}$ and therefore for robust stability the filter has to be designed such that

$$\mu_\Delta(G_{11}^{*F}(i\omega)) < 1, \qquad 0 \leq \omega \leq \pi/T \tag{15.7-6}$$

The superscript $^*$ is used to indicate that in this case $G^F$ is a discrete transfer matrix.

### 15.7.3 Robust Performance Interconnection Structure

If one only cared about the performance at the sample points, then one could use Fig. 15.7-1 to state the robust performance conditions. However, because of the intersample rippling problem, one has to consider the continuous output of the plant and express the robust performance requirements in terms of the approximate sensitivity functions $E_r(s)$ or $E_d(s)$ given by (15.5–4) and (15.5–5).

One can obtain the appropriate interconnection structures of Fig. 12.7-1 by starting from Fig. 15.1-2B. The use of (15.5–2) in the derivation of (15.5–4) and (15.5–5), is equivalent to approximating the function of the sampling operator by $1/T$ for $0 \leq \omega \leq \pi/T$. This approximation is reasonable for signals with small power for $\omega > \pi/T$. Use of $1/T$ in the place of the sampling switch in Fig. 15.1-2B, allows us to derive the matrix $G$ in the block diagram in Fig. 12.7-1A, which is slightly different from the one given by (12.7–13) for the continuous controller.

For $v = d$, $e = y$, we have

$$G_d = \begin{pmatrix} 0 & 0 & h_0\tilde{Q} \\ I & I & h_0\tilde{P}\tilde{Q} \\ -\frac{\gamma}{T}I & -\frac{\gamma}{T}I & 0 \end{pmatrix} \tag{15.7-7}$$

For $v = -r$, $e = y - r$, with $r(s) = h_0(s)r^*(e^{sT})$:

$$G_r = \begin{pmatrix} 0 & 0 & h_0\tilde{Q} \\ I & I & h_0\tilde{P}\tilde{Q} \\ -\frac{\gamma}{T}I & h_0^{-1}I & 0 \end{pmatrix} \tag{15.7-8}$$

Note that in this case the uncertainty block $\Delta$ represents continuous transfer functions as in Sec. 12.7.2.

### 15.7.4 Robust $H_\infty$ Performance Objective

The next step is to transform (15.5–6) into an equivalent SSV condition. By using the equations in Sec. 12.7.2, but with the appropriate $G_v$ instead of $G$ and with $W_2 = W$, $W_1 = I$, we can obtain the corresponding $G_v^F$. Then (15.5–6) is satisfied if and only if

$$\mu_\Delta(G_v^F(i\omega)) < 1, \qquad 0 \le \omega \le \pi/T \tag{15.7-9}$$

where $\Delta = \text{diag}\{\Delta_u, \Delta_p\}$, with $\Delta$ representing the uncertainty block $\Delta$ of Fig. 12.7-1 and $\Delta_p$ the additional block introduced for performance.

We can now write

$$F \triangleq F(z;\Lambda) \tag{15.7-10}$$

where $\Lambda$ is an array with the adjustable filter parameters. The filter design problem can be formulated as an minimization problem over the elements of $\Lambda$. In the filter structure proposed in Sec. 15.7.1, there is one adjustable parameter $\alpha$ for each element of the diagonal filter, or of each of the two diagonal filters, if two are used. Each one of these real parameters, say $\alpha_j$, has to be inside the UC for $F$ to be stable. The stability constraints can be removed from the minimization problem by setting

$$\alpha_j = e^{-T/\lambda_j^2} \tag{15.7-11}$$

where $\lambda_j$ is an element of $\Lambda$. Then any $\lambda_j$ in $(-\infty, \infty)$ produces an $\alpha_j$ in $[0, 1)$. Note that if the parametrization (15.7–11) is used, then it is $\lambda_j^2$ and not $\lambda_j$ that corresponds to a time constant. If one wishes to use a higher order $f_1(z)$ with more parameters in (8.2–1), one can write the denominator of each element of $F$ as the product of polynomials of degree 2 and one of degree 1 if the order is odd. A polynomial of degree 2 with roots inside the UC can be written as $z^2 - (e^{Tp_1} + e^{Tp_2})z + e^{Tp_1+Tp_2}$, where $p_1$, $p_2$ are the roots of $\lambda_2^2 x^2 + \lambda_1^2 x + 1 = 0$ for some value of $\lambda_1$, $\lambda_2$. In this way, the optimization problem is unconstrained in the optimization variables $\lambda_1$, $\lambda_2$, which can take any value in $(-\infty, \infty)$.

Our goal is to satisfy (15.7–9). The filter parameters can be obtained by solving

*Objective O4:*

$$\min_{\Lambda} \max_{0 \le \omega \le \pi/T} \mu_\Delta(G_v^F) \tag{15.7-12}$$

It should be noted however that the optimal solution for Obj. O4, may still not satisfy (15.7–9). The reason is usually that the performance requirements set by the selection of $W$ in (15.5–6) are too tight be to satisfied in the presence of the

model-plant mismatch. In this case one should choose a less tight $W$ and resolve Obj. O4.

Another important point is that satisfaction of the robust performance condition (15.7–9) does not necessarily imply satisfaction of the robust stability condition (15.7–6), which was the case in the continuous controller design. This is so even if the uncertainty descriptions for the continuous plant [used in (15.7–9)] and the discretized plant [used in (15.7–6)] correspond to exactly the same sets of possible plants. The reason is that (15.7–9) was obtained by using the approximations discussed in detail in Sec. 15.5.1, while there are no approximations involved in the derivation of (15.7–6). Note however, that if the uncertainty descriptions for the continuous and the discrete plant are equivalent in the sense discussed in Sec. 15.1.5, then satisfaction of (15.7–9) is usually sufficient for satisfaction of (15.7–6), although this is not guaranteed. As a result of the above discussed possibility, when a solution to Obj. O4 is found, one should check if (15.7–6) holds. If this does not happen, then one can always substitute the robust stability $\mu$ (15.7–6) in Obj. O4 and proceed with the minimization until (15.7–6) becomes less than one.

The type of problem defined by (15.7–12) is nearly identical to that defined by (12.7–25). The only difference is that the search over $\omega$ is limited to $0 \leq \omega \leq \pi/T$ in (15.7–12). This difference disappears, when only a finite number of frequencies is considered, as described in Obj. O4′ in Sec. 12.7.3. Hence the entire procedure and equations of Sec. 12.7.3 carry over to this case.

## 15.8 Illustration of the Design Procedure

The purpose of this section is to demonstrate the IMC design procedure by applying it to a $2 \times 2$ open-loop unstable system.

### 15.8.1 System Description

Let the continuous system be modeled by

$$\dot{x} = Ax + Bu \qquad (10.1-1)$$

$$y = Cx + Du \qquad (10.1-2)$$

where

$$A = \begin{pmatrix} 2.375 & 0.857 & 1.000 \\ -17.719 & -5.500 & -5.250 \\ -14.766 & -6.750 & -7.375 \end{pmatrix} \qquad (15.8-1)$$

$$B = \begin{pmatrix} 0 & 0 \\ 1 & 0 \\ -1 & 1 \end{pmatrix} \qquad (15.8-2)$$

$$C = \begin{pmatrix} 0 & 0.3 & 1.8 \\ 0 & 0 & -4.0 \end{pmatrix} \qquad (15.8-3)$$

$$D = \begin{pmatrix} 0 & 0 \\ 0 & 0 \end{pmatrix} \qquad (15.8-4)$$

The eigenvalues of $A$, which are the poles of the system (see Def. 10.1-3), are located at -1, -10, +0.5. Hence the open-loop system has an unstable pole of multiplicity 1 at 0.5.

From (10.1–7) we obtain the transfer matrix of the system:

$$\tilde{P}(s) = \begin{pmatrix} \frac{-1.5(s-0.2)}{(s-0.5)(s+1)} & \frac{0.3(6s+7.5)}{(s-0.5)(s+10)} \\ \frac{4s-0.5}{(s-0.5)(s+1)} & \frac{-(4s+8.5)}{(s-0.5)(s+10)} \end{pmatrix} \qquad (15.8-5)$$

Note that the unstable pole ($s = 0.5$) appears in *all* elements of $\tilde{P}(s)$, though it has only multiplicity 1. This is not an artifact of the example but rather the generic case for systems described by equations of the type (10.1–1), (10.1–2).

Let us now compute the zero-order hold discrete equivalent of $\tilde{P}(s)$ for a sampling time of $T = 0.1$. This is a reasonable choice, equal to 1/10 of the dominant stable time constant and 1/20 of the unstable time constant of the system. From (15.1–6) we find $\tilde{P}^*(z)$, which can be written in the form (15.1–15):

$$\tilde{P}^*(z) = C(zI - \Phi)^{-1}\Gamma + D \qquad (15.8-6)$$

where $C$ and $D$ are given by (15.8–3) and (15.8–4) and

$$\Phi = \begin{pmatrix} 1.2757 & 1.1138 & 1.0 \\ -0.15462 & 0.44053 & -0.41687 \\ -0.079536 & -0.44598 & 0.60772 \end{pmatrix} \qquad (15.8-7)$$

$$\Gamma = \begin{pmatrix} 0 & 0 \\ 0.071429 & 0 \\ -0.094864 & 0.071429 \end{pmatrix} \qquad (15.8-8)$$

For the design we need some information on the potential model error. We will assume a diagonal input multiplicative uncertainty

$$P^*(z) = \tilde{P}^*(z)(I + L_I^*(z)) \qquad (15.8-9)$$

where

$$L_I^*(z) = \text{diag}\{\ell_1^*(z), \ell_2^*(z)\} \qquad (15.8-10)$$

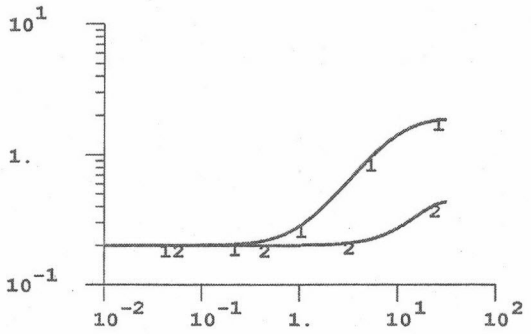


*Figure 15.8-1.* Multiplicative uncertainties $\bar{\ell}_1^*$ and $\bar{\ell}_2^*$.

and $\ell_1^*, \ell_2^*$ are bounded by

$$|\ell_i^*(z)| \leq \bar{\ell}_i^*(z) = \left|0.2\frac{z-p_i}{z-p_i^{10}} \cdot \frac{1-p_i^{10}}{1-p_i}\right| \qquad (15.8-11)$$

with $p_i = e^{-T/\tau_i}$. We will also assume that *all* plants $P^*(z)$ have exactly one unstable pole. The bound (15.8–11) implies that the uncertainty starts to increase around $\omega = 1/\tau_i$ with slope 1 and flattens out after one decade. Also, the low frequency uncertainty can be as much as 20%. The $\tau_i$'s are selected here to correspond to the dominant stable time constants of $\tilde{P}(s)$ associated with the respective inputs, i.e., $\tau_1 = 1$ and $\tau_2 = 0.1$. Bode plots of $\bar{\ell}_1^*, \bar{\ell}_2^*$ are shown in Fig. 15.8-1, for $0 \leq \omega \leq \pi/T$.

### 15.8.2 Design of $\tilde{Q}$

First one has to decide on the type of external input $v$ for which $\tilde{Q}$ will be designed. Here we will consider *step-like* disturbances entering at the plant inputs. The diagonal $V(z)$ is of the form described in Cor. 15.6-1 with

$$v_1(z) = v_2(z) = v^*(z) = \mathcal{Z}\mathcal{L}^{-1}\{v(s)\} \qquad (15.8-12)$$

where $v(s)$ is an appropriate transfer function. Since the $v_i$'s represent the effect of step-like inputs on the plant outputs, $v(s)$ should include both an integrator and a pole at $s = 0.5$. The simplest choice would be $v(s) = s^{-1}(-s+0.5)^{-1}$. However, such an input is "sluggish" and will result in poor robustness (see observation 3 in Sec. 4.1.2). To avoid this problem we select

$$v(s) = \frac{s+0.5}{s(-s+0.5)}$$

The next task is the factorization of $\tilde{P}^*$ into $P_A^*$ and $P_M^*$ (15.6–1). We follow the steps described in Sec. 15.6.4. This procedure yields the matrices $\Phi_A, \Gamma_A, C_A, D_A$ and $\Phi_M, \Gamma_M, C_M, D_M$ that define $P_A^*(z)$ and $P_M^*(z)$ respectively through (15.1–15):

$$\Phi_A = \begin{pmatrix} 1.54714 & 1.50513 & 1.41162 \\ -0.69253 & -0.67372 & -0.63186 \\ -0.098133 & -0.095468 & -0.089537 \end{pmatrix} \qquad (15.8-13)$$

$$\Gamma_A = \begin{pmatrix} -8.27667 & -3.06852 \\ -15.61316 & -4.02293 \\ -3.78625 & -3.05041 \end{pmatrix} \qquad (15.8-14)$$

$$C_A = \begin{pmatrix} -7.0645 \times 10^{-4} & -0.012260 & 0.20435 \\ 0.027830 & 0.13477 & -0.46555 \end{pmatrix} \qquad (15.8-15)$$

$$D_A = \begin{pmatrix} 0 & 0 \\ 0 & 0 \end{pmatrix} \qquad (15.8-16)$$

$$\Phi_M = \begin{pmatrix} 1.27570 & 1.11380 & 1.0 \\ -0.15462 & 0.44053 & -0.41687 \\ -0.079536 & -0.44598 & 0.60772 \end{pmatrix} \qquad (15.8-17)$$

$$\Gamma_M = \begin{pmatrix} 0 & 0 \\ 1 & 0 \\ -1.32810 & 1 \end{pmatrix} \qquad (15.8-18)$$

$$C_M = \begin{pmatrix} -0.017300 & -0.060253 & 0.050708 \\ 0.021810 & 0.12528 & -0.18355 \end{pmatrix} \qquad (15.8-19)$$

$$D_M = \begin{pmatrix} -0.13652 & 0.086180 \\ 0.39111 & -0.30647 \end{pmatrix} \qquad (15.8-20)$$

We also need to factor $V(z)$ according to (15.6–15), but this is trivial since $V(z)$ is diagonal and $v^*(z)$ can be factored as described by (8.1–3).

The final task is to determine $\tilde{Q}(z)$ from (15.6–16). For $W = I$ a state space description (15.1–15) of $\tilde{Q}(z)$ is given by

$$\Phi_Q = \begin{pmatrix} 1.27570 & 1.11380 & 1 & 0 & 0 \\ -0.57541 & -0.50239 & -0.45106 & -2.25465 & -0.80172 \\ 0.013486 & 0.011775 & 0.010572 & 0.058490 & 3.2232 \times 10^{-3} \\ 0 & 0 & 0 & 0.94873 & 0 \\ 0 & 0 & 0 & 0 & 0.94873 \end{pmatrix} \qquad (15.8-21)$$

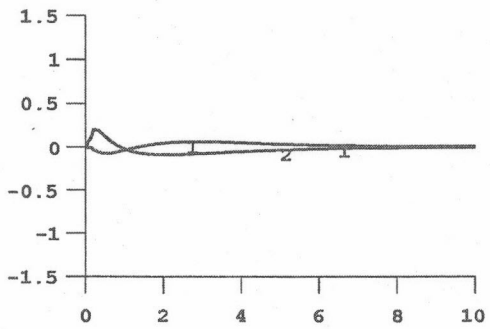


*Figure 15.8-2.* Nominal response to a step change at the plant input. (No filter).

$$\Gamma_Q = \begin{pmatrix} 0 & 0 \\ 81.6566 & 26.2327 \\ -3.09800 & 2.64970 \\ 1 & 0 \\ 0 & 1 \end{pmatrix} \qquad (15.8-22)$$

$$C_Q = \begin{pmatrix} 0.42079 & 0.94292 & 0.034188 & 2.25465 & 0.80172 \\ 0.46584 & 0.79454 & 0.64255 & 2.93590 & 1.06154 \end{pmatrix} \qquad (15.8-23)$$

$$D_Q = \begin{pmatrix} -81.6556 & -26.2327 \\ -105.3488 & -37.4893 \end{pmatrix} \qquad (15.8-24)$$

Figure 15.8-2 shows the response with this controller for the disturbance

$$u'(s) = \begin{pmatrix} s^{-1} \\ s^{-1} \end{pmatrix} \qquad (15.8-25)$$

entering at the plant inputs, when $P = \tilde{P}$. (The same disturbance will be used in all subsequent simulations).

### 15.8.3 Design of $F$

In this section we will design a filter $F(z)$ that guarantees robust stability in the presence of the model-plant mismatch described by (15.8–9). The condition for robust stability is given by (15.7–6). Here $\Delta$ consists of two scalar blocks and

$$G_{11}^{*F} = -\tilde{Q}F\tilde{P}^*\bar{L}_I^* \qquad (15.8-26)$$

where

$$\bar{L}_I^* = \text{diag}\{\bar{\ell}_1^*, \bar{\ell}_2^*\} \qquad (15.8-27)$$

The selection of the filter structure follows Sec. 15.7.1. A simple scalar filter will be used:

$$F(z) = f(z)I \qquad (15.8-28)$$

where $f(z)$ is given by (9.3–3) with $w = 29$. The tuning parameter $\alpha$ in $f_1(z)$ must be in [0,1) and can be parametrized as

$$\alpha = e^{-T/\lambda} \qquad (15.8-29)$$

where $\lambda$ is a positive time constant which becomes the new tuning parameter. We prefer $\lambda$ over $\alpha$ because $\lambda$ has a clear physical meaning and effect as was illustrated in Sec. 9.3.2. Note that the coefficients of $\phi(z)$ are functions of $\lambda$ and are obtained from (9.3–6) and (9.3–9). If one wishes to remove the positivity constraint from the design parameter $\lambda$, then one should use (15.7–11) instead of (15.8–29). In this example however, as in the SISO case, we only have a single design variable to search over, which is a simple optimization problem. Hence (15.8–29) is used here to maintain a clear physical meaning for the optimization variable $\lambda$.

For $F = I$ ($\lambda = \alpha = 0$) we find $\mu(G_{11}^{*F}) = 3.75$, which implies that there exist plants among those described by (15.8–9) for which the closed loop system is unstable. A plot of $\mu$ is shown in Fig. 15.8-3. A search over the parameter $\lambda$ shows that one has to increase $\lambda$ to at least 0.5 to get $\mu = 1.0$ so that robust stability is guaranteed. Further increase of $\lambda$ can reduce $\mu(G_{11}^{*F})$ even further. Plots of $\mu$ for $\lambda = 0.5$ and $\lambda = 1$ can be seen in Fig. 15.8-3.

Note, however, that the lower $\mu$ for $\lambda = 1$ does not necessarily mean that the performance of the system is superior because $\mu(G_{11}^{*F})$ is not the robust performance index. For determining robust performance, one has to select an appropriate performance weight $W$ and compute $\mu(G^F)$ (Sec. 15.7.4). For our particular example, $\tilde{P}(s)$ has an unstable pole at $s = 0.5$ and the uncertainty becomes significant for $\omega > 1$. Therefore there is not much room for performance improvement. The question of robust performance will not be examined any further in this section. The reader is referred to Sec. 12.8 for a detailed example on the design of a filter for robust performance.

Let us now look at some simulations to examine the behavior of the control system when there is model-plant mismatch. The following transfer function was chosen for the "real" continuous plant $P(s)$:

$$P(s) = \tilde{P}(s)(I + L_I(s)) \qquad (15.8-30)$$

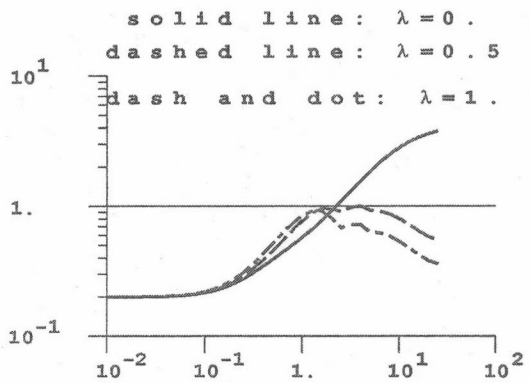


*Figure 15.8-3.* $\mu$ (Robust Stability) for different filter parameters $\lambda$.

where

$$L_I(s) = \begin{pmatrix} -0.2\frac{s+1}{0.1s+1} & 0 \\ 0 & -0.2\frac{0.1s+1}{0.01s+1} \end{pmatrix} \qquad (15.8-31)$$

Note that this $L_I(s)$ does not generate a plant that falls exactly in the class described by (15.8–9, 10, 11), although the steady-state gains and time constants of $L_I(s)$ match those used in (15.8–11) exactly. The reason is that no simple and non-conservative method is available for translating a type of uncertainty description (input multiplicative in this case) from the $s$-domain to exactly the same type in the $z$-domain. As explained in Sec. 15.1.5, such descriptions may be obtained either from first – principles models or via experiments conducted with different sampling rates. For the purposes of this example, (15.8–31) yields a plant sufficiently close to the class described by (15.8–9) to serve our illustration goals.

The responses to the input disturbance (15.8–22) are shown in Fig. 15.8-4 for $\lambda = 0.5$ and in Fig. 15.8-5 for $\lambda = 1$, for both the nominal case ($P = \tilde{P}$) and the case of model-plant mismatch with $P$ given by (15.8–30). Without the IMC filter, the system is unstable for the "real" plant $P$ in (15.8–30) as expected from the large value of $\mu(G_{11}^{*F})$. The nominal response is shown in Fig. 15.8-1. The responses for $\lambda = 1$ are not significantly better than that for $\lambda = 0.5$, although the robust stability $\mu$ is smaller for $\lambda = 1$. This is not surprising because $\mu(G_{11}^{*F})$ is an indicator of stability only.

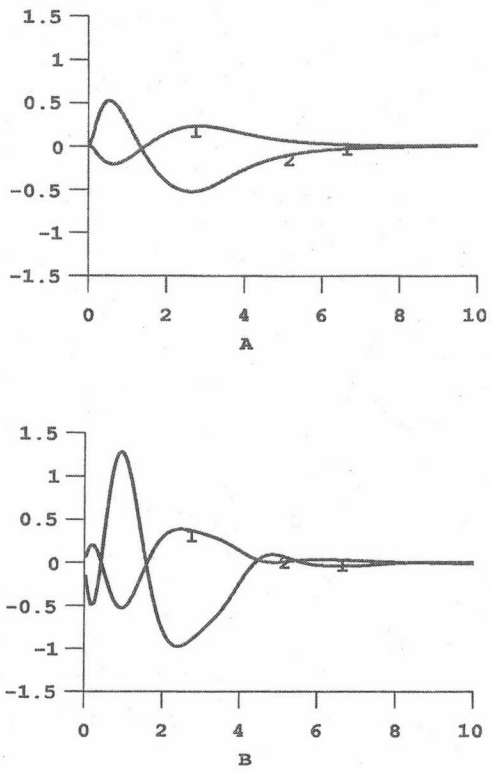


*Figure 15.8-4.* Responses (A) for nominal system and (B) the plant given by (15.8–30) for IMC filter time constant $\lambda = 0.5$.

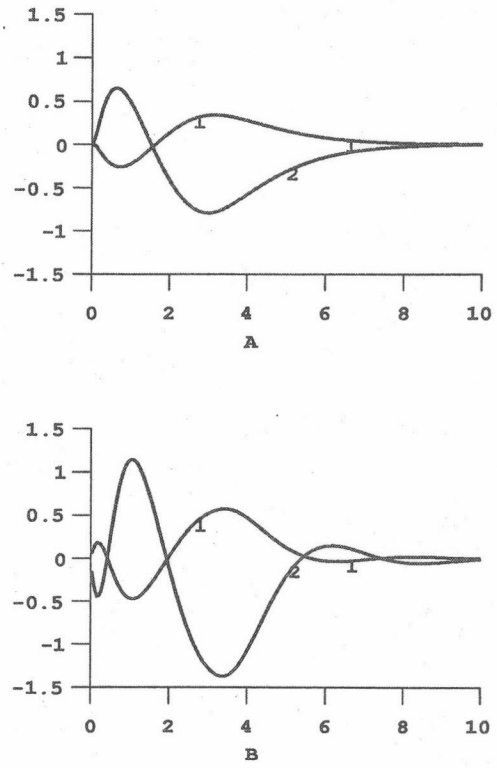


*Figure 15.8-5.* Responses (A) for nominal system and (B) the plant given by (15.8–30) for IMC filter time constant $\lambda = 1.0$.

## 15.9 Summary

For internal stability of the IMC structure, both the plant $P$ and the IMC controller $Q$ have to be stable. For open-loop unstable plants, it is convenient to use the IMC design procedure to design $Q$ and then obtain the classic feedback controller $C$ from (15.1–22) for implementation. Under some mild assumptions about pole-zero cancellations (Sec. 15.2.2), all stabilizing controllers $Q$ for the plant $P^*$ are parametrized by

$$Q(z) = Q_0(z) + Q_1(z) \qquad (15.2-3)$$

where $Q_0$ is an arbitrary proper controller that stabilizes $P^*$ and $Q_1$ is any stable, proper transfer matrix such that $P^*Q_1P^*$ is stable.

*Design Procedure*

*Step 1: Nominal Performance*

First, the stabilizing $H_2^*$-optimal controller $\tilde{Q}_H(z)$ is determined which minimizes the sum of the Sums of Squared Errors that each of the inputs $v^i$ in a set $\mathcal{V} = \{v^i(z) : i = 1, \ldots, n\}$ would cause, when applied to the system separately.

*Objective O3:*

$$\min_{\tilde{Q}}[\Phi(v^1) + \ldots + \Phi(v^n)]$$

where

$$\Phi(v^i) \triangleq \|We^i\|_2^2 = \|W\tilde{E}^*v^i\|_2^2 = \|W(I - P^*\tilde{Q})v^i\|_2^2 \qquad (15.3-14)$$

The unique controller which meets Obj. O3 is given by

$$\tilde{Q}_H = z(P_M^*)^{-1}\{z^{-1}(P_A^*)^{-1}V_M\}_*V_M^{-1} \qquad (15.6-16)$$

where the operator $\{\cdot\}_*$ denotes that after a partial fraction expansion of the operand, only the strictly proper terms are retained, except for those that correspond to poles of $(P_A^*)^{-1}$. The factorization of the plant

$$P^* = P_A^*P_M^* \qquad (15.6-1)$$

into an allpass portion $P_A^*$ and a minimum phase portion portion $P_M^*$ can be accomplished through "inner-outer" factorization (Sec. 15.6.4). The input matrix $V = (\,v^1 \quad v^2 \quad \ldots \quad v^n\,)$ can be factored similarly

$$V = V_MV_A \qquad (15.6-15)$$

In some special cases (Thm. 15.6-3), $\tilde{Q}_H$ is also $H_2^*$-optimal for each of the inputs $v^i$ separately, as well as their linear combinations.

Next, $\tilde{Q}_H$ is modified as described in Sec. 15.6.3 to eliminate the potential problem of intersample rippling:

$$\tilde{Q}(z) = \tilde{Q}_H(z)\tilde{q}_-(z)B(z) \qquad (15.6-33)$$

*Step 2: Robust Stability and Robust Performance*

In this step, the controller $\tilde{Q}$ is augmented by a low-pass filter $F$ such that for the detuned controller $Q = Q(\tilde{Q}, F)$ both the robust stability

$$\mu_\Delta(G_{11}^{*F}(\tilde{P}^*, Q)) < 1, \qquad 0 \le \omega \le \pi/T, \quad \Delta = \Delta_u \qquad (15.7-6)$$

and the robust performance

$$\mu_\Delta(G_v^F(\tilde{P}, Q)) < 1, \qquad 0 \le \omega \le \pi/T, \quad \Delta = \mathrm{diag}\{\Delta_u, \Delta_p\} \qquad (15.7-9)$$

conditions are satisfied. A nonlinear program was formulated (Sec. 15.7-4) to minimize $\mu_\Delta(G^F(\tilde{P}, Q))$ as a function of the filter parameters for a filter with a fixed diagonal structure. For unstable plants the filter has to be identity at the unstable poles of $\tilde{P}^*$. For ill-conditioned plants, two diagonal filters may be necessary to meet the requirement (15.7–9). It should be noted that satisfaction of (15.7–9) does not guarantee satisfaction of (15.7–6), although this is usually so. Hence it should be verified that the optimal solution to (15.7–9) also satisfies (15.7–6).

## 15.10 References

15.1.2. For a discussion on the computation of the matrices $\Phi$ and $\Gamma$ see Åström & Wittenmark (1984).

15.1.3. See the same reference for more details on the Nyquist D-contour for discrete systems.

15.2. For modeling and identification methods for discrete systems see Åström & Wittenmark (1984). Jenkins and Watts (1969) is an excellent reference for identification techniques that result in norm uncertainty bounds for each element or a whole row of the system transfer matrix.

# Part V

# CASE STUDY

# Chapter 16

# LV-CONTROL OF A HIGH-PURITY DISTILLATION COLUMN

In this chapter the high-purity distillation column described in the Appendix will be studied, when reflux (L) and boilup (V) are manipulated to control the top ($y_D$) and bottom ($x_B$) compositions. This column was used as an example on several occasions earlier in this book. The LV-configuration is selected because this choice of manipulated inputs is most common in industrial practice. This does not mean that this is necessarily the best configuration; for example, the $\frac{L}{D}\frac{V}{B}$-configuration may be preferrable.

The distillation column investigated here was chosen to be representative of a large class of moderately high-purity distillation columns. The goal of this chapter is to provide a realistic control design and simulation study for the column. To be realistic at least the issues of uncertainty and nonlinearity must be addressed.

The reader is assumed to be thoroughly familiar with the material in Part III of this book.

## 16.1 Features

### 16.1.1 Uncertainty

We showed in Sec. 13.3.4 that the closed-loop system may be extremely sensitive to input uncertainty when the LV-configuration is used. In particular, inverse-based controllers were found to display severe robustness problems. In a similar manner as in Secs. 11.3.5 and 12.8 we will take uncertainty explicitly into account here when designing and analyzing the controllers via the structured singular value ($\mu$). We will demonstrate that $\mu$ provides a much more efficient tool for comparing and analyzing the effect of various combinations of controllers, uncertainty and disturbances than the traditional simulation approach.

### 16.1.2 Nonlinearity

High-purity distillation columns are known to be strongly nonlinear (see Appendix), and any realistic study should take this into account. Our approach is to base the controller design on a linear model. The effect of nonlinearity is taken care of by analyzing this controller for linearized models at *different operating points*. Furthermore, all simulations will be based on the full nonlinear model.

### 16.1.3 Logarithmic Compositions

Several authors found that the high-frequency behavior of distillation columns is only weakly affected by operating conditions when the *scaled* transfer matrix is considered

$$\begin{pmatrix} dy_D^S \\ dx_B^S \end{pmatrix} = G^S \begin{pmatrix} dL \\ dV \end{pmatrix} \quad , G^S = \begin{pmatrix} \frac{1}{1-y_D^o} & 0 \\ 0 & \frac{1}{1-x_B^o} \end{pmatrix} G \qquad (16.1-1)$$

All plant models and controllers in this chapter are scaled in this manner. $G^S$ is obtained by scaling the outputs with respect to the amount of impurity in each product

$$y_D^S = \frac{y_D}{1-y_D^o}, \quad x_B^S = \frac{x_B}{x_B^o} \qquad (16.1-2)$$

Here $x_B^o$ and $y_D^o$ are the compositions at the nominal operating point. This relative scaling is obtained automatically by using logarithmic compositions

$$Y_D = \ln(1-y_D) \qquad (16.1-3)$$

$$X_B = \ln x_B$$

because

$$dY_D = -\frac{dy_D}{1-y_D}, \quad dX_B = \frac{dx_B}{x_B} \qquad (16.1-4)$$

Furthermore, the use of logarithmic compositions ($Y_D$ and $X_B$) effectively eliminates the effect of nonlinearity at high frequency and also reduces its effect at steady-state. For control purposes the high-frequency behavior is of principal importance. Consequently, if logarithmic compositions are used we expect a linear controller to perform satisfactorily even when the operating conditions are far removed from the nominal operating point for which the controller was designed. Another objective of this chapter is to confirm that this is indeed true.

In most cases the column is operated close to its nominal operating point and there is hardly any advantage in using logarithmic compositions which merely corresponds to a rescaling of the outputs in this case. However, if, for some reason,

the column is taken far away from this nominal operating point, for example, during startup or due to a temporary loss of control, the use of logarithmic compositions may bring the column safely back to its nominal operating point, whereas a controller based on unscaled compositions ($y_D$ and $x_B$) may easily yield an unstable response.

### 16.1.4 Choice of Nominal Operating Point

The design approach suggested by the above discussion is to design a linear controller based on a linearized model for some nominal operating point. What operating point should be used? If an operating point corresponding to both products of high and equal purities is chosen (i.e., $1 - y_D = x_B$ is small), it is easily shown that the steady-state gains and the linearized time constant will change drastically for small perturbations from this operating point. We may therefore question if acceptable closed-loop control can be obtained by basing the controller design on a linearized model at such an operating point. Some authors indicate that this is not advisable, and that a model based on a perturbed operating point should be used. However, as we just discussed, the high-frequency behavior, which is of primary importance for feedback control, shows much less variation with operating conditions. Therefore, *provided* the model gives a good description of the high-frequency behavior, we expect to be able to design an acceptable controller also when the nominal operating point has both products of high purity. This is also confirmed by the results in this chapter.

Therefore, a main conclusion is that acceptable closed-loop performance may be obtained by designing a linear controller based on a linear model at *any* nominal operating point. If large perturbations from steady state are expected then logarithmic compositions should be used to reduce the effect of nonlinearity.

## 16.2 The Distillation Column

The column model is derived in the Appendix. The following simplifying assumptions are made: binary separation; constant relative volatility; constant molar flows; constant holdups on all trays; perfect pressure and level control. The last assumption results in immediate flow response, that is, flow dynamics are neglected. This is somewhat unrealistic, and in order to avoid unrealistic controllers, we will add "uncertainty" at high frequencies to include the effect of neglected flow dynamics when designing and analyzing the controllers.

We will investigate the column at two different operating points. At the nominal operating point, $A$, both products are high-purity and $1 - y_D^o = x_B^o = 0.01$.

Operating point $C$ is obtained by increasing $D/F$ from 0.500 to 0.555 which yields a less pure top product and a purer bottom product; $1 - y_{DC}^{o} = 0.10$ and $x_{BC}^{o} = 0.002$ (subscript C denotes operating point C while no subscript denotes operating point A). We will study the column for the following three assumptions regarding reboiler and condenser holdup

*Case 1:* Almost negligible condenser and reboiler holdup ($M_D/F = M_B/F =$ 0.5 min).

*Case 2:* Large condenser and reboiler holdup ($M_D/F = 32.1$ min, $M_B/F = 11$ min).

*Case 3:* Same holdup as in Case 2, but the composition of the overhead vapor ($y_T$) is used as a controlled output instead of the composition in the condenser ($y_D$).

These three cases will be denoted by subscripts 1, 2 and 3, respectively. The holdup on each tray inside the column is $M_i/F$= 0.5 min in all three cases.

### 16.2.1 Modelling

*Nominal operating point (A).* A 41st order linear model for the columns is easily derived

$$\begin{pmatrix} dy_D \\ dx_B \end{pmatrix} = G(s) \begin{pmatrix} dL \\ dV \end{pmatrix} \qquad (16.2-1)$$

The *scaled* steady-state gain matrix is

$$G(0) = \begin{bmatrix} 87.8 & -86.4 \\ 108.2 & -109.6 \end{bmatrix} \qquad (16.2-2)$$

which yields the following values for the condition number and the 1,1-element in the RGA

$$\gamma(G(0)) = \bar{\sigma}(G(0))/\underline{\sigma}(G(0)) = 141.7 \qquad \lambda_{11}(G(0)) = 35.1$$

However, $\gamma(G)$ and $\lambda_{11}(G)$ are much smaller at high frequencies as seen from Fig. 16.2-1. A very crude model used throughout the earlier chapters is

$$\text{Model 0}: \quad G_0(s) = \frac{1}{1+75s} G(0) \qquad (16.2-3)$$

This model has the same $\gamma(G)$ and $\lambda_{11}(G)$ for all frequencies and is therefore a poor description of the actual plant at high frequency.

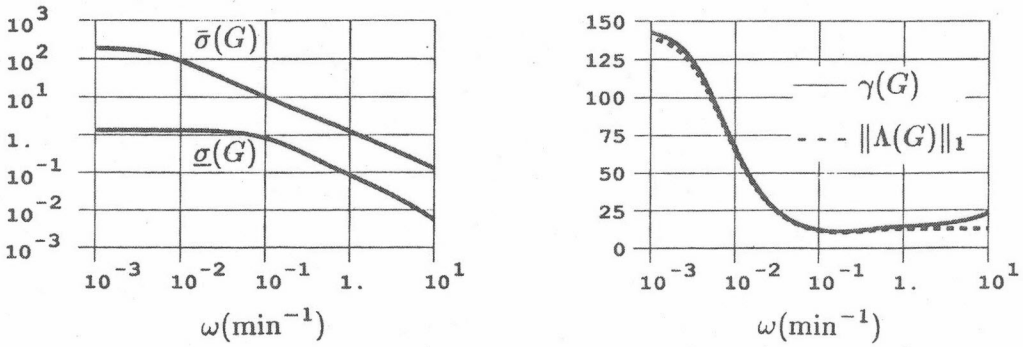


*Figure 16.2-1.* Column A, Case 1 ($G = G_1$). The condition number of the plant is about 10 times lower at high frequencies than at steady state. (Reprinted with permission from *Chem. Eng. Sci.* **43**, 35 (1988), Pergamon Press, plc.)

*Case 1.* For the case of negligible reboiler and condenser holdup the following simple two time-constant model yields an *excellent* approximation of the 41st order linear model.

$$\text{Model 1}: \quad G_1(s) = \begin{pmatrix} \frac{87.8}{1+\tau_1 s} & -\frac{87.8}{1+\tau_1 s} + \frac{1.4}{1+\tau_2 s} \\ \frac{108.2}{1+\tau_1 s} & \frac{-108.2}{1+\tau_1 s} - \frac{1.4}{1+\tau_2 s} \end{pmatrix} \quad \begin{matrix} \tau_1 = 194 \text{ min} \\ \tau_2 = 15 \text{ min} \end{matrix} \qquad (16.2-4)$$

This two state model uses two time constants: $\tau_1$ is the time constant for changes in the external flows and is dominant. $\tau_2$ is the time constant for changes in internal flows (simultaneous change in L and V with constant product rates, D and B). The simple model (16.2–4) matches the observed variation of the condition number with frequency (Fig. 16.2-1).

The effect of the reboiler and condenser holdups (Case 2) can be partially accounted for with Model 1 by multiplying $G_1(s)$ by $\text{diag}\{(1+\tau_D s)^{-1}, (1+\tau_B s)^{-1}\}$, where in our case $\tau_D = M_D/V_T = 10$ min and $\tau_B = M_B/L_B = 3$ min. However, in practice the top composition is often measured in the overhead vapor line (Case 3), rather than in the condenser. $G_1(s)$ provides a good approximation of the plant in such cases.

*Cases 2 and 3.* In order to obtain a low-order model for Cases 2 and 3, we performed a model reduction on the full 41st order model. These reduced order models are denoted by $G_2(s)$ and $G_3(s)$ respectively. A good approximation was obtained with a 5th-order model as illustrated in Fig. 16.2-2.

*Operating point C.* We will return with a discussion of the model for this case in Sec. 16.5 when we also discuss the control of the plant.

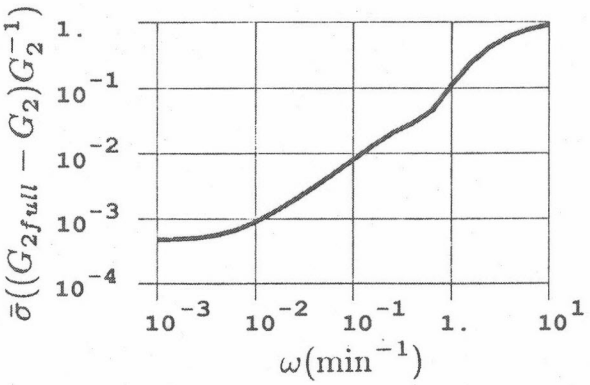


*Figure 16.2-2.* Column A, Case 2. Relative difference between the 5th order model $G_2(s)$ and the 41st order plant $G_{2\text{full}}(s)$. The 5th-order model provides an excellent approximation within the frequency range of interest ($\omega < 1\text{min}^{-1}$). (Reprinted with permission from *Chem. Eng. Sci.*, **43**, 36 (1988), Pergamon Press, plc.)

### 16.2.2 Simulations

The design and analysis of the controllers are based on the linear models $G_1(s), G_2(s)$, and $G_3(s)$. However, except for the five simplifying assumptions stated above, all simulations are carried out with the full *nonlinear* model. (In some cases the changes are so small, however, that the results are equivalent to linear simulations.) To get a realistic evaluation of the controllers *input uncertainty* must be included. Simulations are therefore shown both with and without 20% uncertainty with respect to the change of the two inputs. The following uncertainties are used:

$$\Delta L = (1 + \Delta_1)\Delta L_c, \quad \Delta_1 = 0.2 \qquad (16.2 - 5a)$$

$$\Delta V = (1 + \Delta_2)\Delta V_c, \quad \Delta_2 = -0.2 \qquad (16.2 - 5b)$$

Here $\Delta L$ and $\Delta V$ are the actual changes in manipulated flow rates, while $\Delta L_c$ and $\Delta V_c$ are the desired values as computed by the controller. $\Delta_1 = -\Delta_2$ was chosen to represent the worst combination of the uncertainties (Sec. 13.3.4).

## 16.3 Formulation of the Control Problem

### 16.3.1 Performance and Uncertainty Specifications

The uncertainty and performance specifications are the same as those used elsewhere in this book.

*Uncertainty.* The only source of uncertainty which is considered here is uncertainty on the manipulated inputs (L and V) with a magnitude bound:

$$w_I(s) = 0.2\frac{5s+1}{0.5s+1} \qquad (16.3-1)$$

The bound (16.3–1) allows for an input error of up to 20% at low frequency as was assumed for the simulations (16.2–5). The uncertainty bound (16.3–1) increases with frequency. This allows, for example, for a time delay of about 1 min in the response between the inputs, L and V, and the outputs, $y_D$ and $x_B$. In practice, such delays may be caused by the flow dynamics. Therefore, although flow dynamics are not included in the models or in the simulations, they are partially accounted for in the $\mu$-analysis and in the controller design.

*Performance.* Robust performance is satisfied if

$$\bar{\sigma}(E) = \bar{\sigma}((I+GC)^{-1}) \leq \frac{1}{|w_p|} \qquad (16.3-2)$$

is satisfied for all possible plants $G$. We use the performance weight

$$w_p(s) = 0.5\frac{10s+1}{10s} \qquad (16.3-3)$$

A particular $E$ which exactly matches the bound (16.3–2) at low frequencies and satisfies it easily at high frequencies is $E = 20s/20s+1$. This corresponds to a first-order response with closed-loop time constant 20 min.

### 16.3.2 Analysis of Controllers

Comparison of controllers is based mainly on $\mu$ for robust performance ($\mu_{RP}$). Simulations are used only to support conclusions found using the $\mu$-analysis. The main advantage of the $\mu$-analysis is that it provides a well-defined basis for comparison. On the other hand, simulations are strongly dependent on the choice of setpoints, uncertainty, etc.

The value of $\mu_{RP}$ is indicative of the worst-case response. If $\mu_{RP} > 1$ then the "worst case" does not satisfy our performance objective, and if $\mu_{RP} < 1$ then the "worst case" is better than required by our performance objective. Similarly,

if $\mu_{NP} < 1$ then the performance objective is satisfied for the *nominal* case. However, this may not mean very much if the system is sensitive to uncertainty and $\mu_{RP}$ is significantly larger than one. We will show below that this is the case, for example, if an inverse-based controller is used for our distillation column.

### 16.3.3 Controllers

We will study the distillation column with the following six controllers:

1. *Diagonal PI-controller.*

$$C_{PI}(s) = \frac{0.01}{s}(1+75s)\begin{pmatrix} 2.4 & 0 \\ 0 & -2.4 \end{pmatrix} \qquad (16.3-4)$$

This controller was studied in Sec. 11.3.5 and was tuned to achieve as good a performance as possible while maintaining robust stability (see also Fig. 16.4-1).

2. *Steady-state decoupler plus two PI-controllers.*

$$C_{oinv}(s) = 0.7\frac{(1+75s)}{s}G(0)^{-1} = \frac{0.01(1+75s)}{s}\begin{pmatrix} 27.96 & -22.04 \\ 27.60 & -22.40 \end{pmatrix} \qquad (16.3-5)$$

This controller was tuned to achieve good *nominal* performance. However, the *controller* has large RGA-elements ($\lambda_{11}(C) = 35.1$) at *all* frequencies and we expect the controller to be extremely sensitive to input uncertainty (see Sec. 13.3).

3. *Inverse-based controller based on the linear model $G_1(s)$ for Case 1.*

$$C_{1inv}(s) = \frac{0.7}{s}G_1(s)^{-1} \qquad (16.3-6)$$

At low frequency this controller is equal to $C_{oinv}(s)$. Note that $C_{1inv}(s)$ and $G_1(s)^T$ have the same RGA-elements. Therefore from Fig. 16.2-1 we expect $C_{1inv}(s)$ to be sensitive to input uncertainty at low frequency, but not at high frequency.

4, 5, and 6. *$\mu$-optimal controllers* based on the models $G_0(s), G_1(s)$ and $G_2(s)$. The controllers are denoted $C_{0\mu}(s), C_{1\mu}(s)$ and $C_{2\mu}(s)$, respectively.

These controllers were obtained by minimizing $\sup_\omega \mu(N_{RP})$ for each model using the input uncertainty and performance weights given above. The numerical procedure used for the minimization is the same as mentioned in Sec. 11.3.5. The $\mu$-plots for robust performance for the $\mu$-optimal controllers are of particular interest since they indicate the best *achievable* performance for the plant. Bode plots of the transfer matrix elements of $C_{1\mu}(s)$ and $C_{2\mu}(s)$ are shown in Fig. 16.3-1. Note the similarities between these controllers and the simple diagonal PI controller (16.3–4).

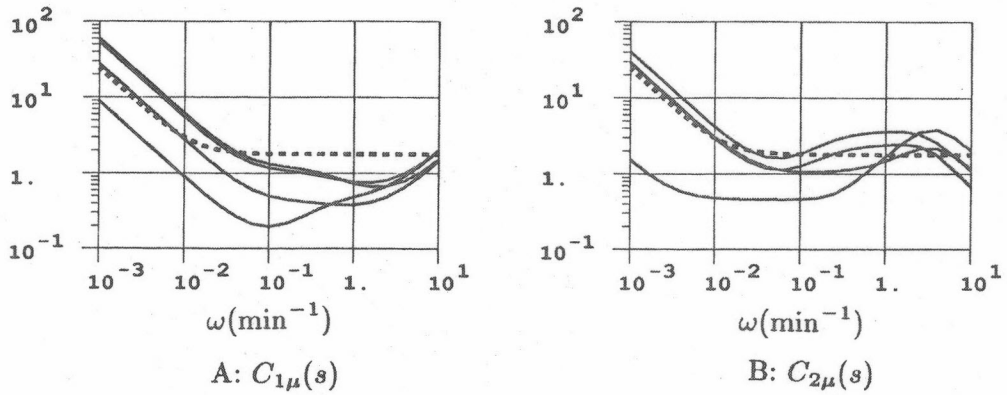


*Figure 16.3-1.* Magnitude plots of elements in $\mu$–optimal controllers $C_{1\mu}(s)$ and $C_{2\mu}(s)$. Dotted line: $C_{PI}(s)$. (Reprinted with permission from *Chem. Eng. Sci.*, **43**, 39 (1988), Pergamon Press, plc.)

At low frequency ($s \to 0$) the six controllers are approximately

$$C_{PI} = \frac{0.01}{s}\begin{pmatrix} 2.4 & 0 \\ 0 & -2.4 \end{pmatrix}$$

$$C_{0inv} = C_{1inv} = \frac{0.01}{s}\begin{pmatrix} 27.96 & -22.04 \\ 27.80 & -22.40 \end{pmatrix}$$

$$C_{0\mu} = \frac{0.01}{s}\begin{pmatrix} 3.82 & -0.92 \\ 1.73 & -3.52 \end{pmatrix}; C_{1\mu} = \frac{0.01}{s}\begin{pmatrix} 6.07 & -0.90 \\ 2.80 & -2.93 \end{pmatrix}; C_{2\mu} = \frac{0.01}{s}\begin{pmatrix} 4.06 & +0.15 \\ 2.85 & -2.93 \end{pmatrix}$$

$\|\Lambda(C)\|_1$ is shown as a function of frequency for the six controllers in Fig. 16.3-2. As expected, the $\mu$-optimal controllers have small RGA-elements, which make them insensitive to input uncertainty. For example, $C_{2\mu}$ is nearly triangular at low frequency and consequently has $\Lambda \cong I$.

## 16.4 Results for Operating Point A

In this section we will study how the six controllers perform at the nominal operating point A for the three assumptions regarding condenser and reboiler holdup (corresponding to the models $G_1(s), G_2(s)$, and $G_3(s)$). The $\mu$-plots for the 18 possible combinations are given in Fig. 16.4-1. A number of interesting observations can be derived from these plots. These are presented below. In some cases the simulations in Figs. 16.4-2 to 16.4-4 are used to support the claims.

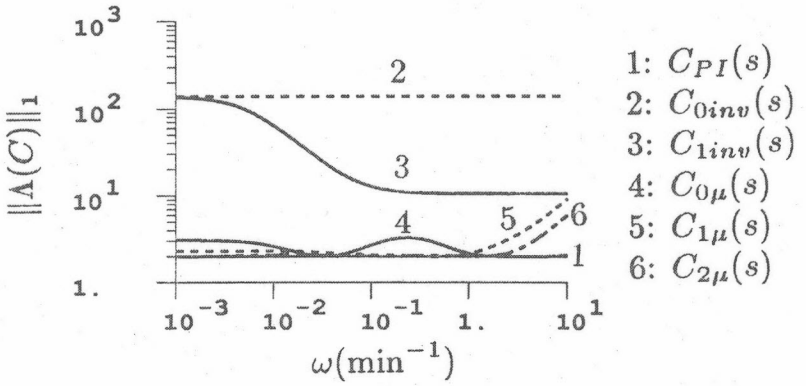


*Figure 16.3-2.* Magnitude of RGA elements of controllers. $\|\Lambda(C)\|_1 = \sum_{i,j} |\lambda_{ij}(C)|$. (Reprinted with permission from *Chem. Eng. Sci.*, **43**, 39 (1988), Pergamon Press, plc.)

### 16.4.1 Discussion of Controllers

$C_{PI}(s)$. The simple diagonal PI-controller performs reasonably well in all cases. $\mu_{NP}$ is higher than one at low frequency, which indicates a slow return to steady state. This is confirmed by the simulations in Fig. 16.4-3 for a feed rate disturbance; after 200 min the column has still not settled. Operators are usually unhappy about this kind of response. The controller is insensitive to input uncertainty and to changes in reboiler and condenser holdup.

$C_{0inv}(s)$. This controller uses a steady-state decoupler. The nominal response is very good for Case 1 (Fig. 16.4-2), but the controller is extremely sensitive to input uncertainty. In practice, this controller will yield an unstable system.

$C_{1inv}(s)$. This controller gives an excellent nominal response for Case 1 (Fig. 16.4-1). This is also confirmed by the simulations in Fig. 16.4-2; the response is almost perfectly decoupled with a time constant of about 1.4 min. Since the simulations are performed with the full-order model, while the controller was designed based on the simple two time-constant model, $G_1(s)$ (16.2-4), this confirms that $G_1(s)$ yields a very good approximation of the linearized plant when the reboiler and condenser holdups are small. The controller is sensitive to the input uncertainty as expected from the RGA analysis. Also note that the controller performs very poorly when the condenser and reboiler holdups are increased. This shows that the controller is also very sensitive to other sources of model-plant mismatch.

$C_{0\mu}(s)$. This is the $\mu$-optimal controller from our previous study which was designed based on the very simplified model $G_0(s)$. The controller performs

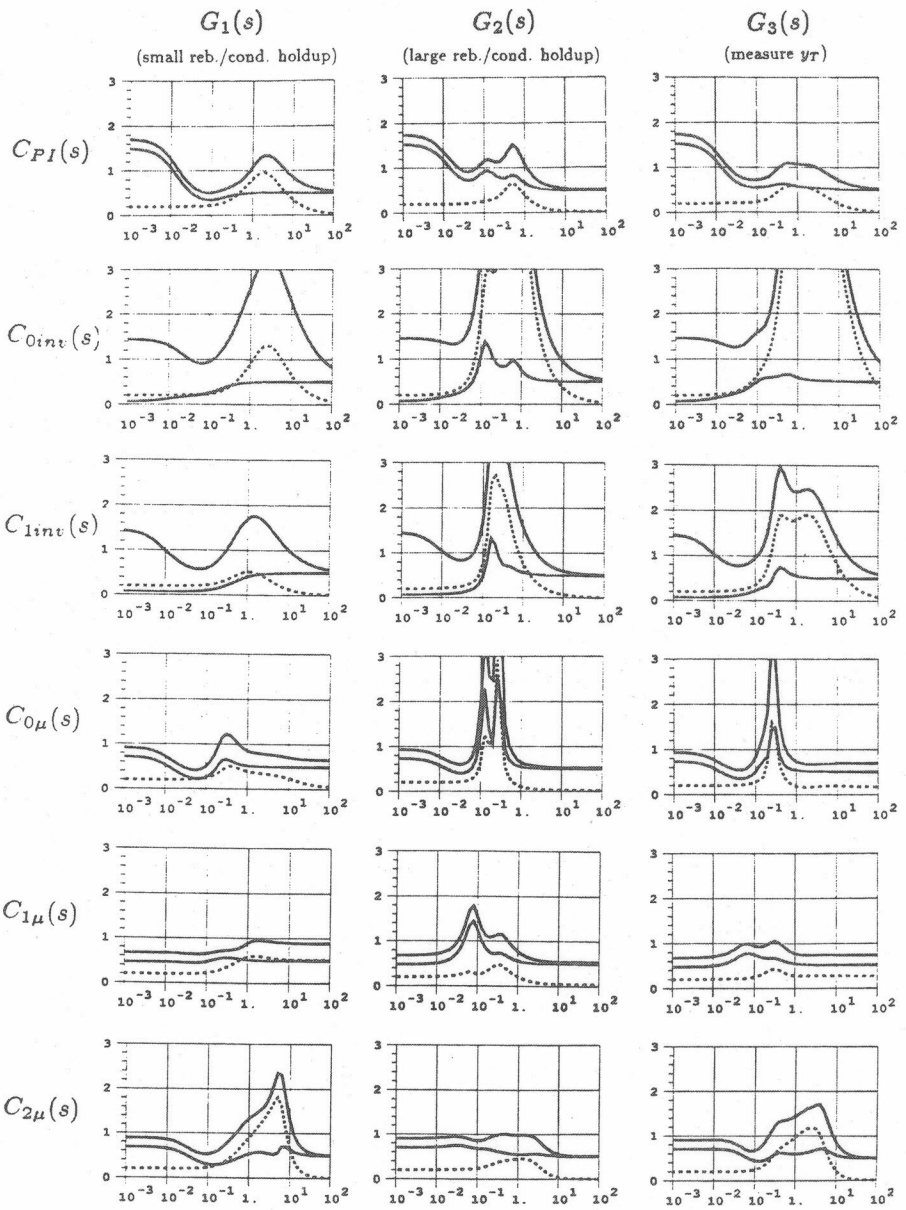


*Figure 16.4-1.* $\mu-$plots for operating point. Upper solid line: $\mu_{RP}$ for robust performance; lower solid line:$\mu_{NP}$ for nominal performance; dotted line: $\mu_{RS}$ for robust stability. (Reprinted with permission from *Chem. Eng. Sci.*, **43**, 40 (1988), Pergamon Press, plc.)

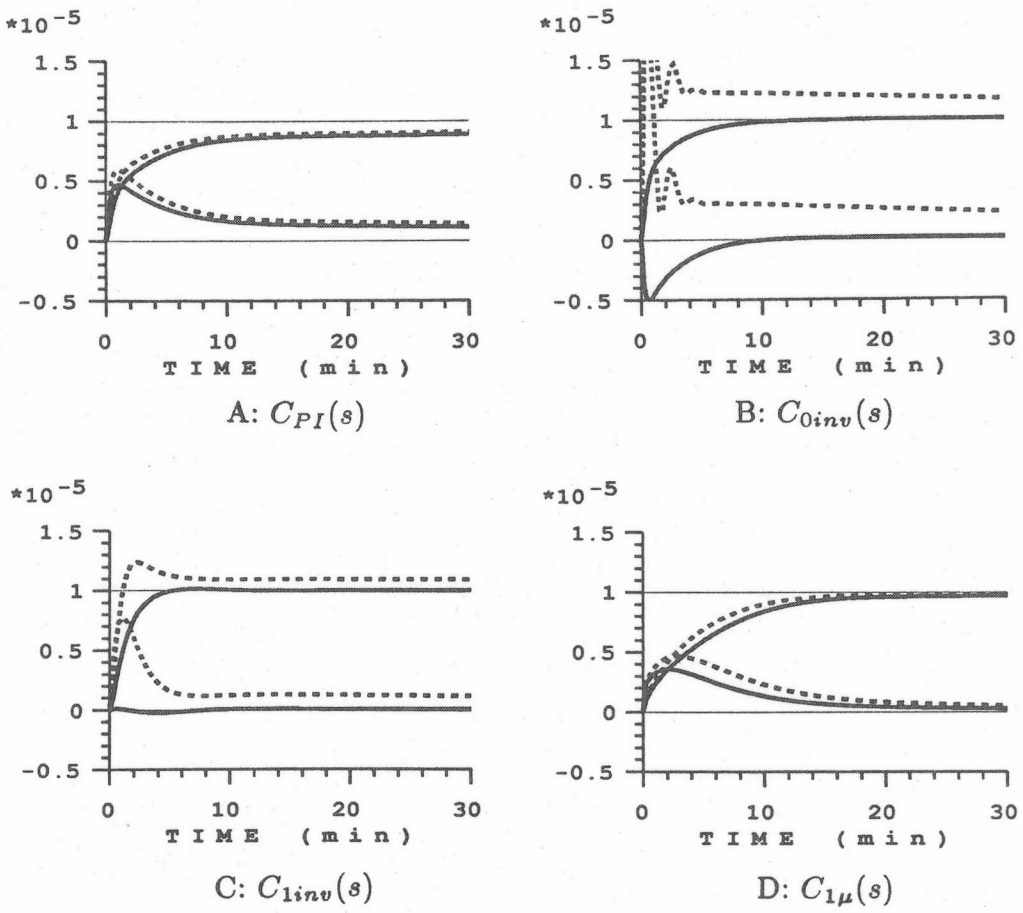


*Figure 16.4-2.* Operating point A, Case 1. Closed-loop response to small setpoint change in $y_D$. Solid lines: no uncertainty; dotted lines: 20% uncertainty on inputs $L$ and $V$ (16.2–5). (Reprinted with permission from *Chem. Eng. Sci.*, **43**, 41 (1988, Pergamon Press, plc.)

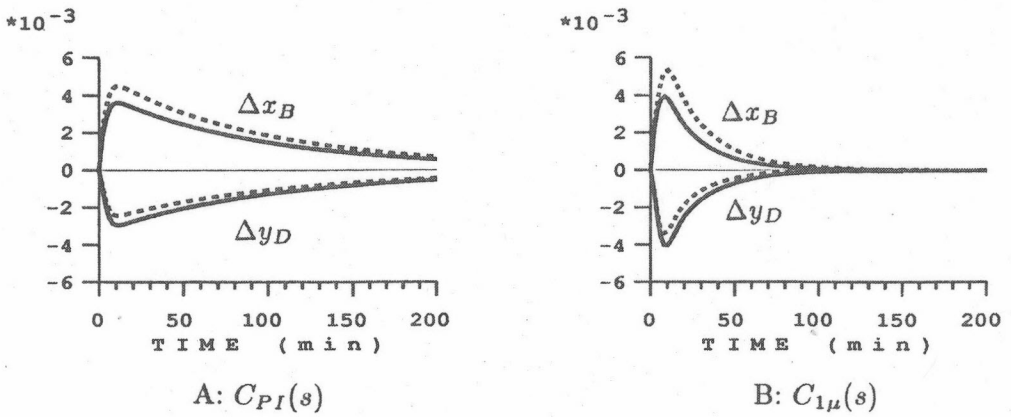


*Figure 16.4-3.* Operating point A, Case 1. Closed-loop response to a 30% increase in feed rate. Solid lines: no uncertainty; dotted lines: 20% uncertainty on inputs $L$ and $V$ (16.2-5). (Reprinted with permission from *Chem. Eng. Sci.*, **43**, 41 (1988), Pergamon Press, plc.)

surprisingly well on the actual plant ($G_1(s)$) when the holdups are negligible. However, the controller is seen to perform very poorly when the holdups in the reboiler and condenser are increased, which shows that the controller is very sensitive to other sources of model inaccuracies (for which it was not designed).

$C_{1\mu}(s)$. This is the $\mu$-optimal controller when there is negligible holdup ($G_1(s)$). The robust performance condition is satisfied for this case since $\mu_{RP} \cong 0.95$. The nominal performance is not as good as for the inverse-based controller $C_{1inv}(s)$; we have to sacrifice nominal performance to make the system robust with respect to uncertainty. The controller shows some performance deterioration when the reboiler and condenser holdups are increased (Case 2). This is not surprising since the added holdup makes the response of $y_D$ and $x_B$ more sluggish; the open-loop response for $y_D$ changes from approximately $(1+194s)^{-1}$ to $((1+194s)(1+10s))^{-1}$ [recall discussion following (16.2–4)]. As expected, the controller is much less sensitive to changes in condenser holdup if the overhead composition is measured in the vapor line (Case 3). Overall, this is the best of the six controllers.

$C_{2\mu}(s)$. This is the $\mu$-optimal controller for the case with considerable reboiler and condenser holdup, and with $y_D$ measured in the condenser ($G_2(s)$). $\mu_{RP} \cong 1.00$ for this case. The nominal response is good in all cases (Fig. 16.4-1), but the controller is very sensitive to uncertainty when the plant is $G_1(s)$ or $G_3(s)$ rather than $G_2(s)$. This is clearly not desirable since changes in condenser and reboiler holdup are likely to occur during normal operation. The observed behavior is not

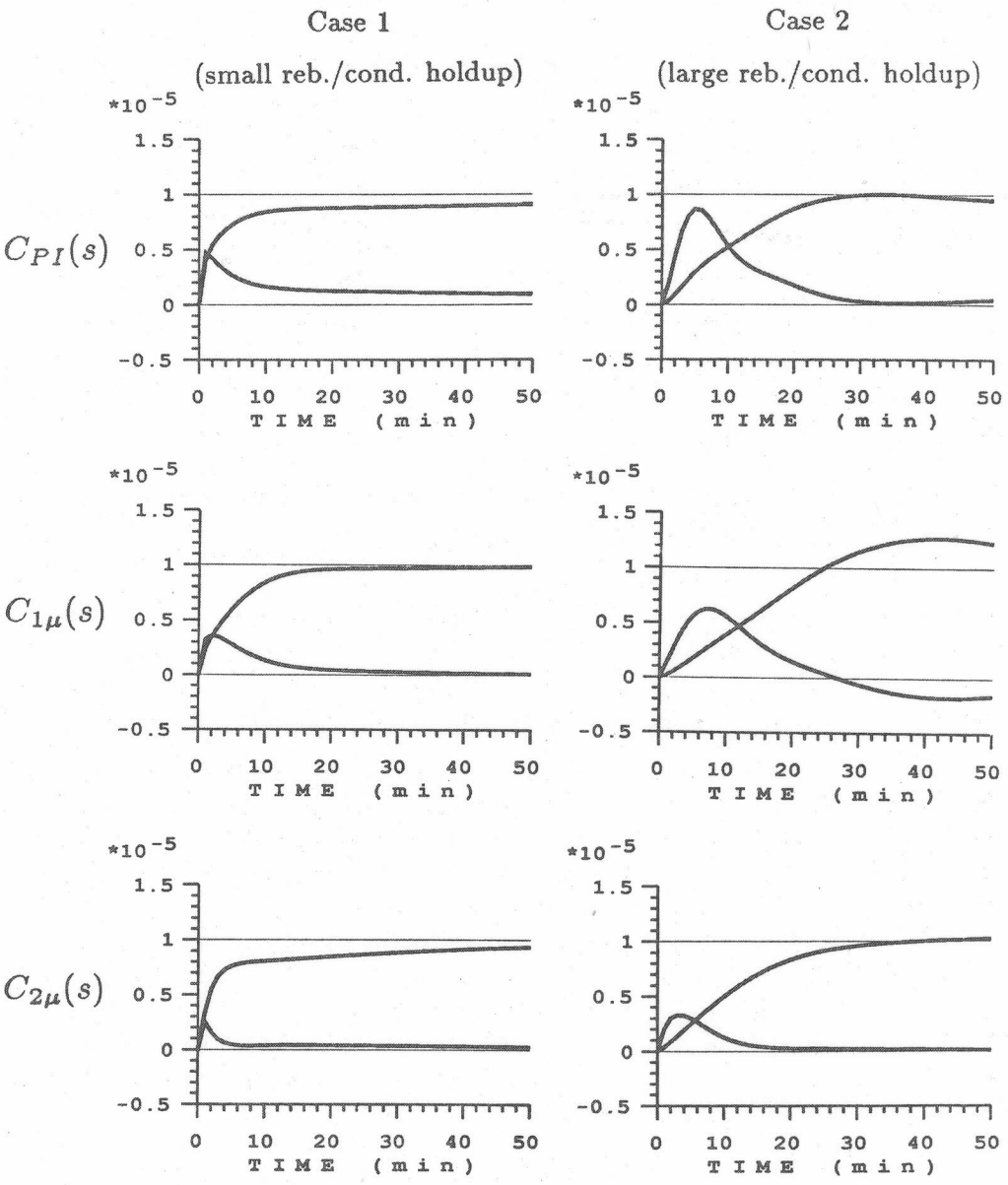


*Figure 16.4-4.* Operating point A. Effect of reboiler and condenser holdup on closed-loop response. No uncertainty. (Reprinted with permission from *Chem. Eng. Sci.*, **43**, 42 (1988), Pergamon Press, plc.)

surprising since the controller includes lead elements at $\omega \cong 0.1$ (Fig. 16.3-1B) to counteract the lags caused by the reboiler and condenser holdups. If these lags are not present in the plant ($G_1(s)$ or $G_3(s)$), the "derivative" action caused by the lead elements results in a system which is very sensitive to uncertainty.

### 16.4.2 Conclusions

- The $\mu$-optimal controller $C_{0\mu}(s)$ for the plant $G_0(s)$ has $\mu_{RP} \cong 1.06$ while the $\mu$-optimal controller $C_{1\mu}(s)$ for the plant $G_1(s)$ has $\mu_{RP} \cong 0.95$. Thus, somewhat surprisingly, the achievable performance is not much better for $G_1(s)$ than for $G_0(s)$, even though $G_0(s)$ is ill-conditioned and has large RGA elements at *all* frequencies, while $G_1(s)$ has large RGA elements only at low frequencies (Fig. 16.2-1). This seems to indicate that large RGA-elements at low frequency imply limitations on the achievable control performance and partially justifies the use of steady-state values of the RGA for selecting the best control configuration.

- However, the use of the more detailed model $G_1(s)$, rather than $G_0(s)$, is still justified since the resulting $\mu$-optimal controller is much less sensitive to changes in reboiler and condenser holdup (which will occur during operation).

- $G_1(s)$ approximates the full-order model very closely as seen from Fig. 16.4-2C; the response is almost perfectly decoupled when there is no uncertainty.

- To avoid sensitivity to the amount of condenser and reboiler holdup, the overhead composition should be measured in the overhead vapor, rather than in the condenser. In practice, temperature measurements *inside* the column are often used to infer compositions, and the dynamic response of these measurements is similar to that when the condenser and reboiler holdup is neglected.

- The simple model $G_2(s)$ is useful for controller design even when the reboiler and condenser holdup is large.

- The main advantage of the $\mu$-optimal controllers over the simple diagonal PI controller is a faster return to steady-state. This can be seen very clearly in Fig. 16.4-3 which shows the closed-loop response to a 30% increase in feed rate.

## 16.5 Effect of Nonlinearity (Results for Operating Point C)

We will not treat nonlinearity as uncertainty because this approach is not rigorous and is also very conservative due to the strong correlation between all the parameters in the model which is difficult to account for. Furthermore, we know from the data in the Appendix that the column is actually *not* as nonlinear as one might expect. Though the steady-state gains may change dramatically, the high frequency behavior, which is of principal importance for feedback control, is much less affected. In particular, this is the case if relative (logarithmic) compositions are used. To demonstrate this fact we compute $\mu$ and show simulations for some of the controllers when the "plant" is $G_C(s)$ rather than $G(s)$.

### 16.5.1 Modelling

The model $G_C(s)$ describes the same column as $G(s)$, but the distillate flow rate $(\frac{D}{F})$ has been increased from 0.5 to 0.555 such that $y_D = 0.9$ and $x_B = 0.002$. For Case 1 ($M_D/F = M_B/F = 0.5$ min), the following approximate model is derived when scaled compositions $(dy_D/0.1, dx_B/0.002)$ are used:

$$G_{C1}(s) = \begin{pmatrix} \frac{16.0}{1+\tau_1 s} & \frac{16.0}{1+\tau_1 s} + \frac{0.023}{1+\tau_2 s} \\ \frac{9.3}{1+\tau_1 s} & \frac{-9.3}{1+\tau_1 s} - \frac{1.41}{1+\tau_2 s} \end{pmatrix} \quad \begin{matrix} \tau_1 = 24.5 \text{ min} \\ \tau_2 = 10 \text{ min} \end{matrix} \qquad (16.5-1)$$

The steady-state gains and time constants are entirely different from those at operating point A (16.2–4). Also note that at steady state $\lambda_{11}(G(0)) = 35.1$ for operating point A, but only 7.5 for operating point C. However, at high-frequency the scaled plants at operating points A and C are very similar. Equations (16.2–4) and (16.5–1) yield:

$$G_1(\infty) = \frac{1}{s}\begin{pmatrix} 0.45 & -0.36 \\ 0.56 & -0.65 \end{pmatrix} \quad \lambda_{11}(\infty) = 3.2 \qquad (16.5-2a)$$

$$G_{C1}(\infty) = \frac{1}{s}\begin{pmatrix} 0.65 & -0.65 \\ 0.38 & -0.52 \end{pmatrix} \quad \lambda_{11}(\infty) = 3.7 \qquad (16.5-2b)$$

Therefore, as we will show, controllers which were designed based on the model $G(s)$ (operating point A) remain satisfactory when the plant is $G_C(s)$ rather than $G(s)$. Recall that the use of a scaled plant is equivalent to using logarithmic compositions ($Y_D$ and $X_B$). The variation in gain with operating conditions is much larger if unscaled compositions are used – both at steady-state and at high frequencies:

$$G_1^{us}(\infty) = \frac{0.01}{s}\begin{pmatrix} 0.45 & -0.36 \\ 0.56 & -0.65 \end{pmatrix} \qquad (16.5-3a)$$

$$G_{C1}^{us}(\infty) = \frac{0.01}{s}\begin{pmatrix} 6.5 & -6.5 \\ 0.08 & -0.10 \end{pmatrix} \qquad (16.5-3b)$$

### 16.5.2 $\mu$-Analysis

The $\mu$-plots with the model $G_C(s)$ and four of the controllers are shown in Fig. 16.5-1 (all four controllers yield *nominally* stable closed-loop systems). For high frequencies the $\mu$-values are almost the same as those found at operating point A. The only exception is the inverse based controller $C_{1inv}(s)$ which is robustly stable at operating point A, but not at operating point C. Again, this confirms the sensitivity of this controller to model inaccuracies. Performance is clearly worse for low frequencies at operating point C (Fig. 16.5-1) than at operating point A (Fig. 16.4-1). This is expected; the controllers were designed based on model A, and the plants are quite different in the low frequency range.

The $\mu$-optimal controller $C_{1\mu}(s)$ satisfies the robust performance requirements also at operating point C when the reboiler and condenser holdups are small. Consequently, with scaled (logarithmic) compositions, a single linear controller is able to give acceptable performance at these two operating points although the linear models are quite different. The main difference between $C_{1\mu}(s)$ and the diagonal PI controller is again that the $\mu$-optimal controller gives a much faster return to steady-state. This is clearly seem from Fig. 16.5-2A.

### 16.5.3 Logarithmic Versus Unscaled Compositions

Figure 16.5-1 shows how controllers, designed based on the *scaled* plant $G(s)$ at operating point A, perform for the *scaled* plant (different scaling factors!) at operating point C; this is equivalent to using logarithmic compositions ($Y_D$ and $X_B$). We know from (16.5–3) that the plant model based on absolute compositions changes much more. Therefore we expect the closed-loop performance to be entirely different at operating ponts A and C when unscaled (absolute) compositions are used. This is indeed confirmed by Fig. 16.5-2B which shows the closed-loop response to a small setpoint change in $x_B$ at operating point C. Fig. 16.5-2B should be compared to Fig. 16.5-2A which shows the same response, but with logarithmic compositions as controlled outputs. In Fig. 16.5-2B (absolute compositions) the response for $x_B$ is significantly more sluggish, but the response for $y_D$ is much faster than in Fig. 16.5-2A (logarithmic compositions). This is exactly what we would expect from a comparison of (16.5–3a) and (16.5–3b). The high-frequency gain for changes in $y_D$ is increased by an order of magnitude and

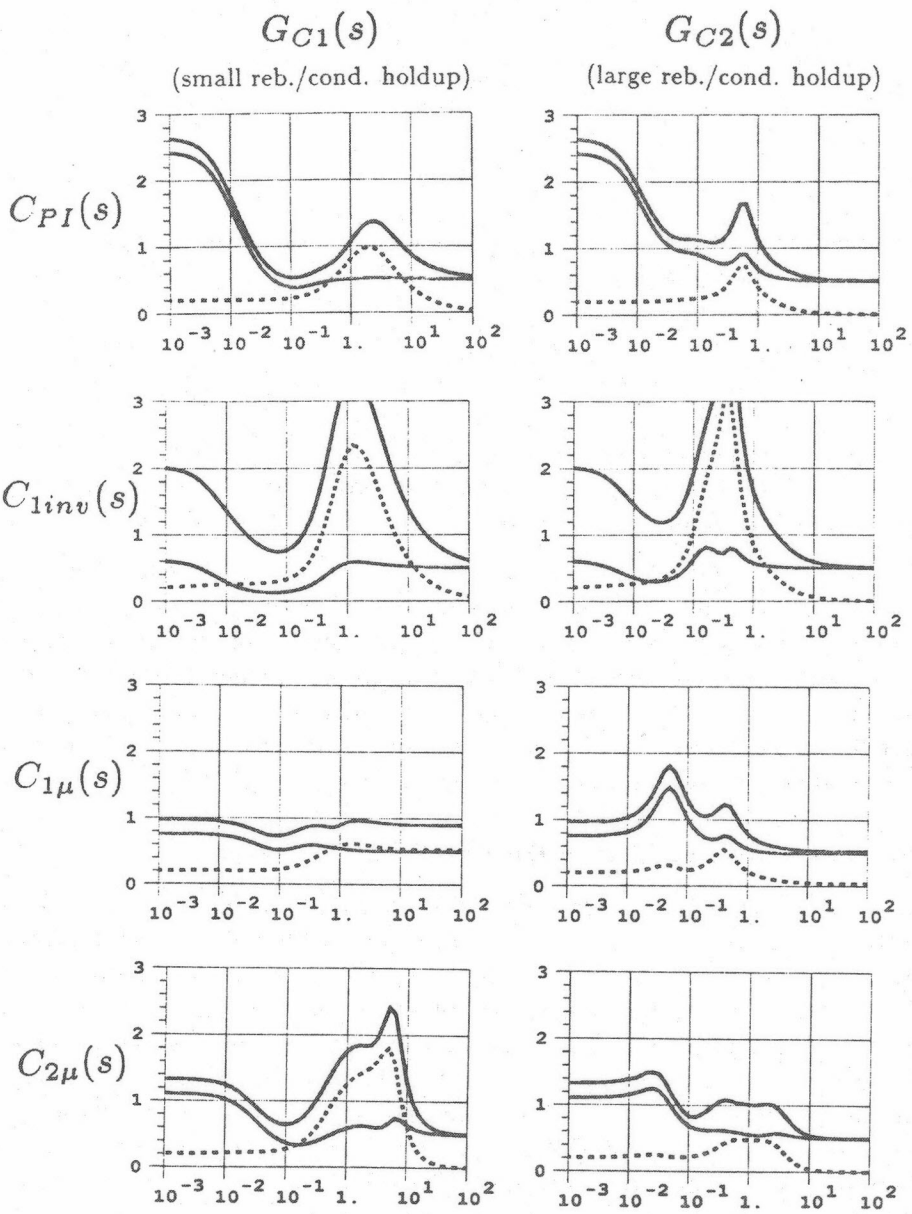


*Figure 16.5-1.* $\mu$–plots for operating point C. Upper solid line: $\mu_{RP}$; lower solid line: $\mu_{NP}$; dotted line: $\mu_{RS}$. (Reprinted with permission from *Chem. Eng. Sci.*, **43**, 44 (1988), Pergamon Press, plc.)

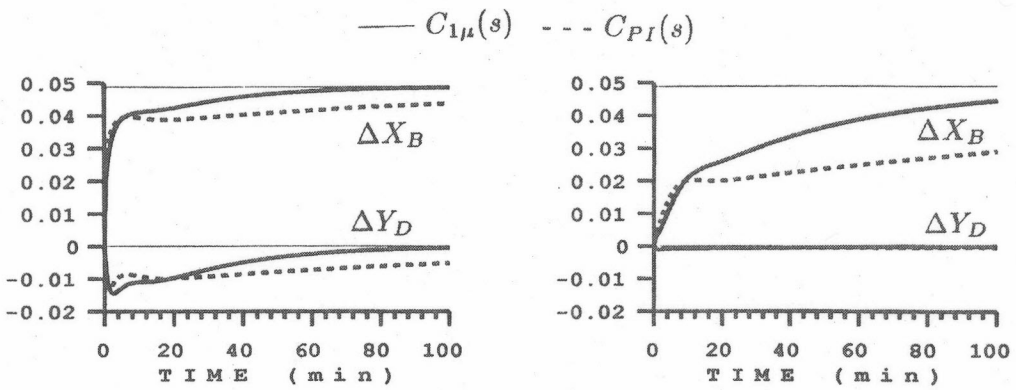


*Figure 16.5-2.* Operating point C, Case 1. Closed-loop response to small setpoint change in $x_B$ ($x_B$ increases from 0.002 to 0.0021) using diagonal PI controller (dotted line) and the $\mu$–optimal controller for operating point A (solid line). Left: logarithmic compositions as controlled outputs (equivalent to using scaled compositions); right: absolute (unscaled) compositions as controlled outputs. No uncertainty. (Reprinted with permission from *Chem. Eng. Sci.*, **43**, 45 (1988), Pergamon Press, plc.)

the gain for changes in $x_B$ is reduced by an order of magnitude. However, recall from (16.5–2) that the gain changes very little when logarithmic compositions are used.

### 16.5.4 Transition from Operating Point A to C

Figure 16.5-3 shows a transition from operating point A ($Y_D = X_B = 4.605$) to operating point C ($Y_D = 2.303, X_B = 6.215$) using logarithmic compositions as controlled ouputs. The desired setpoint change is a first order response with time constant 10 min:

$$\Delta Y_{Ds} = \frac{2.303}{1+10s}\frac{1}{s}, \quad \Delta X_{Bs} = \frac{-1.609}{1+10s}\frac{1}{s}$$

The closed-loop response is seen to be very good. The diagonal controller $C_{PI}(s)$ and the $\mu$-optimal controller $C_{1\mu}(s)$ give very similar responses in this particular case. (However, the $\mu$-optimal controller generally performs better at operating point C as is evident from Figs. 16.5-1 and 16.5-2.) This illustrates that a linear controller, based on the nominal operating point A, can be satisfactory for a large

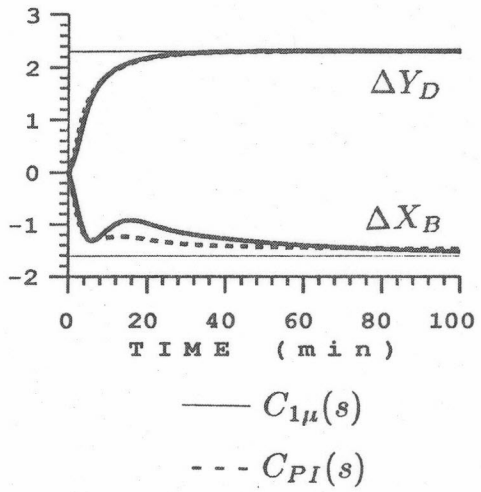


*Figure 16.5-3.* Transition from operating point A to C (Case 1) with controllers $C_{1\mu}$ (solid line) and $C_{PI}$ (dotted line). Logarithmic compositions are used as controlled outputs to reduce the effect of nonlinearity. Desired trajectory is a first-order response with time constant 10 min. No uncertainty. (Reprinted with permission from *Chem. Eng. Sci.*, **43**, 45 (1988), Pergamon Press, plc.)

deviation from this operating point when logarithmic compositions are used.

## 16.6 Conclusions

A single linear controller is able to provide satisfactory control for this high-purity column at widely different operating conditions. To compensate for the plant nonlinearity it is advantageous to use "logarithmic compositions." For small deviations from steady state linear controllers using "absolute compositions" work also well.

The performance with a simple diagonal controller is robust with respect to model-plant mismatch but after an upset the return to steady state can be very sluggish. This particular deficiency can be removed by a $\mu$-optimal controller. Inverse-based controllers, and specifically those involving steady-state decouplers, were shown to be very sensitive to model-plant mismatch.

## 16.7 References

This chapter is abstracted from a paper by Skogestad & Morari (1988a) where the state-space description of the $\mu$-optimal controllers and the reduced order

models for Cases 2 and 3 are also provided. For a general discussion of distillation control the reader is referred to the book by Shinskey (1984) or the thesis by Skogestad (1987). Skogestad and Morari (1987a) have reviewed the current industrial understanding of distillation control from the viewpoint of modern robust control.

16.1.2. The nonlinear behavior was observed specifically by Moczek, Otto & Williams (1963) and Fuentes and Luyben (1983).

16.1.3. The use of "logarithmic compositions" seems to have been first suggested by Ryskamp (1981).

16.1.4. The change of gain and time constant with operating condition was analyzed by Kapoor, McAvoy & Marlin (1986) and Skogestad & Morari (1988d).

16.2.1. The model reduction was performed via "Balanced Realization" (Moore, 1981). The dominant time constant $\tau_1$ can be estimated, for example, from the inventory time constant introduced by Moczek, Otto & Williams (1963). The time constant $\tau_2$ can be obtained by matching the high-frequency behavior as shown by Skogestad & Morari (1988d).

# Appendix

# Dynamic Model of Distillation Column

On many occasions in this book a high purity distillation column is used as an example. In this Appendix all the necessary information is summarized to enable the reader to verify any of the results reported in this book and to use the distillation model as a test case for other analysis and design procedures.

## A.1 Nomenclature and Assumptions

The column is shown in Fig. A.1-1 where most symbols are also defined.

*Symbols:*

| | |
|---|---|
| $M$ | hold up |
| $N$ | number of equilibrium (theoretical) stages |
| $N+1$ | total number of stages including total condenser |
| $N_F$ | feed stage location |
| $F$ | feed rate |
| $z_F$ | mole fraction of light component in feed |
| $q_F$ | fraction liquid in feed |
| $D$ | distillate flow |
| $V$ | boilup |
| $V_T$ | top vapor flow |
| $L$ | reflux flow |
| $B$ | bottom flow |
| $p$ | pressure |
| $q$ | mole fraction of feed which is liquid |
| $x$ | mole fraction of light component in liquid |
| $y$ | mole fraction of light component in vapor |
| $\alpha$ | relative volatility |
| $\kappa$ | linearized VLE-constant |

The unit of mass is kmol and the unit of time is minute.

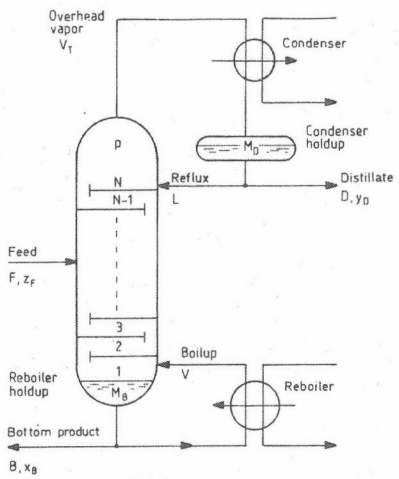


*Figure A.1-1.* Two product distillation column with single feed and total condenser.

*Subscripts:*

| | |
|---|---|
| $i$ | tray $i$ (trays are numbered from bottom with the reboiler as tray |
| $F$ | feed |
| $D$ | distillate |
| $B$ | bottom |
| $T$ | top |

*Assumptions:*

- binary mixture
- constant pressure
- constant relative volatility $\alpha$
- constant molar flows
- no vapor holdup (immediate vapor response, $dV_T = dV_B$)
- constant liquid holdup $M_i$ on all trays (immediate liquid response, $dL_T = dL_B$)
- Vapor-Liquid Equilibrium (VLE) and perfect mixing on all stages

## A.2 Nonlinear Model

Material balances for change in holdup of light component on each tray $i = 2, \ldots, N (i \neq N_F, i \neq N_F + 1)$:

$$M_i \dot{x}_i = L_{i+1} x_{i+1} + V_{i-1} y_{i-1} - L_i x_i - V_i y_i$$

Above feed location $i = N_F + 1$:

$$M_i \dot{x}_i = L_{i+1} x_{i+1} + V_{i-1} y_{i-1} - L_i x_i - V_i y_i + F_V y_F$$

Below feed location, $i = N_F$:

$$M_i \dot{x}_i = L_{i+1} x_{i+1} + V_{i-1} y_{i-1} - L_i x_i - V_i y_i + F_L x_F$$

Reboiler, $i = 1$:

$$M_B \dot{x}_i = L_{i+1} x_{i+1} - V_i y_i - B x_i, \quad x_B = x_1$$

Total condenser, $i = N + 1$:

$$M_D \dot{x}_i = V_{i-1} y_{i-1} - L_i x_i - D x_i, \quad y_D = x_{N+1}$$

VLE on each tray ($i = 1, \ldots, N$), constant relative volatility:

$$y_i = \frac{\alpha x_i}{1 + (\alpha - 1) x_i}$$

Flow rates assuming constant molar flows:

$$i > N_F \text{ (above feed)}: \quad L_i = L, \quad V_i = V + F_V$$

$$i \leq N_F \text{ (below feed)}: \quad L_i = L + F_L, \quad V_i = V$$

$$F_L = q_F F, \quad F_V = F - F_L$$

$$D = V_N - L = V + F_V - L \quad \text{(constant condenser holdup)}$$

$$B = L_2 - V_1 = L + F_L - V \quad \text{(constant reboiler holdup)}$$

Compositions $x_F$ and $y_F$ in the liquid and vapor phase of the feed are obtained by solving the flash equations:

$$F z_F = F_L x_F + F_V y_F$$

*Table A.2-1.* Column Data

| | |
|---|---|
| Relative volatility | $\alpha = 1.5$ |
| No. of theoretical trays | $N = 40$ |
| Feed tray (1=reboiler) | $N_F = 21$ |
| Feed composition | $z_F = 0.5$ |
| Condenser time constant | $M_D/F$: see Ch. 16 |
| Reboiler time constant | $M_B/F$: see Ch. 16 |
| Tray time constant | $M_i/F = 0.5\text{min}$ |

$$y_F = \frac{\alpha x_F}{1 + (\alpha - 1)x_F}$$

The column data and operating conditions used in the book are shown in Tables A.2-1 and A.2-2. The tray compositions are listed in Table A.2-3. The column behavior is highly nonlinear as Fig. A.2-1 illustrates.

*Table A.2-2.* Operating Variables:

| Operating Point | A | C |
|---|---|---|
| $y_D$ | 0.99 | 0.90 |
| $x_B$ | 0.01 | 0.002 |
| $(L/D)_{\min}$ | 3.900 | 3.000 |
| $L/D$ | 5.413 | 4.935 |
| $D/F$ | 0.500 | 0.555 |
| $B/F$ | 0.500 | 0.445 |
| $V/F$ | 3.206 | 3.291 |
| $L/F$ | 2.706 | 2.737 |

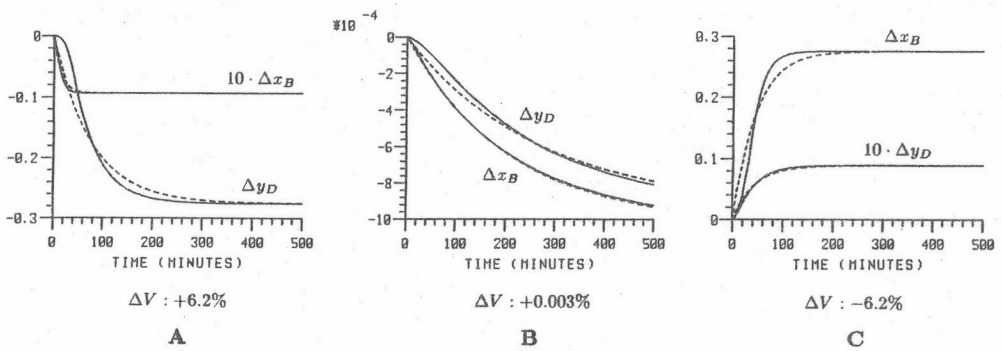


*Figure A.2-1.* (—) Nonlinear open loop responses $\Delta y_D$ and $\Delta x_B$ for changes in boilup $V$ (reflux $L$ constant). ( - - - ) Approximation with linear first order response. (Different time constants for A, B and C). A: $V + 6.2\%$, B: $V + 0.003\%$, C: $V - 6.2\%$.

*Table A.2-3.* Tray compositions for operating conditions A and C.

| Tray | A | | C | |
|---|---|---|---|---|
| | $x$ | $y$ | $x$ | $y$ |
| 41 | 0.99000001 | 0.00000000 | 0.89999998 | 0.00000000 |
| 40 | 0.98507464 | 0.99000001 | 0.85714287 | 0.89999998 |
| 39 | 0.97891331 | 0.98584270 | 0.80946749 | 0.86436397 |
| 38 | 0.97124165 | 0.98064220 | 0.75826764 | 0.82472157 |
| 37 | 0.96174449 | 0.97416693 | 0.70532095 | 0.78214854 |
| 36 | 0.95007116 | 0.96615076 | 0.65266412 | 0.73812300 |
| 35 | 0.93584847 | 0.95629781 | 0.60229003 | 0.69433850 |
| 34 | 0.91870391 | 0.94429302 | 0.55585837 | 0.65245205 |
| 33 | 0.89830160 | 0.92982209 | 0.51450431 | 0.61384380 |
| 32 | 0.87439108 | 0.91260135 | 0.47878328 | 0.57945764 |
| 31 | 0.84686637 | 0.89241952 | 0.44873506 | 0.54975533 |
| 30 | 0.81582677 | 0.86918712 | 0.42401719 | 0.52477002 |
| 29 | 0.78162557 | 0.84298790 | 0.40405512 | 0.50421697 |
| 28 | 0.74489015 | 0.81412017 | 0.38817218 | 0.48761836 |
| 27 | 0.70649838 | 0.78311342 | 0.37568399 | 0.47441158 |
| 26 | 0.66750675 | 0.75070858 | 0.36595631 | 0.46402755 |
| 25 | 0.62903917 | 0.71779740 | 0.35843393 | 0.45593894 |
| 24 | 0.59216058 | 0.69532860 | 0.35264966 | 0.44968402 |
| 23 | 0.55776387 | 0.65420103 | 0.34822109 | 0.44487435 |
| 22 | 0.52649474 | 0.62516826 | 0.34484178 | 0.44119197 |
| 21 | 0.49872494 | 0.59877533 | 9.34226966 | 0.43838206 |
| 20 | 0.47416389 | 0.57493830 | 0.29737207 | 0.38832030 |
| 19 | 0.44553304 | 0.54654711 | 0.25339118 | 0.33734646 |
| 18 | 0.41298330 | 0.51345152 | 0.21191093 | 0.28741339 |
| 17 | 0.37701508 | 0.47582585 | 0.17416464 | 0.24031939 |
| 16 | 0.33849627 | 0.43424863 | 0.14091858 | 0.19746466 |
| 15 | 0.29860669 | 0.38972306 | 0.11246721 | 0.15971924 |
| 14 | 0.25870702 | 0.34361297 | 8.87127668E-02 | 0.12741737 |
| 13 | 0.22015929 | 0.29749119 | 6.92852587E-02 | 0.10044810 |
| 12 | 0.18414706 | 0.25293222 | 5.36631495E-02 | 7.83913583E-02 |
| 11 | 0.15154333 | 0.21130413 | 4.12711129E-02 | 6.06550165E-02 |
| 10 | 0.12285385 | 0.17361607 | 3.15471478E-02 | 4.65858951E-02 |
| 9 | 9.82341841E-02 | 0.14045265 | 2.39814352E-02 | 3.55459340E-02 |
| 8 | 7.75578097E-02 | 0.11199372 | 1.81338135E-02 | 2.69563195E-02 |
| 7 | 6.05053641E-02 | 8.80929977E-02 | 1.36372205E-02 | 2.03172937E-02 |
| 6 | 4.66509089E-02 | 6.83813393E-02 | 1.01931207E-02 | 1.52121522E-02 |
| 5 | 3.55311297E-02 | 5.23663759E-02 | 7.56312115E-03 | 1.13019431E-02 |
| 4 | 2.66932649E-02 | 3.95125374E-02 | 5.55941742E-03 | 8.31601024E-03 |
| 2 | 1.42609123E-02 | 2.12399177E-02 | 2.87815696E-03 | 4.31103166E-03 |
| 1 | 9.99999978E-03 | 1.49253728E-02 | 2.00000009E-03 | 2.99700303E-03 |

## A.3 Linearized Model

We linearize the material balance on each tray ($dL_i = dL, \quad dV_i = dV$):

$$M_i\dot{x}_i = L_{i+1}dx_{i+1} - (L_i + K_iV_i)dx_i + K_{i-1}V_{i-1}dx_{i-1} + (x_{i+1} - x_i)dL - (y_i - y_{i-1})dV$$

Here $K_i$ is the linearized VLE-constant:

$$K_i = \frac{dy_i}{dx_i} = \frac{\alpha}{(1 + (\alpha - 1)x_i)^2}$$

and $y_i, x_i, L_i$ and $V_i$ are the steady-state values at the nominal operating point. Written in the standard state variable form in terms of deviation variables the model becomes

$$\dot{x} = Ax + Bu, \qquad y = Cx$$

where $x = (dx_1, \ldots, dx_{N+1})^T$ are the tray compositions, $u = (dL, dV)^T$ are the manipulated inputs and $y = (dy_D, dx_B)^T$ are the controlled outputs. The state matrix $A = \{a_{i,j}\}$ is tri-diagonal:

$$\begin{array}{lll} i \neq N+1: & a_{i,i+1} = L_{i+1}/M_i \\ & a_{i,i} = -(L_i + K_iV_i)/M_i \\ i \neq 1: & a_{i,i-1} = K_{i-1}V_{i-1}/M_i \end{array}$$

Input matrix $B = \{b_{i,j}\}$:

$$\begin{array}{ll} i \neq N+1: & b_{i,1} = (x_{i+1} - x_i)/M_i, \quad b_{N+1,1} = 0 \\ i \neq 1, i \neq n+1: & b_{i,2} = -(y_i - y_{i-1})/M_i, \quad b_{N+1,2} = 0, \quad b_{1,2} = (y_1 - x_1)/M_1 \end{array}$$

Output matrix C:

$$C = \begin{pmatrix} 0 & 0 & 0 & \ldots & 0 & 1 \\ 1 & 0 & \ldots & 0 & 0 & 0 \end{pmatrix}$$

The condenser drum is assumed to be under perfect level control

$$V = L + D$$

Thus, if a different set of manipulated variables, $U = (dD, dV)^T$ is employed the new model is obtained via the linear transformation

$$\begin{pmatrix} dD \\ dV \end{pmatrix} = \begin{pmatrix} -1 & 1 \\ 0 & 1 \end{pmatrix} \begin{pmatrix} dL \\ dV \end{pmatrix}$$

*Table A.4-1.* Gain Information

| Operating Point | A | C |
|---|---|---|
| $G_{LV}(0)$ | $\begin{pmatrix} 0.878 & -0.864 \\ 1.082 & -1.096 \end{pmatrix}$ | $\begin{pmatrix} 1.604 & -1.602 \\ 0.01865 & -0.02148 \end{pmatrix}$ |
| $G^s_{LV}(0)$ (scaled compositions) | $\begin{pmatrix} 87.8 & -86.4 \\ 108.2 & -109.6 \end{pmatrix}$ | $\begin{pmatrix} 16.0 & 16.023 \\ 9.3 & -10.71 \end{pmatrix}$ |
| RGA $\lambda_{11}(0)$ | 35.1 | 7.5 |
| $G_{LV}(\infty)$ | $\frac{0.01}{s}\begin{pmatrix} 0.45 & -0.36 \\ 0.56 & -0.65 \end{pmatrix}$ | $\frac{0.01}{s}\begin{pmatrix} 6.5 & -6.5 \\ 0.08 & -0.10 \end{pmatrix}$ |
| $G^s_{LV}(\infty)$ | $\frac{1}{s}\begin{pmatrix} 0.45 & -0.36 \\ 0.56 & -0.65 \end{pmatrix}$ | $\frac{1}{s}\begin{pmatrix} 0.65 & -0.65 \\ 0.38 & -0.52 \end{pmatrix}$ |
| $\lambda_{11}(\infty)$ | 3.2 | 3.7 |

## A.4 Gain Information

From the gain information in Tables A.4-1 through A.4-3 one can see that the nonlinearity appears mostly in the low-frequency range and is much less pronounced for high frequencies. The time constant ($\tau$ = 75min) used in the simulations represents an average value based on the simulations shown in Fig. A.2-1.

*Table A.4-2.* Singular Value Decomposition of Gain Matrices

| Configuration | *LV* | *DV* |
|---|---|---|
| $G(0)$ | $\begin{pmatrix} 0.878 & -0.864 \\ 1.082 & -1.096 \end{pmatrix}$ | $\begin{pmatrix} -0.878 & 0.014 \\ -1.082 & -0.014 \end{pmatrix}$ |
| RGA $\lambda_{11}$ | 35.1 | 0.45 |
| Condition number $\kappa$ | 141.7 | 70.8 |
| $SVD;\ G = U\Sigma V^H$ | | |
| $U$ | $\begin{pmatrix} -0.625 & 0.781 \\ -0.781 & -0.625 \end{pmatrix}$ | $\begin{pmatrix} -0.630 & 0.777 \\ -0.777 & -0.630 \end{pmatrix}$ |
| $\Sigma$ | $\begin{pmatrix} 1.972 & 0 \\ 0 & 0.0139 \end{pmatrix}$ | $\begin{pmatrix} 1.393 & 0 \\ 0 & 0.0197 \end{pmatrix}$ |
| $V$ | $\begin{pmatrix} -0.707 & 0.708 \\ 0.708 & 0.707 \end{pmatrix}$ | $\begin{pmatrix} 1.000 & -0.001 \\ 0.001 & 1.000 \end{pmatrix}$ |

*Table A.4-3.* Disturbance gains for LV-configuration.

| | $x_F$ | $F$ | $q_F$ | $V_d$ |
|---|---|---|---|---|
| $dy_D$ | 0.881 | 0.394 | 0.868 | 0.864 |
| $dx_B$ | 1.119 | 0.586 | 1.092 | 1.096 |

# References


Arkun, Y., V. Manousiouthakis and A. Palazoglu, "A Case Study of Decoupling Control in Distillation." *Ind. Eng. Chem. Process Des. Dev.*, **23**, 93-101 (1984).

Åström, K. J., "Frequency Domain Properties of Otto Smith Regulators." *Int. J. Control,* **26**, 307-314 (1977).

Åström, K. J., P. Hagander and J. Sternby, "Zeros of Sampled Systems." *Automatica*, **20**, 31-38 (1984).

Åström, K. J. and B. Wittenmark, *Computer Controlled Systems,* Prentice-Hall, Englewood Cliffs, NJ (1984).

Bellman, R., *Introduction to Matrix Analysis,* McGraw-Hill Book Company, New York (1970).

Bjork, A. and T. Elfring, "Algorithms for Confluent Vandermonde Systems." *Numer. Math.*, **18**, 44-60 (1973).

Black, H. S. "Inventing the Negative Feedback Amplifier." *IEEE Spectrum*, 55-60 (1977).

Bode, H. W., "Feedback – The History of an Idea." in *Selected Papers on Mathematical Trends in Control Theory.*" Dover, NY, 106-123 (1964).

Bristol, E. H., "On a New Measure of Interaction for Multivariable Process Control." *IEEE Trans. Autom. Control*, **AC-11**, 133-134 (1966).

Bristol, E. H., "A New Process Interaction Concept, Pinned Zeros." *Internal Report of the Foxboro Co.*, Boston, MA (1980).

Brosilow, C. B., "The Structure and Design of Smith Predictors from the Viewpoint of Inferential Control." *Proc. of Joint Automatic Control Conf.*, Denver, CO (1979).

Bruns, D. D. and C. R. Smith, "Singular Value Analysis: A Geometrical Structure For Multivariable Processes." *AIChE Winter Meeting*, Orlando, Fla. (1982).

Buckley, P. S., W. L. Luyben and J. P. Shunta, *Design of Distillation Column Control Systems.* Instrument Society of America, Research Triangle Park, NC (1985).

Chen, S., *Control System Design for Multivariable Uncertain Processes.*, Ph.D. Thesis, Chem. Eng. Dept., Case Western Reserve University, Cleveland, OH (1984).

Chu, C. C., *$H_\infty$-Optimization and Robust Multivariable Control*, Ph.D. Thesis, University of Minnesota, Minneapolis, MN (1985).

Churchill, R. V. and J. W. Brown, *Complex Variables and Applications*, McGraw-Hill, New York (1984).

Cohen, G. H. and G. A. Coon, "Theoretical Considerations of Retarded Control." *Trans. ASME*, **75**, 827 (1953).

Cutler, C. R. and B. L. Ramaker, "Dynamic Matrix Control - A Computer Control Algorithm." *AIChE National Mtg.*, Houston, TX (1979); also *Proc. Joint Autom. Control Conf.*, San Francisco, CA (1980).

Dahlquist, G., A. Björck (translated by N. Anderson), *Numerical Methods*, Prentice-Hall, Englewood Cliffs, NJ (1974).

Dailey, R. L., *Conic Sector Analysis for Digital Control Systems with Structured Uncertainties*, Ph.D. Thesis, California Institute of Technology, Pasadena, CA (1987).

Davison, E. J., "Multivariable Tuning Regulators: The Feedforward and Robust Control of a General Servomechanism Problem." *IEEE Trans. Autom. Control*, **AC-21**, 35-47 (1976).

Desoer, C. A. and A. N. Gündes, "Decoupling Linear Multi-Input Multi-Output Plants by Dynamic Output Feedback." *IEEE Trans. Autom. Control*, **AC-31**, 744-750 (1986).

Desoer, C. A. and C. A. Lin, "A Comparative Study of Linear and Nonlinear MIMO Feedback Configurations". *Intl. J. Syst. Sci.*, **16**, 789-813 (1985).

Desoer, C. A. and J. D. Schulman, "Zeros and Poles of Matrix Transfer Functions and Their Dynamical Interpretation." *IEEE Trans. Circuits and Systems*, **CAS-21**, 3 (1974).

Desoer, C. A. and M. Vidyasagar, *Feedback Syst ns: Input-Output Properties*, Academic Press, New York (1975).

Doukas, N. and W. Luyben, "Control of estream Columns Separating Ternary Mixtures." *Anal. Instrum.*, **16**, 51-58 (1978).

Doyle, J. C., "Analysis of Control Systems With Structured Uncertainty." *IEE Proc., Part D*, **129**, 242 (1982).

Doyle, J. C., *Lecture Notes – ONR/Honeywell Workshop on Advances on Multivariable Control* (1984).

Doyle, J. C., "Structured Uncertainty in Control System Design." *Proc. IEEE Conf. on Decision and Control*, Ft. Lauderdale, FL (1985).

Doyle, J. C., R. S. Smith and D. F. Enns, "Control of Plants with Saturation Nonlinearities." *Proc. American Control Conf.*, Minneapolis, MN, 1034-1039 (1987).

Doyle, J. C. and G. Stein, "Multivariable Feedback Design: Concepts for a Classical/Modern Synthesis." *IEEE Trans. Autom. Control*, **AC-26**, 4 (1981).

Doyle, J. C. and J. E. Wall, "Performance and Robustness Analysis for Structured Uncertainty." *Proc. IEEE Conf. on Decision and Control*, Orlando, FL (1982).

Economou, C. G. and M. Morari, "Internal Model Control – 6. Multiloop Design." *Ind. Eng. Chem. Proc. Des. & Dev.*, **25**, 411-419 (1986).

Fan, M. K. H. and A. L. Tits, "Characterization and Efficient Computation of the Structured Singular Value." *IEEE Trans. Autom. Control*, **AC-31**, 734-743 (1986).

Feingold, D. G. and R. S. Varga, "Block Diagonally Dominant Matrices and Generalizations of the Gerschgorin Circle Theorem." *Pacific J. Maths.*, **12**, 1241-1250 (1962).

Foss, A. S., "Critique of Chemical Process Control Theory." *AIChE J.*, **19**, 209 (1973).

Francis, B. A., *A Course in $H_\infty$ Control Theory. Lecture Notes in Control and Information Sciences,* Springer-Verlag, Berlin (1987).

Frank, P. M., *Entwurf von Regelkreisen mit vorgeschriebenem Verhalten*, G. Braun, Karlsruhe (1974).

Franklin, G. F., J. D. Powell and A. Emami-Naeini, *Feedback Control of Dynamic Systems*, Addison-Wesley, Reading, MA (1986).

Fuentes, C. and W. L. Luyben, "Control of High – Purity Distillation Columns." *Ind. & Eng. Chem. Process Des. Dev.*, **22**, 361-366 (1983).

Gantmacher, F. R., *The Theory of Matrices,* Chelsea Publishing Co., New York (1959).

Garcia, C. E. and M. Morari, "Internal Model Control – 1. A Unifying Review and Some New Results. " *Ind. Eng. Chem. Process Des. & Dev.*, **21**, 308-323 (1982).

Garcia, C. E. and M. Morari, "Internal Model Control – 2. Design Procedure for Multivariable Systems." *Ind. Eng. Chem. Process Des. & Dev.*, **24**, 472-484 (1985a).

Garcia, C. E. and M. Morari, "Internal Model Control – 3. Multivariable Control Law Computation and Tuning Guidelines." *Ind. Eng. Chem. Process Des. & Dev.*, **24**, 484-494 (1985b).

Giloi, W., *Zur Theorie und Verwirklichung einer Regelung für Laufzeitstrecken nach dem Prinzip der ergänzenden Rückführung*, Ph.D. Thesis, TH Stuttgart (1959).

Golub, G. H. and C. F. Van Loan, *Matrix Computations.* Johns Hopkins University Press, Baltimore, MD (1983).

Grosdidier, P. and M. Morari, "Interaction Measures for Systems Under Decentralized Control." *Automatica*, **22**, 309-319 (1986).

Grosdidier, P., M. Morari and B. R. Holt, "Closed Loop Properties from Steady State Gain Information." *Ind. Eng. Chem. Fundam.*, **24**, 221-235 (1985).

Hanus, R., M. Kinnaert and J. L. Henrotte, "Conditioning Technique, a General Anti-Windup and Bumpless Transfer Method." *Automatica*, **23**, 729-739 (1987).

Holt, B. R. and M. Morari, "Design of Resilient Processing Plants – V. The Effect of Deadtime on Dynamic Resilience." *Chem. Eng. Sci.*, **40**, 1229-1237 (1985a).

Holt, B. R. and M. Morari, "Design of Resilient Processing Plants – VI. The Effect of Right-Half-Plane Zeros on Dynamic Resilience." *Chem. Eng. Sci.*, **40**, 59-74 (1985b).

Horowitz, I. M., *Synthesis of Feedback Systems,* Academic Press, London (1963).

Horowitz, I. "Some Properties of Delayed Controls (Smith Predictors)." *Int. J. Control*, **38**, 977-990 (1983).

Isermann, R., *Digital Control Systems,* Springer-Verlag, Berlin (1981).

Jenkins, G. M. and D. G. Watts, *Spectral Analysis and its Applications,* Holden-Day, San Francisco, CA (1969).

Kantor, J. C. and R. N. Andres, "Characterization of 'Allowable Perturbations' for Robust Stability." *IEEE Trans. Autom. Control*, **AC-28**, 107-109 (1983).

Kapoor, N., T. J. McAvoy and T. E. Marlin, "Effect of Recycle Structure on Distillation Tower Time Constant." *AIChE J.*, **32**, 411-418 (1986).

Kestenbaum, A., R. Shinnar and F. E. Thau, "Design Concepts for Process Control." *Ind. & Eng. Chem. Proc. Des. & Dev.*, **15**, 2 (1976).

Kouvaritakis, B. and M. Latchman, "Necessary and Sufficient Stability Criterion for Systems with Structured Uncertainties: The Major Principal Direction Alignment Principle." *Int. J. Control*, **42**, 575-598 (1985).

Kucera, V., "State Space Approach to Discrete Linear Control." *Kybernetika*, **8**, 233 (1972).

Kuo, B. C., *Digital Control Systems,* Holt, Rinehart and Winston, New York (1980).

Kwakernaak, H. and R. Sivan, *Linear Optimal Control Systems,* Wiley-Interscience, New York (1972).

Laub, A. J., "A Schur Method for Solving Riccati Equations." *IEEE Trans. Automatic Control*, **AC-24**, 913-921 (1979).

Laub, A. J. and B. C. Moore, "Calculation of Transmission Zeros Using QZ Techniques." *Automatica*, **14**, 557 (1978).

Laughlin, D. L., K. G. Jordan and M. Morari, "Internal Model Control and Process Uncertainty: Mapping Uncertainty Regions for SISO Controller Design." *Int. J. Control*, **44**, 1675-1698 (1986).

Lehtomaki, N. A., *Practical Robustness Measures in Multivariable Control System Analysis.*, Ph.D. Thesis, Dept. of Electrical Eng. and Computer Sci., Massachusetts Institute of Technology, Cambridge, MA (1981).

Lewin, D. R., R. E. Heersink, A. Skjellum, D. L. Laughlin, D. E. Rivera and M. Morari, "ROBEX: Robust Control Synthesis via Expert System." *Proc. 10th IFAC World Congress, Munich*, **6**, 369-374 (1987).

Limebeer, D. J. N., "The Application of Generalized-Diagonal Dominance to Linear System Stability Theory." *Int. J. Control*, **36**, 185-212 (1982).

Locatelli, A., F. Romeo, R. Scattolini and N. Schiavoni, "A Parameter Optimization Approach to the Design of Reliable Robust Decentralized Regulators." *Laboratorio di Controlli Automatici*, Politecnico di Milano, Relazione Interna, **82-7** (1982).

Lunze, J., "Notwendige Modellkenntnisse zum Entwurf robuster Mehrgrössenregler mit I-Charakter." *Messen, Steuern, Regeln*, **25**, 608-612 (1982).

Lunze, J., "Untersuchungen zur Autonomie der Teilregler einer Dezentralen Regelung mit I-Charakter." *Messen, Steuern, Regeln*, **26**, 451-455 (1983).

Lunze, J., "Determination of Robust Multivariable I-Controllers by Means of Experiment and Simulation." *Syst. Anal. Model. Simul.*, **2**, 227-249 (1985).

Luyben, W. L., "Distillation Decoupling." *AIChE J.*, **16**, 198-203 (1970).

Maxwell, J. C., "On Governors," *Proc. of the Royal Society of London*, **16**, 270-283 (1867/68); in *Mathematical Trends in Control Theory*, R. Bellman and R. Kalaba, eds., Dover, NY, 3-17 (1964).

Mayr, O., *The Origins of Feedback Control*, MIT Press, Cambridge, MA (1970).

McAvoy, T. J., *Interaction Analysis, ISA Monograph*, ISA, Research Triangle Pk (1983).

Mees, A. I., "Achieving Diagonal Dominance." *Systems and Control Letters*, **1**, 155-158 (1982).

Mijares, G., J. D. Cole, N. W. Naugle, H. A. Preisig and C. D. Holland, "A New Criterion for the Pairing of Control and Manipulated Variables." *AIChE J.*, **32**, 1439-1449 (1986).

Moczek, J. S., R. E. Otto and T. J. Williams, "Approximation Model for the Dynamic Responses of large Distillation Columns." *Proc. 2nd IFAC Congress*, Basel (1963); also published in *Chem. Eng. Progress Symp. Series*, **61**, 136-146 (1965).

Molinari, B. P., "The Stabilizing Solution of the Algebraic Riccati Equation." *SIAM J. Control*, **11**, 262-271 (1973).

Moore, B. C., "Principal Component Analysis in Linear Systems: Controllability, Observatibility, and Model Reduction," *IEEE Trans. Autom. Control*, **AC-26**, 17-32 (1981).

Morari, M., "Design of Resilient Processing Plants-III. A General Framework for the Assessment of Dynamic Resilience." *Chem. Eng. Sci.*, **38**, 1881-1891 (1983a).

Morari, M., "Robust Stability of Systems with Integral Control." *Proc. IEEE Conf. on Decision and Control*, San Antonio, TX, 865-869 (1983b).

Morari, M., "Robust Stability of Systems with Integral Control." *IEEE Trans. Autom. Control*, **AC-30**, 574-577 (1985).

Morari, M., W. Grimm, M. J. Oglesby and I. D. Prosser, "Design of Resilient Processing Plants – VII. Design of Energy Management System for Unstable Reactors – New Insights." *Chem. Eng. Sci.*, **40**, 187-198 (1985).

Morari, M., S. Skogestad and D. E. Rivera, "Implications of Internal Model Control for PID Controllers. " *Proc. of American Control Conf.*, San Diego, CA, 661-666 (1984).

Morari, M., E. Zafiriou and B. R. Holt, "Design of Resilient Processing Plants – X. New Characterization of the Effect of RHP Zeros." *Chem. Eng. Sci.*, **42**, 2425-2428 (1987).

Nett, C. N. and V. Manousiouthakis, "Euclidean Condition and Block Relative Gain: Connections, Conjectures and Clarifications." *IEEE Trans. Autom. Control*, **5**, 405-407 (1987).

Nett, C. N. and H. Spang, "Control Structure Design: A Missing Link in the Evolution of Modern Control Theories." *Proc. American Control Conf.*, Minneapolis, MN (1987).

Nett, C. N. and J. A. Uthgenannt, "An Explicit Formula and an Optimal Weight for the 2-Block Structured Singular Value Interaction Measure." *Automatica*, **24**, 261-265 (1988).

Newton, G. C., L. A. Gould and J. F. Kaiser, *Analytical Design of Feedback Controls,* Wiley, New York (1957).

Niederlinski, A., "A Heuristic Approach to the Design of Linear Multivariable Interacting Control Systems." *Automatica*, **7**, 691-701 (1971).

Nyquist, H., "Regeneration Theory." *Bell Syst. Tech. J.*, **11**, 126-147 (1932).

Osborne, E. E., "On Pre-Conditioning of Matrices." *I. Assoc. Comput. Mach.*, **7**, 338-345 (1960).

Palmor, Z. J. and R. Shinnar, "Design of Advanced Process Controllers." *AIChE J.*, **27**, 793-805 (1981).

Postlethwaite, I. and Y. K. Foo, "Robustness with Simultaneous Pole and Zero Movement across the $j\omega$-Axis." *Automatica*, **21**, 433-443 (1985).

Postlethwaite, I. and A. G. J. MacFarlane, *A Complex Variable Approach to the Analysis of Linear Multivariable Feedback Systems,* Springer Verlag, Berlin (1979).

Prett, D. M. and R. D. Gillette, "Optimization and Constrained Multivariable Control of a Catalytic Cracking Unit." *AIChE National Mtg.*, Houston, TX (1979); also *Proc. Joint Autom. Control Conf.*, San Francisco, CA (1980).

Ramkrishna, D. and N. R. Amundson, *Linear Operator Methods in Chemical Engineering with Appication to Transport and Chemical Reaction Systems,* Prentice-Hall, Englewood Cliffs, NJ (1985).

Richalet, J. A., A. Rault, J. L. Testud and J. Papon, "Model Predictive Heuristic Control: Applications to an Industrial Process." *Automatica*, **14**, 413-428 (1978).

Rijnsdorp, J. E., "Interaction in Two-Variable Control Systems for Distillation Columns – I." *Automatica*, **1**, 15-28 (1965).

Rivera, D. E., S. Skogestad and M. Morari, "Internal Model Control. 4. PID Controller Design." *Ind. Eng. Chem. Proc. Des. & Dev.*, **25**, 252-265 (1986).

Rivera, D. E., *Modeling Requirements for Process Control.* Ph.D. Thesis, California Institute of Technology (1987).

Rosenbrock, H. H., *Computer Aided Control System Design,* Academic Press, London (1974).

Ryskamp, C. J., "Explicit Versus Implicit Decoupling in Distillation Control." *Chemical Process Control 2 Conf.*, Sea Island, GA, Jan. 18-23 (1981), (T. F. Edgar and D. E. Seborg, eds.), United Engineering Trustees (1982), available from AIChE.

Sandell Jr., N. and M. Athans, "On 'Type L' Multivariable Linear Systems." *Automatica*, **9**, 171-176 (1973).

Seneta, E., *Non-Negative Matrices,* John Wiley, New York (1973).

Shinskey, F. G., *Distillation Control, Second Edition*, McGraw Hill, New York (1984).

Skogestad, S., *Studies on Robust Control of Distillation Columns.*, Ph.D. Thesis, California Institute of Technology, Pasadena, CA (1987).

Skogestad, S. and M. Morari, "Control Configurations for Distillation Columns." *AIChE J.*, **33**, 1620-1635 (1987a).

Skogestad, S. and M. Morari, "Design of Resilient Processing Plants-IX. Effect of Model Uncertainty on Dynamic Resilience." *Chem. Eng. Sci.*, **42**, 1765-1780 (1987b).

Skogestad, S. and M. Morari, "Implications of Large RGA-Elements on Control Performance." *Ind. & Eng. Chem. Research*, **26**, 2323-2330 (1987c).

Skogestad, S. and M. Morari, "Effect of Disturbance Directions on Closed Loop Performance." *Ind. Eng. Chem. Research*, **26**, 2029-2035 (1987d).

Skogestad, S. and M. Morari, "LV-Control of a High-Purity Distillation Column." *Chem. Eng. Sci.* , **43**, 33-48 (1988a).

Skogestad, S. and M. Morari, "Robust Performance of Decentralized Control Systems by Independent Designs." *Proc. American Control Conf.*, Minneapolis, MN, 1325-1330 (1987); *Automatica*, submitted (1988b).

Skogestad, S. and M. Morari, "Some New Properties of the Structured Singular Value." *IEEE Trans. Autom. Control*, in press (1988c).

Skogestad, S. and M. Morari, "Understanding the Dynamic Behavior of Distillation Columns." *Ind. Eng. Chem. Research*, in press (1988d).

Skogestad, S., M. Morari and J. C. Doyle, "Robust Control of Ill-Conditioned Plants: High Purity Distillation." *IEEE Trans. Autom. Control*, in press (1988).

Smith, C. A. and A. B. Corripio, *Principles and Practice of Automatic Process Control,* John Wiley & Sons, New York, NY (1985).

Smith, O. J. M., "Closer Control of Loops with Dead Time." *Chem. Eng. Progress*, **53(5)**, 217-219 (1957).

Stanley, G. M., M. Marino-Gallaraga and T. J. McAvoy, "Short Cut operability Analysis. 1. The Relative Disturbance Gain." *Ind. Eng. Chem. Process Des. Dev.*, **24**, 1181-1188 (1985).

Stein, G., "Beyond Singular Values and Loop Shapes." *unpublished manuscript* (1985).

Stephanopoulos, G., *Chemical Process Control. An Introduction to Theory and Practice,* Prentice-Hall, Englewood Cliffs, NJ (1984).

Stewart, G. C., *Introduction to Matrix Computations,* Academic Press, New York (1973).

Strang, G., *Linear Algebra and Its Applications. Second Edition,* Academic Press, New York (1980).

Thompson, P. M., *Conic Sector Analysis of Hybrid Control Systems.*, Ph.D. Thesis, Massachusetts Institute of Technology, Cambridge, MA (1982).

Toijala (Waller), K. and K. Fagervik, "A Digital Simulation Study of Two-Point Feedback Control of Distillation Columns." *Kemian Teollisuus*, **29**, 1-12 (1982).

Vidyasagar, M., *Control System Synthesis - A Factorization Approach,* MIT Press, Cambridge, MA (1985).

Vidyasagar, M., H. Schneider and B. A. Francis, "Algebraic and Topological Aspects of Feedback Stabilization." *IEEE Trans. Automatic Control*, **AC-27**, 880 (1982).

Vyshnegradskii, I. A., "On Controllers of Direct Action." *Izv. SPB Tekhnolog. Inst.* (1877).

Wolfe, C. A. and J. S. Meditch, "Theory of System Type for Linear Multivariable Servomechanisms." *IEEE Trans. Automatic Control*, **AC-22**, 36-46 (1977).

Youla, D. C., J. J. Bongiorno and H. A. Jabr, "Modern Wiener-Hopf Design of Optimal Controllers – Part I. The Single Input-Output Case." *IEEE Trans. Autom. Control*, **AC-21**, 3-13 (1976).

Youla, D. C., H. A. Jabr and J. J. Bongiorno, "Modern Wiener-Hopf Design of Optimal Controllers – Part II. The Multivariable Case." *IEEE Trans. Autom. Control*, **AC21**, 319-338 (1976).

Zafiriou, E., *A Methodology for the Synthesis of Robust Control Systems for Multivariable Sampled-Data Processes*, Ph.D. Thesis, California Institute of Technology, Pasadena, CA (1987).

Zafiriou, E. and M. Morari, "Digital Controllers for SISO Systems. A Review and a New Algorithm." *Int. J. Control*, **42**, 855-876 (1985).

Zafiriou, E. and M. Morari, "Design of Robust Controllers and Sampling Time Selection for SISO Systems." *Int. J. Control*, **44**, 711-735 (1986a).

Zafiriou, E. and M. Morari, "Design of the IMC Filter by Using the Structured Singular Value Approach." *Proc. American Control Conf.*, Seattle, WA, 1-6 (1986b).

Zafiriou, E. and M. Morari, "Digital Controller Design for Multivariable Systems with Structural Closed–Loop Performance Specifications." *Int. J. Control*, **46**, 2087-2111 (1987).

Zames, G., "Feedback and Optimal Sensitivity: Model Reference Transformations, Multiplicative Seminorms and Approximate Inverses." *IEEE Trans. Autom. Control*, **AC-26**, 301-320 (1981).

Zames, G. and B. A. Francis, "Feedback, Minimax Sensitivity and Optimal Robustness." *IEEE Trans. Autom. Control*, **AC-28**, 585 (1983).

Ziegler, J. G. and N. B. Nichols, "Optimum Settings for Automatic Controllers." *Trans. ASME*, **64**, 759-768 (1942).

Zirwas, H. C., *Die ergänzende Rückführung als Mittel zur schnellen Regelung von Regelstrecken mit Laufzeit,* Ph.D. Thesis, TH Stuttgart (1958).

# Index


— Symbols —

2-norm, 19, 215, 217, 225, 232

— A —

A/D converter, 143, 151
Åström, 139, 164, 182, 434
Actuator uncertainty, 223
Aliasing, 145
Allpass, 13, 58, 61
Amplitude-ratio, 215
Amundson, 5
Andres, 291
Anti-aliasing prefilter, 145, 154, 164, 393
  unstable systems, 189
Arkun, 357
Athans, 234

— B —

Balanced realization, 296, 325, 457
Bandwidth, 24
  sampled-data, 158
Batch reactor
  uncertainty, **254**
Bellman, 233
Björck, 326
Bjork, 110
Black, 1
Block diagonal, 367, 371, 375, 390
Bode, 1
Bode plot, 215, 444
Bode stability criterion, 222
Bongiorno, 325
Bristol, 291, 357
Brosilow, 56, 140
Brown, 5
Bruns, 233
Buckley, 110

— C —

Calculus of residues, 61
Cascade control, 135ff
Causal, 11, **12**
  MIMO system, **206**
  sampled-data, **146**
    MIMO, 395
Characteristic equation, 206, 365
Characteristic loci, 366, 390
Characteristic polynomial, 219, 232, 365
Chen, 84
Chu, 309, 326
Churchill, 5
Classic controllers, 132
Classic feedback, 42
  IMC implications, 113
  MIMO system, 217
  sampled-data, 143ff, **393**
Cohen, 113, 123, 125, 139
Column
  dominance, 372
Complementary sensitivity function,

24ff, 299
IMC, 45
MIMO system, 227
sampled-data, 151ff
MIMO, **401**
unstable systems, 86, 92, 100
Condition number, 224, 241, 344, 346
as sensitivity measure, 258ff
distillation, 440
minimized, 344
scaling, 338
Constraints, 44, 49
actuator, 328
Control structure, 327, 360
Controller
diagonal, 333, 339, 347, 351, 356, 361
distillation, 444
inverse-based, 339, 346, 348, 351
distillation, 437, 444
$\mu$-optimal, 445–446, 449, 451
Controller implementation, 44, 85
Controller parametrization, 3, 44
MIMO, 296ff
unstable systems, **87**
sampled-data, **184**
Coon, 113, 123, 125, 139
Corripio, 139
Cutler, 3, 56

— D —

D/A converter, 145, 393
Dahlin, 164
Dahlquist, 326
Dailey, 164
Davison, 389
Deadbeat controllers, 164, 169, 182
Deadtime, 115, 327
error, 125
uncertainty, 75, 178
Decentralized control, 359ff
Decentralized integral controllable, **361**, 363ff, 375, 387
$2 \times 2$ systems, 376
Decoupler, xv, 333, 341, 346, 357, 446
distillation, 444
one-way, 341, 343, 347, 351
Decoupling, 351
ideal, 347
simplified, 347
steady state, 347
Desoer, 5, 38, 233, 356–357
Diagonal dominance, 372, 384, 390
generalized, 373, 375, 378, 390
Directionality, 327, 332, 351
Distillation, 5, 118, 333ff, 346, 349, 356–357, 376, 383
additive uncertainty, 262
base level control, 104ff
sampled-data, **200**
DV configuration, 349ff
element uncertainty, 261
high-purity, 271ff, **320**
input uncertainty, 242, 252
logarithmic compositions, 438, 453, 457
LV configuration, 334, 349ff, 437ff
model, 459ff
nonlinearity, 438
Disturbance
condition number, 329ff, 333, 347, 351
direction, **328**, 329–330
Dominance
column, 372
generalized, 374
row, 373

Doukas, 376
Doyle, xv, 2, 38, 56, 234, 291–292, 326
Dynamic Matrix Control, 3

— E —

Economou, 390
Edgar, 164
Eigenvalue, 206, 213
Eigenvector, 211
Elfring, 110
Enns, 56
Euclidean norm, **209**

— F —

Fagervik, 357
Fan, 291, 357
Feedforward control, 5, 58, 131ff
Feingold, 390
Field, 208
Filter
  IMC, **52**, 64ff
    ill-conditioned plants, 312, 315, 321
    interconnection structure, 313ff
    interpretation, 99ff, 195ff
    MIMO, 311ff
    MIMO, sampled-data, 420ff
    sampled-data, 170ff
    sampled-data, unstable systems, 193ff
    speed of response, 65
    unstable systems, 96ff
  time constant, 71
Foo, 291–292
Foss, xv
Francis, 4, 110, 201
Frank, 55–56, 84, 110
Franklin, 5
Frobenius norm, **209**, 211
Fuentes, 457

— G —

Gündes, 357
Gain margin, 139
Gantmacher, 233
Garcia, 3, 56, 182, 291
Gershgorin bands, 390
Gillette, 56
Giloi, 55
Golub, 110
Gould, 1, 38, 55, 84
Grosdidier, 291, 389–390

— H —

Hagander, 164
Hanus, 56
Henrotte, 56
Hermitian matrix, 212–213
Hilbert space, 89, 185, 402
Holt, 38, 233, 291, 326, 356–357, 389
Horowitz, 38, 140
$H_2$ objective, 34
$H_2$-optimal control, **58**
  MIMO
    set of inputs, 306ff
    specific input, 302ff
  MIMO system, **228**
  unstable systems, 88ff
$H_2^*$-optimal control, 165ff, 185ff, 413
  MIMO, 406ff
    set of inputs, 410ff
    specific input, 407ff
$H_\infty$ objective, 35

$H_\infty$-optimal control, 28, **29**
MIMO system, 230
sampled-data, **159**

— I —

Ill-conditioned, 225, 333, 346–347, 351, 451
IMC, *see*
• Internal Model Control
IMC design, **50**
application to a first-order deadtime system, 75ff
MIMO, 298ff
sampled-data, **168**
illustration, 424ff
MIMO, 406ff, 419ff
summary, 74
MIMO, **324**
MIMO, sampled-data, 433
sampled-data, **162**, 181
sampled-data, unstable systems, 199
unstable systems, 103
unstable systems
sampled-data, **188**
Improper, **12**
MIMO system, **206**
sampled-data, **146**
MIMO, 395
Induced norm, 211
$\infty$-norm, 30, 216–217, 231–232
Inner product, 215
Inner-outer factorization, 303, 309ff
sampled-data, 416ff
Input direction, 213
Input specification, 19ff
MIMO system, 225ff
Input weight, 19
Integral control, 291, 361, 384
robust performance, 71
robust stability, 67, 70, 244ff
Integral controllable, 362ff
Integral square error, 28, 61
Integral stabilizable, 362ff
Interaction Measure, 360, 367ff, 389
diagonal dominance, 372
generalized diagonal dominance, 373
IMC, 372
$\mu$, **374**, 390
Rijnsdorp, 375
Interactions, 342–343, 351
Internal Model Control, 3, 5, **41**, 56, 293ff; *see also*
• IMC
sampled-data, **147**, 397
Intersample rippling, 143, **155**, 168, 181, 192, 200
MIMO, 413ff
Inverse
approximate, 57
Inverse response, **13**, 327
Inversion, 48
Isermann, 164

— J —

Jabr, 325
Jenkins, 434

— K —

Kaiser, 1, 38, 55, 84
Kalman, 2
Kantor, 291
Kapoor, 457
Kestenbaum, xv

Kinneart, 56
Koppel, 390
Kouvaritakis, 291
Ktesibios, 1
Kucera, 182
Kuo, 164
Kwakernaak, 182, 201, 233, 326

— L —

Latchman, 291
Laub, 233, 326
Laughlin, 84
Lead compensator, 140
Lehtomaki, 291
Lewin, 139
Limebeer, 390
Lin, 38
Linear Fractional Transformation, 278ff, 379
Linear Quadratic ($H_2$-) Optimal Control, **28**, 216
Linear Quadratic ($H_2^*$-) Optimal control
  discrete, **158**
Linear quadratic optimal control
  MIMO system, **228**
Linearization, 15
Locatelli, 389
Loop shaping, 31, 34, 36, 240–241
Lunze, 389
Luyben, 110, 357, 376, 457

— M —

MacFarlane, 233, 390
Manousiouthakis, 291, 357
Marino-Galarraga, 356
Marlin, 457
Matrix norm, 224
Maxwell, 1
Mayr, 1
McAvoy, 356, 390, 457
Measurement device, 145, 293
  dynamics
    IMC design, 54
Measurement noise, 25
Meditch, 234
Mees, 390
Mijares, 389
Minimal realization, 296
Minimum phase, **13**, 58, 114
Moczek, 457
Model Algorithmic Control, 3
Model error
  Smith predictor, 129
Model reduction, 139
Model uncertainty, 4, 14, 41, 49
  MIMO System, 15, 223
  sampled-data, 149, **397**
Molinari, 326
Moore, 233, 325, 457
Morari, 3, 38, 56, 139, 164, 182, 233, 291–292, 326, 356–357, 389–390, 456–457
Multiloop controllers, 5

— N —

Neglected dynamics, **255**
Nett, 291, 389–390
Newton, 1, 38, 55–56, 84
Nichols, 113, 123, 125, 139
Niederlinkski, 390
Noncausal, **12**
  MIMO system, **206**
  sampled-data, **146**
    MIMO, 395

Nonminimum phase, xv, **13**, 48, 114
  MIMO system, 208
  unstable systems, 107
Norm
  compatible, 210, 221, 233
  consistent, 233
  Euclidean, 209
  Frobenius, 209, 211
  function space, **215**
  induced, 210–211
  matrix, 208ff
    compatible, 370
  operator, 210
  spectral, 209, 211
  vector, 208ff
Normal rank, 206–207
Normed space, 209
Nyquist, 1, 366
Nyquist band, **16**, 68, 73, 79, 82, 223, 237
Nyquist contour, 220, 232, 366
Nyquist region, 73
Nyquist stability criterion, 31, 205
  MIMO system, 217ff, 368

— O —

Offset, 27, 114, 343
Operator norm, 210
  induced, 216
Osborne, 291
Otto, 457
Output direction, 213

— P —

Padé approximation, 15, 115
  error caused, 120
Pairing, 365
Pairing problem, 360
Palmor, 139
Palozoglu, 357
Parseval's theorem, 20, 28, 215
Partial fraction expansion, 58, 133
Perfect control, **47**, 245, 343
Performance, 34
  achievable, 444
  IMC, 45
  nominal, 23ff
    $H_2$ objective, **300**
    $H_2^*$ objective, 402ff
    $H_\infty$ objective, **404**
    IMC, 50–51
    IMC design, 57, 74, 103
    MIMO system, 227ff
    MIMO, IMC design, 298, 300ff, 324
    MIMO, sampled-data, **401**
    MIMO, sampled-data, IMC design, 433
    sampled-data, 151
    sampled-data, $H_\infty$ objective, 159
    sampled-data, IMC design, 165, 199
    sampled-data, unstable systems, 184ff
    unstable systems, 88ff
  robust, 11, 22, 34ff
    decentralized control, 379ff, 382
    $H_2$ objective, 161, 268ff
    $H_\infty$ objective, 162, 262ff, 318ff, 406, 423
    IMC, 51
    IMC design, 70, 74–75, 103
    input uncertainty, 381
    interconnection structure, 422
    MIMO, $H_\infty$ objective, 315ff
    MIMO, IMC design, 299, 301,

310ff, 325
MIMO, sampled-data, 405ff
MIMO, sampled-data, IMC design, 434
sampled-data, **161**, 164
sampled-data, IMC design, 176ff, 182, 200
sampled-data, unstable systems, 198
summary, **287**
unstable systems, 102
specification, 72
distillation, 443
weights, 262
Perron-Frobenius Theorem, 374, 390
Phase margin, 139
PID controller, xv, 5, 114ff
Pinned zero, 342
Poles, 206
sampled-data
MIMO, **396**
Polynomial matrix, 365
Postlethwaite, 233, 291–292, 390
Prediction, 12
Predictor, 126
Prefilter, 26, 53
Prett, 56
Process design, 344
Process model, **14**
MIMO system, 222
sampled-data, 149
Proper, 11, **12**
MIMO systems, **206**
sampled-data, **146**
MIMO, 395
strictly, **12**, **206**
sampled-data, **146**
sampled-data,MIMO, 395

— R —

Ramaker, 3, 56
Ramkrishna, 5
Reactor, 67
Realization, 206
Relative Disturbance Gain, 356
Relative Gain Array, xv, 338; *see also* • RGA
as sensitivity measure, 258ff
Reset windup, 44
Return difference operator, 219, 232, 368
RGA, 347, 351, 357, 363, 366, 375, 445, 451; *see also* • Relative Gain Array
distillation, 440
of the controller, 345
RHP zeros, 58–59, 114, 136, 327, 357, 384
degree, 339
MIMO system, 208
performance limitations, 339ff
Richalet, 2, 56
Rijnsdorp, 390
Rivera, 139
ROBEX software, 139
Robust, 34
Robustness, 4
Rosenbrock, 326, 390
Rotation, 213
Routh test, 365
Ryskamp, 457

— S —

Sampling
effect on nominal performance, 157
effect on robustness, 176–177

effect on zeros, 164
frequency, 144
selection of sampling time, 178ff, 182
switch, 143, 151
Sandell, 234
Saturation, 44
Scalar controller, 338
Scali, 84
Schulman, 356
Schur's formulae, 219
Semi-proper, **12**
sampled-data, **146**
Seneta, 390
Sensitivity function, 24ff, 233, 299
IMC, 45
MIMO system, 227
sampled-data, 151ff
MIMO, **401**, 405
unstable systems, 86
Sensitivity operator, 229, 233
Sensor uncertainty, 223
Setpoint prediction, 168, **413**
Shinnar, 139
Shinskey, 457
Shunta, 110
Singular value, 211ff, 232
Singular value decomposition, 212, 337
Singular vector, 213
Sivan, 182, 201, 233, 326
Skogestad, 139, 291–292, 356–357, 389–390, 456–457
Small gain theorem, **221**, 233, 370, 389
Smith, 55–56, 139, 233
Smith Predictor, xv, 5, 55–56, 123, 126ff
model error, 129
robust tuning, 130
stability
internal, 126
Space
linear, 208
Spang, 389
Spectral norm, **209**, 211
Spectral radius, 211, 221
Spectrum, 20, 30, 226
Square-integrable, 215
SSV, 357, 374
Structured Singular Value, 344
Stability
internal, 21ff
IMC, 41, 150
MIMO, 221, **295**
MIMO, sampled-data, **396**, 399ff
sampled-data, **147**
sampled-data, unstable systems, **183**
Smith predictor, 126
unstable systems, **85**
nominal, 21
decentralized control, 382
robust, 11, 22, 31ff, 68, 236ff
decentralized control, 378
IMC, 50, 52
IMC design, 66, 74–75, 103
interconnection structure, 421
MIMO, IMC design, 298, 301, 310ff
MIMO, sampled-data, **404**
MIMO, sampled-data, IMC design, 434
sampled-data, **160**, 164
sampled-data, IMC design, 174, 182, 199
sampled-data, unstable systems, 198
structured uncertainty, 247ff

summary, **287**
unstable systems, 101
Stanley, 356
Stein, 38, 234, 291
Stephanopoulos, 5
Sternby, 164
Stewart, 233
Stochastic optimal control, 25
Strang, 5
Structured Singular Value, 36, 38, 248ff, 281ff, 291, 299, 349, 371
robust performance, **264**, 269ff
sampled-data, 422–423
System Type, **27**; *see also* • Type
IMC, 46
MIMO, **298**
sampled-data, 154ff, 164, 166, 168, 172, 189

— T —

Thompson, 164
Time constant
closed loop, 114
Time delay, 11, 13–14, 115, 126, 128, 136, 222
Time-varying, 151, 161
Tits, 291, 357
Toijala, 357
Transfer matrix, 206
Two-degree-of-freedom controller, **25**, 104, 340
IMC, 46, 52
unstable systems, 94ff
Type, 60, 64; *see also* • System Type
system type
MIMO system, **228**, 234

— U —

Uncertainty, **223**
actuator, 344, 349
additive, 17, 236, 244
integral control, 246
interconnection structure, 313
perfect control, 245
batch reactor, 254
block input, 346
diagonal input, 344, 346, 357
distillation column, 242
element-by-element, 344
input, **223**
diagonal, 351
distillation, 442
inverse multiplicative output, 236, **242**
multiplicative, 17, **223**, 344
at plant output, 223
integral control, 246
perfect control, 245
multiplicative input, 236, **240**, 244, 252, 266, 280
diagonal, 344
interconnection structure, 314
sampled-data, 425
multiplicative output, 236, **239**, 244, 252, 265, 280, 299, 344
interconnection structure, 314
parametric, **254**
structured, **235**
transfer matrix elements, **257**
interconnection structure, 314
unstructured, 235ff
weights, 262
worst-case, 348, 357
Uncertainty description, 234
Uncertainty region, 16
general

unstable systems, 102
norm-bounded
unstable systems, 101
Uncertainty specification
distillation, 443
Unitary, 225
Unitary matrix, 212
Uthgenannt, 390

— V —

Vandermonde form, 110
VanLoan, 110
Varga, 390
Vidyasagar, 4–5, 38, 110, 233, 291
Vogel, 164
Vyshnegradskii, 1

— W —

Wall, 291
Watt, 1
Watts, 434
Weight
input weight, 225, 229–230
output weight, 229–230
performance weight
example, 383
selection, 229
uncertainty weight
example, 384
Wiener, 55
Wiener-Hopf factorization, 2
Williams, 457
Windup, 44
Wittenmark, 139, 164, 182, 434
Wolfe, 234

— Y —

Youla, xv, 2, 56, 110, 325

— Z —

Zafiriou, 164, 182, 291, 326, 356
Zames, xv, 2, 38, 56, 110, 201
Zero direction, 339ff, 343
Zero polynomial, 207
Zero-order hold, **145**, 393
Zeros
MIMO system, **207**
pinned zero, 342
sampled-data
MIMO, 396
Ziegler, 113, 123, 125, 139
Zirwas, 55